THE ROLE OF PYRIDINE NUCLEOTIDES IN QUINONE-INDUCED CELL DEATH

Winston Antonio Morgan

Submitted to the University of London
for examination for the degree of
Doctor of Philosophy December 1992.

Department of Toxicology
School of Pharmacy,
University of London,
29-39 Brunswick Square, London WC1N, 1AX.

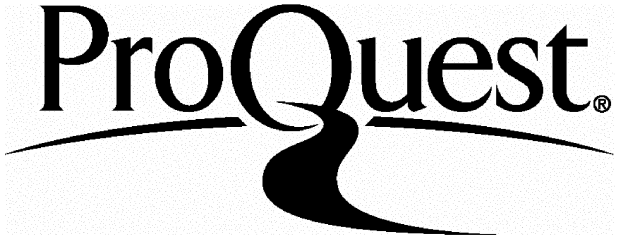

ABSTRACT-The depletion of the pyridine nucleotide NAD^+ observed during oxidative stress has often been attributed to hydrolysis. However recently an interconversion of NAD(H) to NADP(H) was proposed. Using rat hepatocytes, the changes in pyridine nucleotides induced by several redox cycling quinones as well as the organic hydroperoxide tert-butyl hydroperoxide (tBH) were investigated. The exposure of rat hepatocytes to redox cycling quinones such as 2,3-dimethoxy-1,4-naphthoquinone (2,3-diOMe-1,4-NQ) or to tBH resulted in a rapid depletion of NAD^+. The depletion of NAD^+ was accompanied by an increase in nicotinamide. In hepatocytes preincubated for one hour with inhibitors of poly(ADP-ribose)polymerase then exposed to either 2,3-diOMe-1,4-NQ or tBH, the rate of NAD^+ depletion was significantly reduced. 2,3-diOMe-1,4-NQ induced extensive oxidation of NADPH which was followed by an increase in level of $NADP^+$ + NADPH. The increase in $NADP^+$ + NADPH was equivalent to the decrease in NAD^+ and no change in the total pyridine nucleotide { NAD(H) + NADP(H) } level was observed. In hepatocytes exposed to tBH, the oxidation of NADPH was not accompanied by an increase in the level of $NADP^+$ + NADPH and a decrease in total pyridine nucleotides was observed. These observations suggest that during oxidative stress, the depletion of NAD^+ results from the activation of poly(ADP-ribose)polymerase which hydrolyses NAD^+ to nicotinamide and that the depletion of NAD^+ is independent of the increase in NADP(H).

The activation of poly(ADP-ribose)polymerase and the depletion of NAD^+ are often associated with DNA damage. In human myeloid leukaemic cells (K562), both 2,3-diOMe-1,4-NQ and menadione induced DNA strand breaks at very early time points (< 5 min). The strand breaks induced by both quinones were inhibited by the iron chelator 1,10-phenanthroline. Where strand breaks are rapidly repaired, cell proliferation is unaffected. Conversely at concentrations which cause extensive strand breakage less strand scission repair is observed and the rate of cell proliferation is significantly inhibited. These results suggest that a brief exposure to low concentrations of some redox cycling quinones results in a delayed cell death, preceded by DNA damage and the depletion of NAD^+.

This thesis is dedicated to my mother.

EVA.

ACKNOWLEDGEMENTS

The completion of this thesis would not have been possible without the help, support and advice of several people.

I would like to thank Dr J. Timbrell for his invaluable help during the last few months of this thesis. In particular for the manner in which he coped with a potentially difficult situation. I would also like to thank Dr A. Kortenkamp for his helpful suggestions in writing this thesis. Thankyou also to Dr J. Hartley and all at the Department of Oncology, UCMSM.

Thankyou to all members of Department of Toxicology, past and present for being there and for making working in a cold dark basement interesting; John Mooney, Simin (Dr Ghatenah), Cathy (Dr Waterfield), Michael Butterworth, Adrian Keene, Mark Raffray, Ruth Draper, Mary Fagg and Zahida Ahmed. A special thankyou to Adrian Rodgers for his "sage-like" knowledge of all subjects.

Thankyou to all members of the Centre for Drug Delivery Research especially Ijeoma.

I would like to thank all members of family for their interest encouragement and support.

Finally, but by no means least thankyou to my fiancée Stephanie for her love encouragement and constant support, without which I could not have completed this thesis.

CONTENTS

FIGURES

TABLES

ABBREVIATIONS

ARA-C	Arabinofuranosylcytosine
ATP	Adenosine triphosphate
ADP	Adenosine diphosphate
AZQ	3,6-bis(ethoxycarbonylamino)-2,5-bis(1-aziridinyl)-1,4-benzoquinone
BSA	Bovine serum albumin
BABQ	2,5-bis(1-aziridinyl)-1,4-benzoquinone
CQ	3-(2-carbamoyloxy)-1-(methoxyethyl)-2,5-bis(1-aziridinyl)-1,4-benzoquinone
DMS	Dimethyl sulphate
DMSO	Dimethyl sulphoxide
EDTA	Ethylenediaminetetraacetic acid
EGTA	Ethyleneglycol-bis-(aminoethyl ether)N,N,N,N'-tetraacetic acid
GSH	Glutathione reduced
GSSH	Glutathione oxidized
HEPES	(N-[2-hydroxyethyl]piperazine-N'-[2ethanesulphonic acid])
$OH^{\cdot}$	Hydroxyl radical
H_2O_2	Hydrogen peroxide
MTT	Thiazolyl Blue
NAD^+	Nicotinamide adenine dinucleotide
NADH	Nicotinamide adenine dinucleotide reduced
$NADP^+$	Nicotinamide adenine dinucleotide phosphate
NADPH	Nicotinamide adenine dinucleotide phosphate reduced
NAMN	Nicotinate mononucleotide
NMN	Nicotinamide mononucleotide
NMNG	N-methyl-N-nitro-N-nitrosoguanidine
$O_2^{\cdot-}$	Superoxide anion radical
o-PT	o-phthalaldehyde
PCA	Perchloric acid
PES	Phenasine ethanosulphate
PRPP	5-Phosphoribosyl-1-pyrophosphate
SOD	Superoxide dismutase
tBH	tert-Butyl Hydroperoxide
TW13	2,5-bis(1-aziridinyl)-1,4-benzoquinone
TQ25	2,5-bis(1-aziridinyl)-3-bromo-6-ethyl- 1,4-benzoquinone
2,3-diOMe1,4-NQ	2,3-dimethoxy-1,4-naphthoquinone

CHAPTER 1

INTRODUCTION

1.1 OVERVIEW

In recent years there has been an increasing interest in pyridine nucleotides and their role in the mechanisms of chemically induced cell injury [Cohen and Stubberfield, 1990]. Alterations in the level and redox status of cellular pyridine nucleotides (NAD^+, NADH, $NADP^+$, NADPH) prior to the loss of membrane integrity has been widely reported in mammalian cells during oxidative stress [Smith et al, 1987; Stubberfield and Cohen, 1988]. Many cytotoxic chemicals including menadione and tert-butyl hydroperoxide cause the oxidation and hydrolysis of mitochondrial pyridine nucleotides; this is believed to lead to the perturbation of intracellular Ca^{2+} homeostasis and cell death from the activation Ca^{2+}-dependent proteases, phospholipases and endonucleases [Lotscher et al, 1980; Boobis et al, 1989]. Additionally, compounds such as hydrogen peroxide are known to cause DNA damage and the depletion of NAD^+ [Schraufstatter et al, 1986b].

A number of studies have demonstrated that the depletion of NAD^+ results from DNA damage and the activation of poly(ADP-ribose)polymerase, which hydrolyses NAD^+ as a source of ADP-ribose during DNA repair [Gaal et al, 1987]. Furthermore, following extensive DNA damage, the depletion of NAD^+ and the subsequent loss of ATP has been proposed as a cellular suicide response to prevent the survival of cells which suffer extensive DNA damage [Berger, 1985].

Recently a novel explanation was suggested to account for the depletion of NAD^+ observed during oxidative stress. Stubberfield and Cohen (1989) and later Yamamoto

and Farber (1992) found that during oxidative stress the depletion of NAD^+ was independent of the activation of poly(ADP-ribose)polymerase. They proposed that the depletion of NAD^+ was instead due to an interconversion of NAD^+ to NADP(H) in an attempt to combat the effects of oxidative stress, by increasing the cells reducing capacity. However, as poly(ADP-ribose)polymerase is normally activated following DNA strand breakage, an alternative interpretation of the studies above is that either chemically-induced oxidative stress does not result in DNA damage or that during oxidative stress the process of DNA repair is abrogated by nucleotide interconversion.

1.1.1 AIMS

Quinones are increasingly encountered both in the environment and as therapeutic agents. Recently a number of widely differing and contradictory mechanisms have been proposed to explain their cytotoxicity in mammalian cells. These studies will investigate the relationship between pyridine nucleotide changes and cytotoxicity in rat hepatocytes induced by several bis-aziridinylbenzoquinones. Although the mechanisms of action of the bis-aziridinylbenzoquinones have been widely studied, their effects on cellular pyridine nucleotides have never been extensively investigated. This study will also examine the evidence for pyridine nucleotide interconversion using a number of redox cycling quinones and tert-butyl hydroperoxide. The fate of NAD^+ during oxidative stress is also extensively investigated using poly(ADP-ribose)polymerase inhibitors and radiolabelled nicotinamide. Finally the relationship between quinone-induced DNA strand breakage, pyridine nucleotide changes and cytotoxicity is investigated.

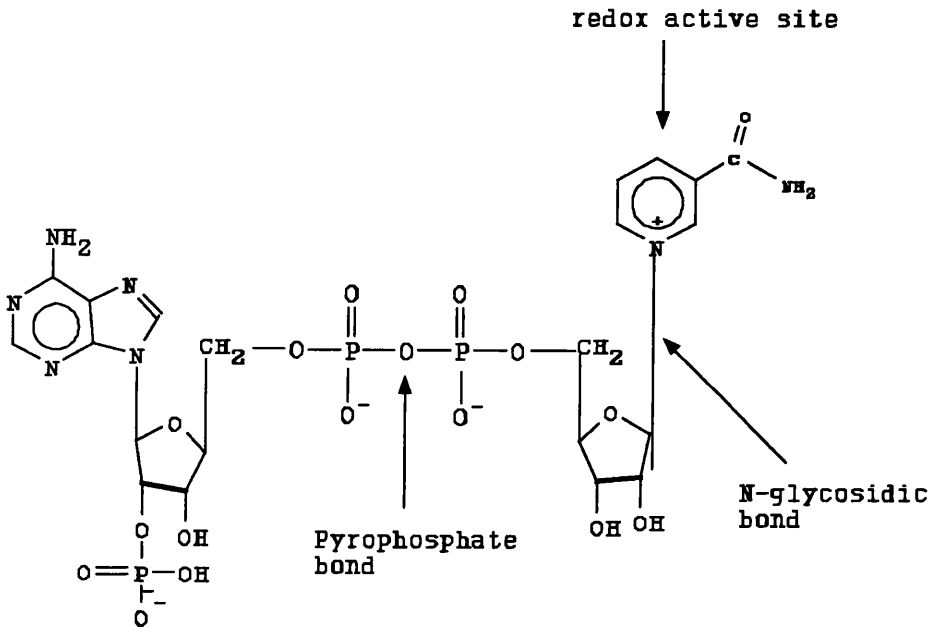

Fig. 1.1 Nicotinamide adenine dinucleotide phosphate, reduced form ($NADP^+$).

1.2 Pyridine Nucleotides

Nicotinamide dinucleotides were first discovered in the 1930's as coenzymes of dehydrogenase [Warburg et al, 1935]. Basically they consist of two mononucleotides, 5'AMP and nicotinamide nucleotide linked by a pyrophosphate bond (Fig. 1.1). Alternatively the dinucleotide can also be described as the adenosine diphosphate ribosyl moiety (ADP-ribose) attached to nicotinamide through a β-N-glycosidic linkage (Fig.1.1). The name pyridine nucleotide refers to the redox-active pyridine derivative, the nicotinamide moiety. Since their discovery pyridine nucleotides have been found to perform numerous biochemical functions including: (a) the oxidation and reduction of the pyridine ring allows the nucleotide to perform its central role in biological oxidation [Bucher, 1970]; (b) the splitting of the pyrophosphate bond in adenylation

of prokaryote DNA ligase [Little et al, 1967]; and (c) the transfer of the ADP-ribosyl moiety to an acceptor as in ADP-ribosylation of proteins or to water in the NAD^+ glycohydrolase reaction [Nishizuka et al, 1968].

1.2.1 Distribution and Cellular Compartmentation of the Pyridine Nucleotides

The pyridine nucleotide content of different cell types and tissues have been widely studied [Kaplan et al, 1957; Tischler et al, 1969; Heldt et al, 1965]. Distribution of the two forms of the nucleotide, NAD(H) and NADP(H) differ markedly between liver, heart, skeletal muscle and brain (Table 1). Some years ago Kaplan (1985) proposed that the two pyridine nucleotide systems (NAD^+ and $NADP^+$) had different metabolic functions. Whereas NADH is oxidized by the mitochondria to yield ATP, NADPH appears to be involved in reductive synthetic systems.

TABLE 1 Content of nicotinamide nucleotides in rat tissues and amounts present in mitochondrial compartments (From Sies, 1982)

Tissue	$NADH+NAD^+$ nmol/gram wet weight	% mitochondrial	$NADPH+NADP^+$ nmol/gram wet weight	% mitochondrial
Liver	804	20	428	65
Skeletal muscle	593	21	27	65
Heart	854	53	141	78
Brain	450	18	41	35

Hence, tissues such as skeletal muscle contain relatively high levels of NADH and low levels of NADP, while tissues such as liver with high synthetic activity contain high levels of NADPH [Sies, 1982]. At present information on the regulation of subcellular distribution of the pyridine nucleotides is limited. Cellular NAD^+ undergoes rapid turnover, while biosynthesis takes place in different cellular compartments. For example mitochondrial nucleotide levels are maintained despite the slow rate of penetration of the nucleotide through the inner mitochondrial membrane and the low rate of synthesis within the mitochondria [Purvis and Lowenstein, 1961].

The subcellular distribution of the nucleotides may be quantified in terms of mitochondrial and extramitochondrial compartments. NAD(H) is found predominantly in the extramitochondrial compartments where it exists mainly in the oxidized form (NAD^+), while NADP(H) is found predominantly in the mitochondria where it exists mainly in the reduced form (NADPH) (Table 2). Generally the degree of reduction of the nucleotides is dependent on the availability of energy.

TABLE 2. Subcellular distribution of pyridine nucleotides in rat liver. (From Sies 1982)

	nmol per gram liver wet weight		
Nucleotide	Mitochondrial	Extramitochondrial	Total
NADH	66	24	90
NAD^+	66	504	570
NADH + NAD^+	132	528	660
NADPH	236	65	301
$NADP^+$	16	47	63
NADPH + $NADP^+$	252	112	364

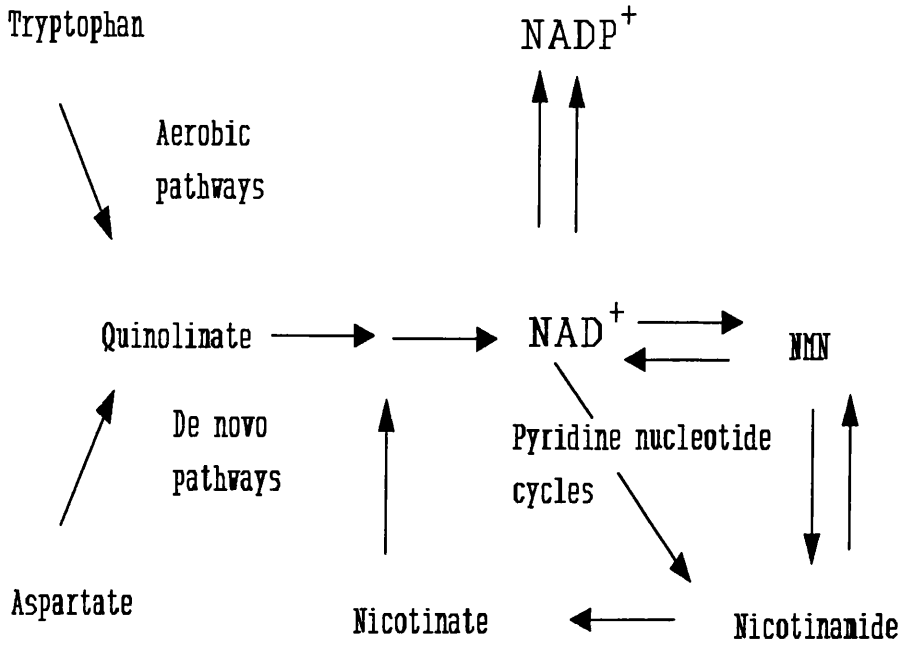

Fig. 1.2 Overview of pyridine nucleotide biosynthetic and salvage pathways (From White, 1982)

1.2.2 Maintenance of Intracellular Pyridine Nucleotides

The maintenance of intracellular pyridine nucleotides levels is determined by the balance between biosynthesis, hydrolysis and recycling. Under circumstances where there is increased hydrolysis of NAD^+ such as following DNA damage, a decrease in the total pyridine nucleotides results. Conversely, the intraperitoneal injection of rats with nicotinamide, which acts as a precursor in the biosynthesis of NAD^+ as well as an inhibitor of NAD^+ hydrolysis results in a threefold increase in the level of NAD^+

in the liver [Lagunas et al, 1970].

1.2.3 Pyridine Nucleotide Biosynthesis

Quinolinate (2,3-pyridinedicarboxylic acid) is a major precursor of the biosynthesis of the pyridine nucleotides. At least four distinct synthetic pathways to quinolinate have been identified (Fig. 1.2) [White, 1982]. In organisms able to synthesize quinolinate, there seems to be only a single pathway for the conversion of quinolinate to the pyridine nucleotides (Fig. 1.2). Quinolinate is converted to NAD^+ via nicotinamide mononucleotide and deamido nicotinamide adenine dinucleotide (Fig. 1.3). The nicotinamide mononucleotide (NMN) may also be formed from nicotinate (niacin) a common vitamin as well as a product of pyridine nucleotide metabolism. The conversion of nicotinate or quinolinate to NAD^+ is via a three step pathway called the Preiss-Handler pathway, when available nicotinate is the preferred precursor in the synthesis of NAD^+ [Priess and Handler, 1958a; Priess and Handler, 1958b; Mclean et al, 1973]. Intermediates in the Preiss-Handler pathway are formed in different cellular compartments; the first intermediate, nicotinate mononucleotide is formed in the cytoplasm, it is then transported to the nucleus where it reacts with ATP to form deamido-NAD^+ [Imsande and Handler, 1961]. The final amidation reaction takes place in the cytoplasm (Fig. 1.3) [Kaplan, 1961].

The mechanisms which regulate the formation of $NADP^+$ from NAD^+ are unknown at present. However, the reaction is thought to be catalysed by a specific NAD^+ kinase and may take place in either the cytosol or mitochondria [White, 1982]. Increased NAD^+ kinase activity has been observed in mammary glands during

pregnancy, while the reduced nucleotides are thought to inhibit the activity of NAD^+ kinase [Kaplan, 1985].

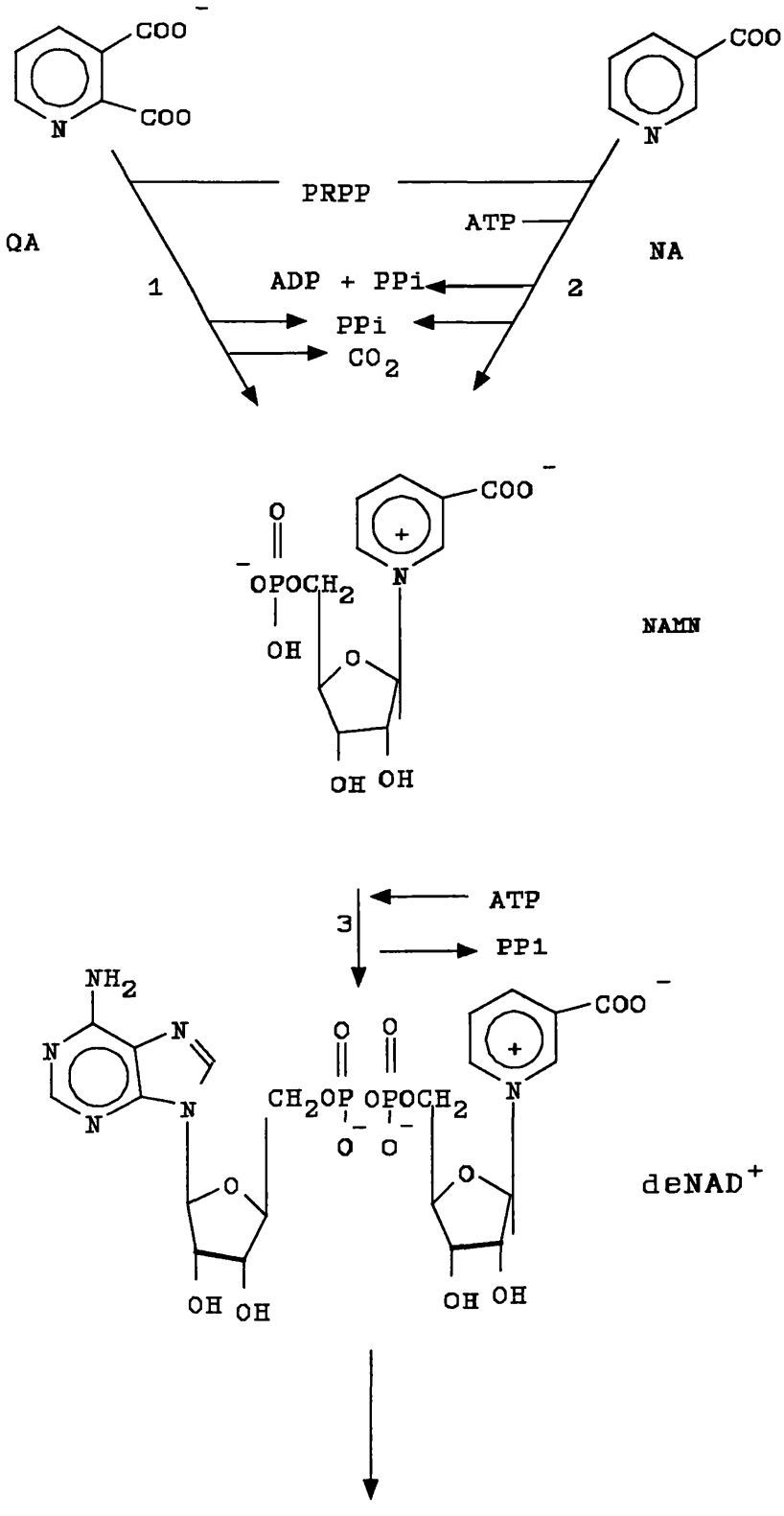
COO⁻
COO
N
COO⁻
N
PRPP
ATP
QA
NA
1
ADP + PPi
2
PPi
CO2
COO⁻
O
OPOCH2
OH
O
N
NAMN
OH OH
ATP
3
PP1
NH2
N
N
N
N
COO⁻
O O
CH2OP OPOCH2
O⁻ O⁻
O
O
N
deNAD+
OH OH
OH OH

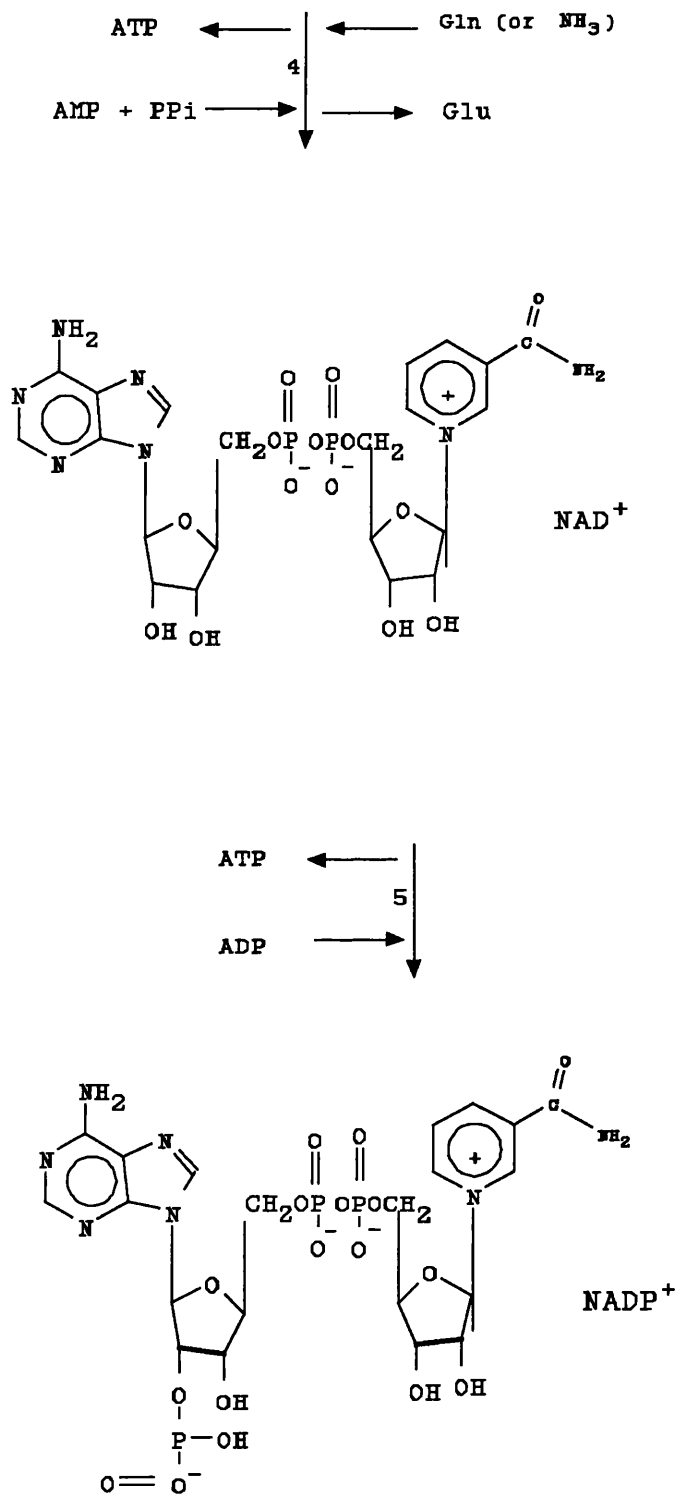

Fig. 1.3 The biosynthesis of NAD^+ and $NADP^+$ from quinolinate (QA) and nicotinate (NA), via nicotinate mononucleotide (NAMN) and deamido nicotinamide adenine dinucleotide ($deNAD^+$) [Kaplan, 1982]. Reactions 2,3 and 4 constitute the Preiss-Handler pathway. Enzymes involved in the above are: 1. Quinolinate phosphoribosyltransferase (which requires phosphoribosyl pyrophosphate, PRPP); 2. Nicotinate phosphoribosyltransferase; 3. Nicotinate mononucleotide adenyltransferase; 4. NAD^+ synthetase; 5. NAD^+ kinase.

1.2.4 The Pyridine Nucleotide Cycles

The majority of NAD^+-requiring enzymes catalyze oxidation-reduction reactions. However, pyridine nucleotides are also involved in reactions which result in the hydrolysis of NAD^+. Cleavage of the *N*-glycosidic bond or the pyrophosphate linkage of NAD^+ liberates nicotinamide or nicotinamide mononucleotide respectively, both are inert in oxidation-reduction reactions and must be salvaged by the pyridine nucleotide cycle (Fig. 1.4) [Gholson, 1966].

Isotope studies have revealed that cells do not contain significant amounts of the intermediates in the pyridine nucleotide cycle, suggesting the cycles are either very efficient or they play a quantitatively minor role in pyridine nucleotide metabolism [Foster and Baskowsky-Foster, 1980]. Isotope studies also revealed that half the cell's NAD^+ is lost in 1.0 ± 0.3 hours and only 5% of NAD^+ formation is due to biosynthesis, the remainder being due to recycling [Rechsteiner et al, 1976]. The nucleus is thought to play an important role in recycling of NAD^+ as the half-life of the nucleotide increases to 10 hours in enucleated cells [Rechsteiner and Cantanzarite, 1974]. Within the nucleus NAD^+ is the substrate for poly(ADP-ribose)polymerase [Hayaishi and Ueda, 1977].

The NAD^+ molecule may be hydrolysed at several points, generating a number of intermediates [Gholson, 1966]. Several recycling pathways have been identified, enabling intermediates to join the cycle at various stages (Fig. 1.4) [White, 1982]. For example nicotinamide can either be recycled via nicotinate or directly to the mononucleotide. Nicotinamide liberated in the nucleus must be transported to the cytoplasm to be converted to the mononucleotide. Both DNA ligase and NAD^+ pyrophosphatase are capable of forming the nicotinamide mononucleotide from NAD^+,

which may be resynthesized to NAD^+ by certain mammals. Although several recycling pathways have been identified, not all tissues are able to utilise them [Greenbaum and Pinder, 1968; Striffer and Benes, 1971; Foster and Baskowsky-Foster, 1980]. The efficiency of the salvage pathways means that the pyridine nucleotides are conserved by most cells. In general nicotinamide is not degraded. However, in mammals a modified nicotinate derivative N-methylnicotinamide appears in the urine [Lindquist and Olivera, 1971; Chaykin et al, 1965; Kaplan, 1961].

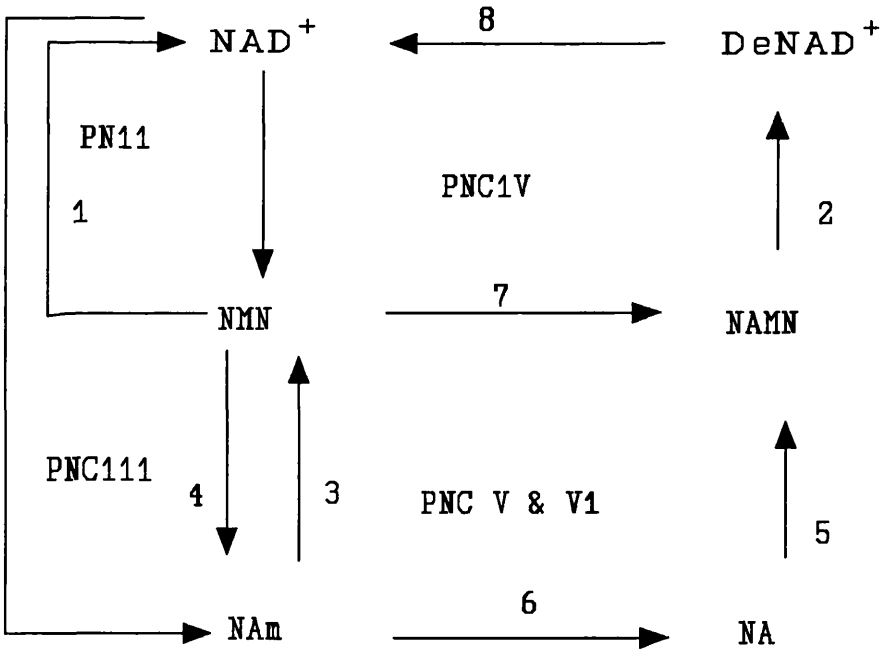

Fig 1.4 The Pyridine nucleotide cycles (PNC) and salvage pathways to regenerate NAD^+ from nicotinamide mononucleotide (NMN) or nicotinamide (NAm). PNC1V, PNCV and PNCV1 converts NMN and or NAm to intermediates of the Priess-Handler pathway (nicotinate (NA), via nicotinate mononucleotide (NAMN) and deamido nicotinamide adenine dinucleotide ($deNAD^+$)). PNC11 and PN111 are similar to the other cycles except the deamidation and reamidation reactions are not involved as recyling is not dependent on the reactions of the synthetic pathway. Enzymes involved in the above are: 1. Nicotinamide mononucleotide adenyltransferase; 2. Nicotinate mononucleotide adenyltransferase; 3 NMN nucleosidase; 4. Nicotinamide phosphoribosyltransferase; 5. Nicotinate phosphoribosyltransferase; 6. Nicotinamidase; 7. NMN amidase; 8. NAD^+ synthetase.

1.3 Quinones

Quinones are cyclic structures containing two or more carbonyl groups. They are found throughout the animal and plant kingdoms where they function primarily as components of the electron transport chain in respiration and photosynthesis [Thomson, 1971; Nohl et al, 1986; Hatefi, 1985].

TABLE 3. Sources and uses of some quinones.

Quinone	Source	Use
Lawsone	Henna	Dye
Phylloquinone	Animals	Vitamin K1
Adriamycin	Streptomyces sp.	Anticancer agent
Echinochromes	Sea Urchins	Pigments
Benzoquinones	Insects	Toxic defence
Phenanthrene quinone	Urban particulate matter	Pollutants
Anthraquinone	Diesel exhaust	
Mitomycin C	Streptomyces cultures	Antibiotic

Contact with quinones may result from a number of sources including exposure to cigarette smoke, diesel exhaust or through diet [Pryor et al, 1983; Schutzle, 1983; Ames, 1983]. Quinones are also widely used as therapeutic agents such as antibiotics and in cancer chemotherapy (Table 3) [Nohl et al, 1986; Blum and Carter, 1974; Carter and Crook, 1974].

Quinones occur in a variety of forms from the very simple benzoquinones and naphthoquinones to the more complex benzo[*a*]pyrene-1,6-dione (Fig. 1.5). Despite

their structural diversity most quinone chemistry is governed by the polarizing effects of the two carbonyl groups, while the cytotoxicity of most quinones can be attributed to their ability to act either as electrophiles or as oxidants [Monks et al, 1992].

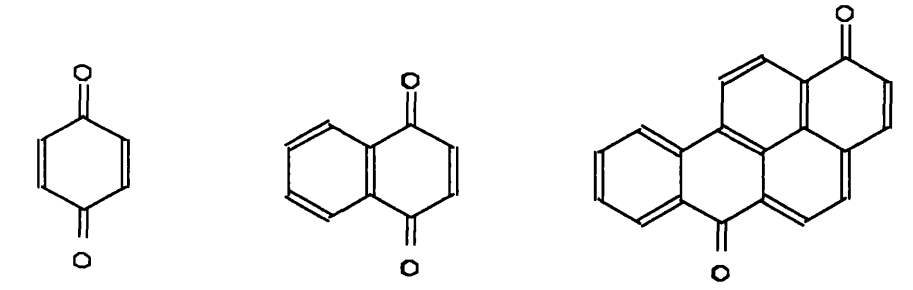

Fig. 1.5 Examples of quinone structures.

1.3.1 Redox Cycling and Oxidative Stress

The mechanisms of cytotoxicity of quinones has been extensively studied. Increasingly a number of studies have focused on the role of redox cycling and oxidative stress in quinone-induced cytotoxicity [Monks et al, 1992]. Quinones may be sequentially reduced by one electron steps to the semiquinone radical and hydroquinone in the presence of a suitable electron donor such as NAD(P)H (Fig. 1.6)

[Kappus, 1986]. In the presence of molecular oxygen, the semiquinone may be auto-oxidized back to the parent quinone, which is then available for re-reduction in a futile redox cycle [Kappus and Sies, 1981]. Evidence of redox cycling includes a disproportionate consumption of molecular oxygen, reducing equivalents (NAD(P)H, GSH) and the generation of active oxygen species in excess of the concentration of the quinone [Monks, et al. 1992]. The one electron reduction of quinones may be catalyzed by a number of flavoproteins including microsomal NADH-cytochrome b_5 reductase, microsomal NADPH-cytochrome P450 reductase and mitochondrial NADH-ubiquinone oxidoreductase [Powis and Appel, 1986].

The reduction of molecular oxygen by the semiquinone (or hydroquinone) generates the superoxide anion from which a series of active oxygen species may be generated [Powis and Appel, 1986; Kappus and Sies, 1981]. Under circumstances where the generation of active oxygen species ($O_2^{\cdot-}$, H_2O_2 and $HO^{\cdot}$) overwhelms the cell's antioxidant defences (GSH, superoxide dismutase, catalase, NAD(P)H) a state of oxidative stress is said to exist [Sies, 1985; Cadenas, 1985].

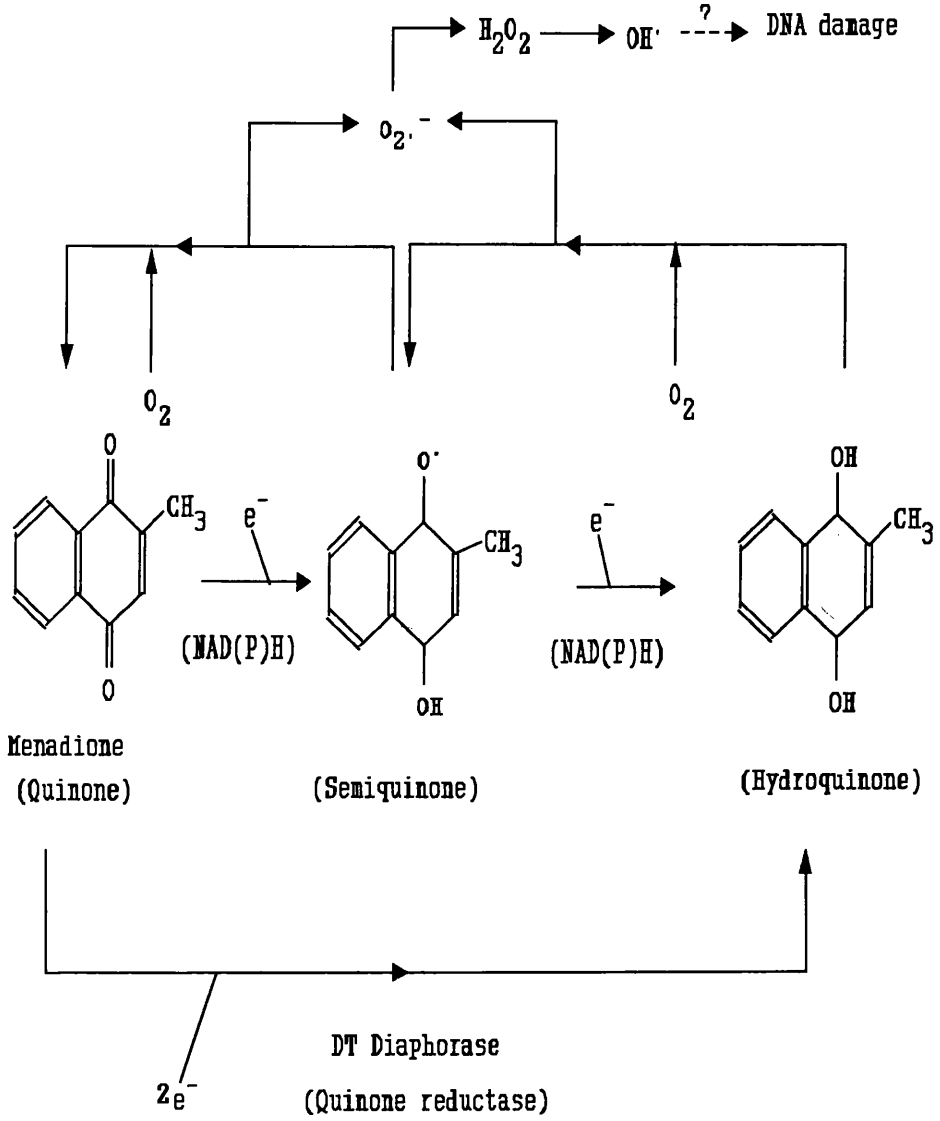

Fig. 1.6 Proposed mechanism of redox cycling of quinones

Quinones may also undergo a two electron reduction to the hydroquinone catalyzed by the enzyme DT-diaphorase (NAD(P)H-quinone oxidoreductase), the hydroquinone may be conjugated to glucuronide or sulphate groups then excreted from the cell in what is thought to be a detoxification process [Lind et al, 1982; Thor et al, 1982].

Certain quinones are also thought to undergo a two electron redox cycle mediated by DT-diaphorase [Cohen and Stubberfield, 1990].

1.4 Superoxide Anion, Hydrogen Peroxide and the Hydroxyl Radical

The generation of the superoxide anion radical during redox cycling of certain quinones is the starting point in the generation of a series of potentially damaging active oxygen species (eq 1) [Chance et al, 1979].

$$O_2 \xrightarrow{+e^-} O_2^{\cdot-} \xrightarrow[2H^+]{+e^-} H_2O_2 \xrightarrow{+e^-} HO^{\cdot} + HO^- \quad (1)$$

The one electron reduction of molecular oxygen by the semiquinone generates the superoxide anion which is capable of acting as both oxidant and reductant, this property enables it to spontaneously dismutate to hydrogen peroxide (eq. 2). The dismutation to hydrogen peroxide may also be mediated by the enzyme superoxide dismutase [McCord and Fridovich, 1969].

$$O_2^{\cdot-} + O_2^{\cdot-} + 2H^+ \longrightarrow H_2O_2 + O_2 \quad (2)$$

Although both the superoxide anion and hydrogen peroxide may react with biological substances, neither is responsible for the oxidative damage observed during quinone-induced oxidative stress. Damage is thought to result from the generation of the hydroxyl radical [Fee and Valentine, 1977; Bus and Gibson, 1984; Imlay and Linns, 1988]. The highly reactive hydroxyl radical may be generated by a series of reactions first described by Haber and Weiss (1934). They proposed that the hydroxyl radical is formed by the reaction of $O_2^{\cdot-}$ with H_2O_2 (eq. 3), the reaction is normally

slow but is thought to be catalysed by iron (or copper) salts in biological systems (eq. 4 & 5) in the Fenton reaction [Halliwell and Gutteridge, 1984].

$$O_2^{\cdot-} + H_2O_2 \longrightarrow O_2 + HO^{\cdot} + OH^- \quad (3)$$

$$O_2^{\cdot-} + Fe^{3+} \longrightarrow O_2 + Fe^{2+} \quad (4)$$

$$Fe^{2+} + H_2O_2 + H^+ \longrightarrow Fe^{3+} + H_2O + HO^{\cdot} \quad (5)$$

The hydroxyl radical can cause damage to cellular constituents by a number of reactions including electron transfer, hydrogen abstraction as well as addition to lipids, proteins, polysaccharides and nucleic acids [Halliwell and Aruoma, 1991]. Damage is normally restricted to sites where the radical is generated as the reactivity of the hydroxyl radical limits diffusion [Sies and Cedenas, 1983].

1.4.1 Antioxidant Defence Mechanisms

A number of antioxidant defence mechanism have evolved in both procaryotic and eukaryotic cells to protect against the harmful effects of active oxygen species ($O_2^{\cdot-}$, H_2O_2 and OH^-), resulting from the sequential univalent reduction of molecular oxygen.

Superoxide dismutase catalyses the dismutation of the superoxide anion to hydrogen peroxide and oxygen [Thor et al, 1982]. In E. coli grown under hyperbaric oxygen the enzyme is induced while in mutant strains where the enzyme is diminished, reduced oxygen tolerance is observed [Halliwell and Gutteridge, 1984]. Cells are also protected by catalase and glutathione peroxidase. Catalase is an iron-containing enzyme located mainly in the peroxisome, it catalyses the reduction of two molecules of H_2O_2 to water

and oxygen [Nohl et al, 1986; Ames, 1983; Jones, 1985]. GSH peroxidase is thought to be more effective than catalase as it is widely distributed in the cytosol and mitochondria, at sites where the active oxygen species can be generated [Jones et al 1981]. Furthermore GSH peroxidase is also capable of removing both H_2O_2 and organic hydroperoxides [Chance et al 1979].

1.5 Reaction of Quinones with Nucleophiles

In addition to their ability to redox cycle, quinones may readily react with certain cellular nucleophiles such as reduced glutathione additionally they may react with the sulphydryl group in certain proteins and amino acids [Monks et al, 1992]. The reaction may either occur spontaneously or it may be catalyzed by enzymes such as GSH *S*-transferase [Chasseaud, 1979]. The interaction of quinones with nucleophilic groups may lead to toxicity by a number of mechanisms including inhibition of critical thiol groups in enzymes or by interfering with cellular thiol balance. Most reactions of quinones with nucleophiles proceed via nucleophilic Michael addition forming hydroquinone thioethers [Monks et al, 1992].

1.6 Bioreductive Activation

The concept of bioreductive activation has been used to describe the mechanism of a number of quinone-containing therapeutic agents [Lin et al, 1972]. Compounds such as diaziquone (AZQ) contain not only the quinone moiety but also two alkylating aziridine groups. Reduction of the quinone moiety is thought to facilitate the protonation of the aziridine ring leading to the formation of the aziridinium ion, the required species for alkylation (Fig. 1.7) [Gutierrez et al 1986]. Bioreductive activation

can lead to cross-links between DNA molecules and between DNA and proteins [Szmigiero et al, 1984]. However, as compounds such as diaziquone are capable of causing DNA damage by alkylation through aziridinium ion as well as via the generation of active oxygen species, the exact mechanism of action of such compounds remains unresolved [Silva and O'Brien, 1989].

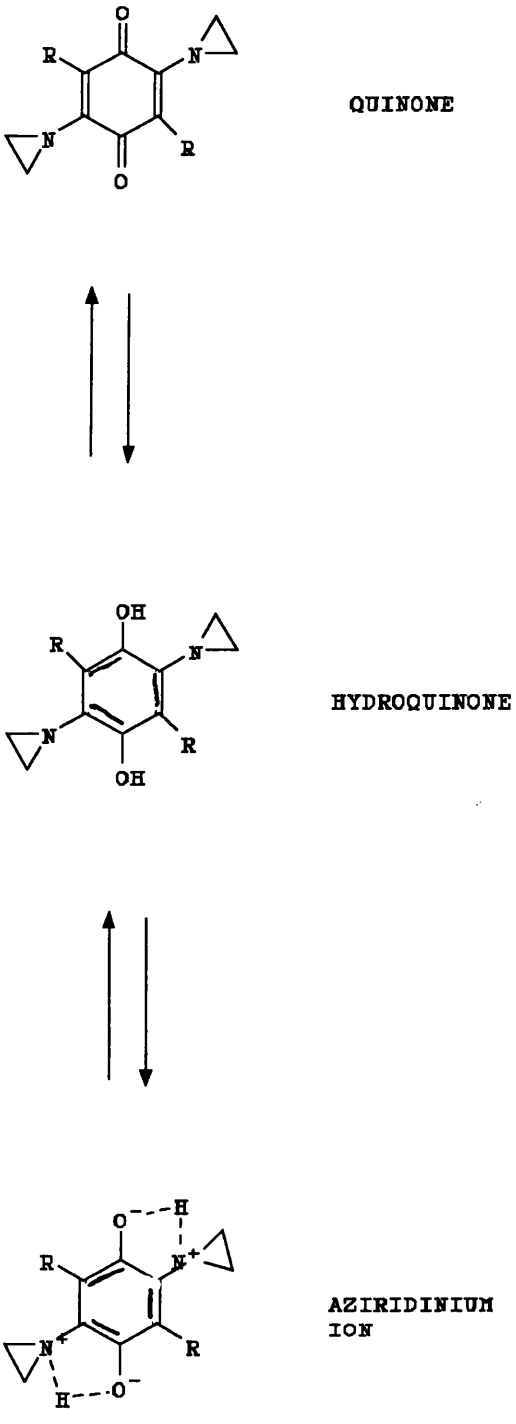

Fig. 1.7 Proposed mechanism for the protonation and activation of the aziridine rings of diaziquone (Gutierrez et al 1986).

1.7 ADP-ribosylation

The ADP-ribosylation of proteins is a form of post-translational modification in which NAD^+ is consumed as a source of ADP-ribose [Ueda and Hayaishi, 1985]. The process involves the hydrolysis of the NAD^+ molecule at the β-N-glycosidic linkage releasing the ADP-ribose moiety and nicotinamide. Two forms of ADP-ribosylation have been identified: mono(ADP-ribosyl)ation involves the attachment one ADP-ribosyl moiety to protein via a N-glycosidic bond, while poly(ADP-ribosyl)ation involves the attachment of multiple moieties via an O-glycosidic linkage (Fig. 1.8) [Hayaishi and Ueda, 1977]. The N-glycosidic linkage of mono(ADP-ribosyl)ation is resistant to neutral NH_2OH treatment while poly(ADP-ribose) is cleaved, this difference is exploited when determining the relative amount of ribosylation of a protein [Hiltz et al, 1982].

The predominant site for mono(ADP-ribosyl)ation is the mitochondria where the reaction is mediated by either NAD^+-glycohydrolase or ADP-ribosyltransferase [Moser et al, 1983; Richter et al, 1983]. In the mitochondria mono(ADP-ribosyl)ation is thought to play a critical role in the release of Ca^{2+} [Richter and Frei, 1985]. In contrast, the vast majority of the poly(ADP-ribosyl)ation take place in the nucleus, where the ribosylation of nuclear proteins plays a critical role in DNA repair, in the control of the cell cycle and in cellular differentiation [Ueda and Hayaishi, 1985; Shall, 1989]. The polymerization reaction is catalyzesd by poly(ADP-ribose)polymerase which is found in virtually all eukaryotic cells [Ueda and Hayaishi, 1985].

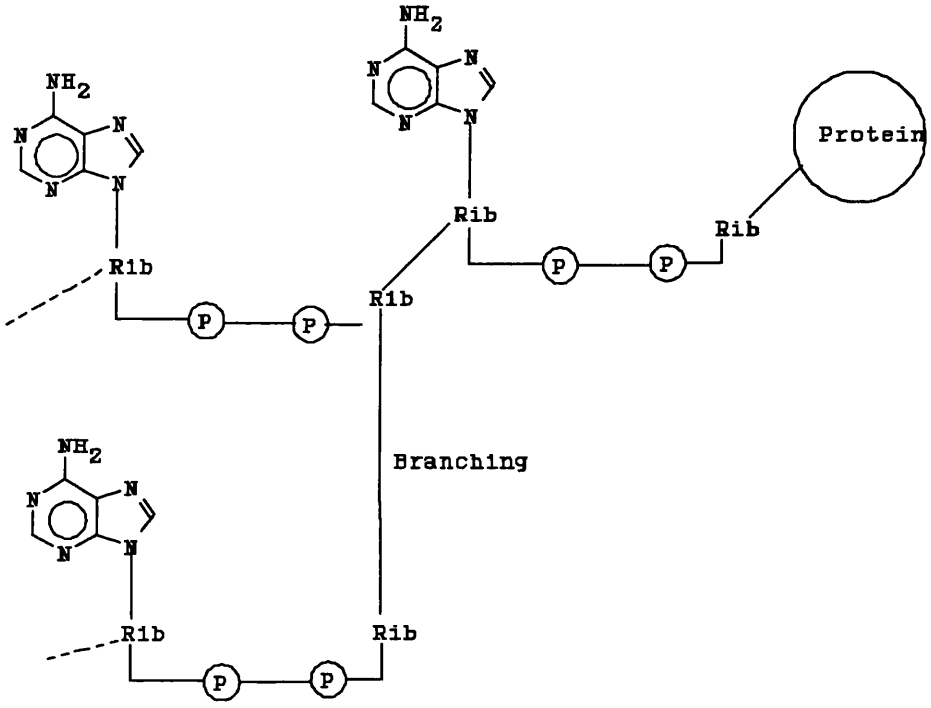

Fig. 1.8 Structure of protein bound Poly(ADP-ribose).

1.7.1 Poly(ADP-ribose)polymerase

Under normal physiological conditions mono(ADP-ribosyl)ation predominates over poly(ADP-ribosyl)ation (> 10 fold) [Ueda and Hayaishi, 1985]. However, evidence from a number of studies strongly suggests that during oxidative stress, the activation of poly(ADP-ribose)polymerase is primarily responsible for the consumption of NAD^+ [Berger, 1985; Schraufstatter et al, 1986b].

Poly(ADP-ribose)polymerase has been purified from various animal tissues. The results from a number of purification studies reveal a molecular weight range of the enzyme estimated between 112,000 and 135,000 using gel electrophoresis [Althaus and Richter, 1987]. Further analysis reveals a simple globular protein with a 30% alpha-helical conformation [Ito et al, 1979]. The enzyme consists of three functional domains: a substrate binding moiety; a DNA binding domain and an automodification site [Kameshita et al, 1984]. Four reactions have been attributed to the activity of poly(ADP-ribose)polymerase: (i) the attachment of the ADP-ribosyl moiety of NAD^+ to the acceptor protein; (ii) the elongation of the protein-bound ADP-ribosyl residues to form a polymer; (iii) the addition of ADP-ribose residues which branch away from the linear polymer; (iv) abortive NADase activity [Kawaichi et al, 1980; Kawaichi et al, 1981; Bauer et al, 1986]. The activity of poly(ADP-ribose)polymerase is almost completely dependent on DNA and is stimulated by Mg^{2+} and polycations such as histones and polyamines [Kawamura et al 1981]. Although the enzyme binds single-stranded DNA effectively the polymerase remains inactive [Ogushi et al, 1980]. Conversely, enzyme activity has been observed with short double stranded fragments of DNA, with a minimum length of only 8 to 10 base pairs necessary for activity

[Ueda and Hayaishi, 1985; Berger and Pertzold, 1985]. Free strand ends of DNA are also important in activating the enzyme, hence covalently closed-circular plasmid DNA is an ineffective activator unless the DNA is first linearized by endonuclease treatment [Berger and Pertzold, 1985; Benjamin and Gill, 1980]. Binding of the enzyme to DNA is also thought to alter its Km for NAD^+ [Niedergang et al, 1979].

Histones appear to play a dual role in the activity of poly(ADP-ribose)polymerase. They not only stimulate enzyme activity, but also act as acceptors of ribosylation [Berger and Pertzold, 1985; Okayama et al, 1977; Yoshihara et al, 1977]. Similarly poly(ADP-ribose)polymerase is a primary acceptor of the ADP-ribosyl polymer, automodification affects the activity of the enzyme resulting in an increase in its Km for NAD^+ and a lowering of the V_{max} [Kawaichi et al, 1981]. The extent of automodification is dependent on the presence of Mg^{2+}, in the absence of Mg^{2+} exogenously added acceptor proteins become modified [Tanaka et al, 1979; Tanaka et al, 1985]. Although poly(ADP-ribosyl)ation is stimulated by Mg^{2+}, other metal ions such as Cu^{2+}, Zn^{2+}, and Cd^{2+} inhibit the reaction [Ito et al, 1979].

1.7.2 DNA Repair and Poly(ADP-ribose)polymerase

The DNA repair systems are extraordinarily diverse and effective, it has been calculated that there is a 50% chance of bacterial genes remaining unaltered after 100 million duplications. Perhaps the predominant DNA repair mechanism is excision repair [Shall, 1989]. Basically the removal of defective or unnatural bases is achieved by cleaving the base-sugar bond or by making an endonucleolytic incision on the 5'side of the lesion then excising the lesion by endonuclease cleavage. Finally the lesion is patched by replication and ligation (Fig. 1.9)[Hanawalt et al, 1983]. There

is overwhelming evidence that poly(ADP-ribose)polymerase is necessary for efficient DNA excision repair [Durkacz et al, 1980]. Agents which cause DNA damage also cause a decrease in the level of pyridine nucleotide NAD^+, while inhibitors of poly(ADP-ribose)polymerase inhibit excision repair [Shall, 1989]. The available evidence suggests that ADP-ribosylation regulates the ligation stage of DNA repair as poly(ADP-ribose)polymerase inhibitors do not inhibit incision or the removal of defective bases [Creissen and Shall, 1982].

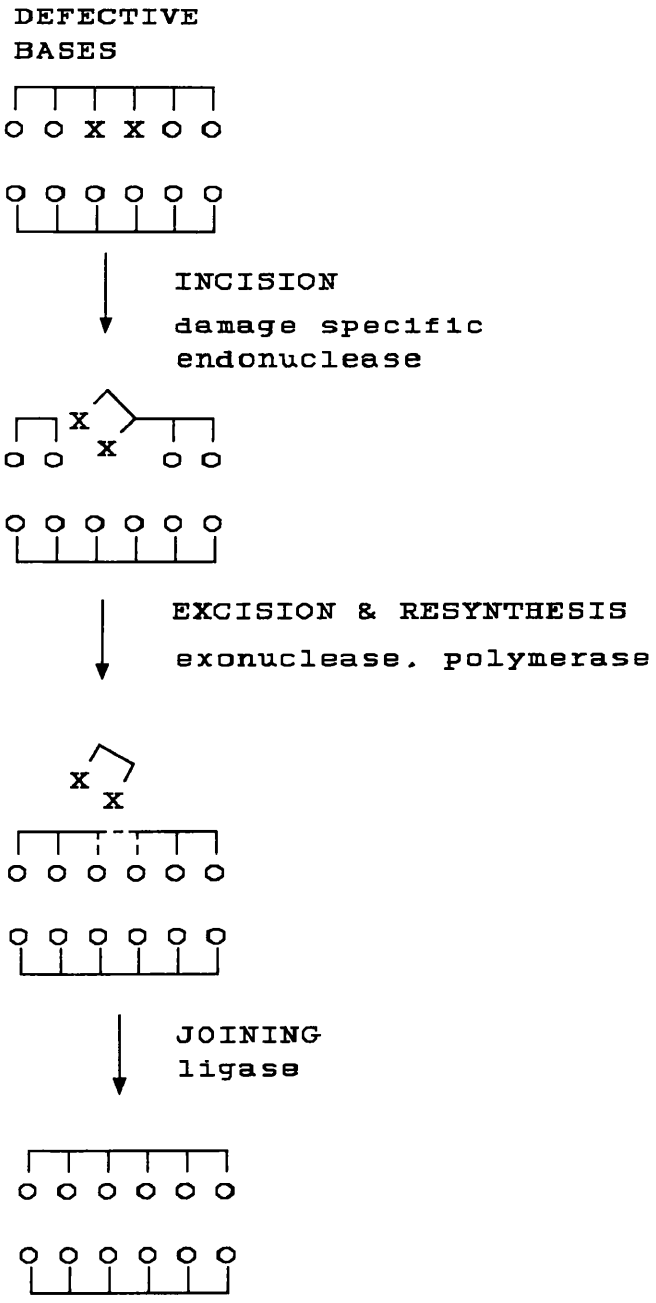

Fig. 1.9 Scheme for DNA excision-repair..

There is also widespread evidence suggesting that inhibitors do not block DNA repair synthesis and that under certain circumstances repair synthesis is stimulated by inhibitors [James and Lehmann, 1982].

Following DNA damage there is an increase in the activity of DNA ligase II, the activation of this enzyme is prevented by poly(ADP-ribose)polymerase inhibitors, while the activity of DNA ligase I is unaffected by DNA damage [Creissen and Shall, 1982]. The exact mechanism of activation of the ligase remains unclear, it has been suggested that DNA ligase II is attached to a controlling regulatory peptide which dissociates on ribosylation leaving the catalytic subunit activated. Alternatively the ligase activity may be effected by modulating the binding of the enzyme at sites to be rejoined. Additionally, ADP-ribosylation may alter the chromatin structure, thus aiding DNA repair [Shall, 1989].

1.7.3 Additional roles of Poly(ADP-ribose)polymerase.

In addition to its role in DNA repair, poly(ADP-ribosyl)ation also plays a important role in sister chromatid exchange [Ueda and Hayaishi, 1985]. The polymerase is thought to be involved in the ligation of strand breaks broken during the exchange. Additionally during cell differentiation there is a 3 fold increase in the activity of poly(ADP-ribose)polymerase [Althaus and Richter 1987]. Thus poly(ADP-ribose)polymerase inhibitors are able to prolong sister chromatid exchange, prevent differentiation and cause cell cycle arrest at the G2 phase [Kidwell et al, 1882].

1.7.4 Poly(ADP-ribose)polymerase Inhibitors

In recent years, a number of inhibitors of poly(ADP-ribose)polymerase have been

identified. Most compounds were found to be structural analogues of either the nicotinamide or the adenine moiety [Purnell and Whish, 1980]. Studies with the analogues of the nicotinamide moiety noticed the importance of the carboxyamide group in position 2, 3 or 4 of the pyridine ring. Studies with benzamide suggested that the ring nitrogen was of less importance, hence nicotinamide and benzamide are potent inhibitors while nicotinic acid and benzoic acid show no inhibitor properties (Fig. 1.10) (Althaus and Richter, 1987). Studies with purine analogues show differing results, theophylline exhibits potent inhibitor properties while caffeine is a less effective inhibitor (Fig. 1.10) [Purnell and Whish, 1980; Althaus and Richter, 1987; Sims et al, 1982].

	Compound	% inhibition
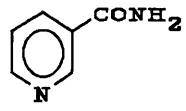	Nicotinamide	89
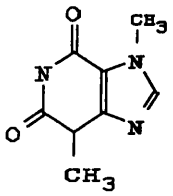	CAFFEINE	35
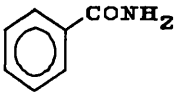	Benzamide	96
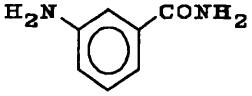	3-aminobenzamide	96
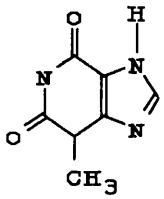	Theophylline	89
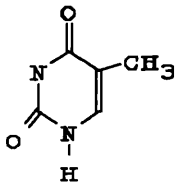	Thymine	75
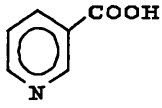	Nicotinic Acid	0
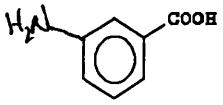	3-aminobenzoic acid	0

Fig. 1.10 Examples of poly(ADP-ribose)polymerase inhibitors

1.8 Mechanisms of Cell Death During Oxidative Stress

Following a toxic insult, cell death is usually preceded by a number of morphological and biochemical changes. Two morphologically distinct patterns of cell death have been recognized: apoptosis and necrosis, while a number of biochemical changes have been associated with the loss of membrane integrity [Fawthrop et al, 1991; Boobis et al, 1989; Orrenius et al, 1989].

1.8.1 Necrosis and Apoptosis

Necrotic cell death usually occurs under pathological conditions. Cells undergoing necrosis are characterised by swelling before the eventual disruption of internal and external membranes. Prior to cell death there is blebbing of the plasma membrane. Cells may undergo a reversible pre-necrotic phase in which the endoplasmic reticulum becomes dilated and some mitochondrial swelling may occur. Irreversible necrotic change occurs when there is abrupt swelling and disruption of the mitochondrial structure [Boobis et al, 1989; Orrenius et al, 1989; Wyllie, 1980].

In contrast, apoptosis or programmed cell death is a process in which cell killing occurs in a controlled manner such as in the resorption of the tadpole tail, the regression of certain tumours and in thymocytes exposed to glucocorticoids [Wyllie and Morris, 1982]. Additionally apoptosis is observed in the mechanism of cell killing of certain chemical toxins such as tributyltin and 2,3,7,8-trtrachlorodibenzo-*p*-dioxin [McConkey et al 1989a; Aw et al, 1990]. In all these circumstances cell death is characterised by a series of morphologically similar changes usually beginning with widespread plasma membrane blebbing [Wyllie et al, 1984]. A cell undergoing

apoptosis usually rounds up and severs contacts with the adjoining cells, their chromatin undergoes condensation and fragmentation into oligonucleosome length fragments [Fawthrop et al, 1991; Boobis et al, 1989; Wyllie et al, 1984].

1.8.2 Intracellular Calcium.

A perturbation of intracellular Ca^{2+} homeostasis is observed in cells prior to both necrosis and apoptosis and is thought to be involved the mechanism of cell killing of both processes [Fawthrop et al, 1991]. The fragmentation of DNA into oligonucleotide-length fragments characteristic of apoptotic cells has been demonstrated to result from the activation of a Ca^{2+} dependent endonuclease. Furthermore the chelation of cytostolic free Ca^{2+} with quin-2 not only prevents activation of the endonuclease but also cell death [McConkey et al, 1989b]. Elevated intracellular Ca^{2+} may result in the activation of a number of degradative enzymes. Calcium-activated phospholipases and proteases have been implicated in the degradation of membrane phospholipids and cytoskeletal proteins respectively [Chien et al, 1979; Mellgren, 1987; Mirabelli et al, 1989]. Increased cytosolic Ca^{2+} is also known to cause the dissociation of actin microfilaments from α-actinin which serves as intermediates in the association of microfilaments with actin-binding proteins in the plasma membrane [Mirabelli, 1988].

1.8.3 Reactive Metabolites and Protein-thiol Modification

A number of chemicals which cause lethal cell injury are chemically reactive electrophilic species. The nucleophilic centres in protein sulphydryl groups are most susceptible to electrophilic attack [Fawthrop et al, 1991]. Many compounds are

cytotoxic through the formation of reactive intermediates which may affect the cellular levels of glutathione and protein thiols, either through oxidation or adduct formation. There is an excellent correlation between the covalent binding of certain electrophilic species and tissue necrosis [Gillette, 1974]. Modification of the sulphydryl groups of certain enzymes may result in their inactivation [Tee et al, 1986]. A number of toxicants including menadione and *tert*-butyl hydroperoxide are thought to modify the thiol-groups in Ca^{2+}-transporting ATPases resulting in increased intracellular calcium [Moore et al, 1985].

1.8.4 Lipid Peroxidation

Several toxins are first metabolised to electrophilic free radicals before they cause lethal cell injury [Boobis et al, 1989]. It has been suggested that free radicals initiate peroxidative damage to membrane lipids by interacting with polyunsaturated fatty acids to form lipid radicals. These react with unsaturated fatty acids to form lipid hydroperoxides and further peroxy radicals in a cascade which consumes the membrane lipids and increases membrane permeability and resulting in cell death [Kappus, 1987; Streeter et al, 1984].

1.8.5 Depletion of Pyridine Nucleotides and ATP

The redox status of mitochondrial pyridine nucleotides plays an important role in Ca^{2+} homeostasis [Fawthrop et al, 1991]. Compounds such as menadione, carbon tetrachloride and benzoquinone are known to oxidize or arylate critical thiol groups in mitochondrial NAD(P)H dehydrogenases and increase NAD(P)H oxidation [Canbonera and Azzone, 1988]. The inability to re-reduce $NADP^+$ together with a

decrease in the NAD(P)H/NAD(P) ratio favours the release of calcium from the mitochondria, the uncoupling of oxidative phosphorylation and ATP depletion [Fawthrop et al 1991]. The depletion of ATP will lead to the impairment of other calcium-regulating systems in the endoplasmic reticulum and plasma membrane [Moore et al 1985].

The depletion of pyridine nucleotides and ATP is also observed in cells which suffer DNA damage. This activates poly(ADP-ribose)polymerase which consumes NAD^+ during DNA excision repair. The permanent depletion of NAD^+ and ATP following extensive DNA damage has been proposed as a suicide mechanism to prevent the perpetuation of damaged DNA [Gaal et al, 1987].

1.8.6 DNA Damage During Oxidative Stress

Aerobic organisms constantly produce reactive oxygen species including the superoxide radical, hydrogen peroxide and hydroxyl radical [Freidovich, 1983]. Similarly, exposure to ionizing radiation leads to homolytic fission of oxygen-hydrogen bonds in water to produce the hydroxyl radical [Von Sonntag, 1987]. Oxidative stress results when the generation of these reactive oxygen species overwhelms the cells antioxidant defences. Cells subjected to oxidative stress may suffer severe metabolic dysfunction including peroxidation of membrane lipids, increased intracellular calcium, decreased pyridine nucleotides and DNA damage [Halliwell and Aruoma, 1991; Starke et al, 1986; Fawthrop et al 1991]. In particular single and double strand breaks in DNA have been observed in a wide range of mammalian cells during oxidative stress [Cantoni et al, 1986].

Neither H_2O_2 nor $O_2^{\cdot-}$ undergo any chemical reaction with DNA as measured by

strand breakage or by chemical changes in the deoxyribose, purines or pyrimidines [Lasko et al, 1980; Aruoma et al, 1989; Mello Fello and Meneghini, 1984]. It is envisaged that H_2O_2 which crosses biological membranes enters the nucleus and reacts with ions of iron or copper which are bound to DNA, thus generating the highly reactive hydroxyl radical in close proximity to the DNA [Halliwell and Aruoma, 1991]. Oxidative stress may also trigger a series of events which leads to the activation of certain nuclease enzymes. Increased intracellular calcium is thought to activate the Ca^{2+}-dependent endonuclease responsible for the fragmentation of DNA during apoptosis [Orrenius et al 1989].

Reactive oxygen species and in particular the hydroxyl radical can attack all components of DNA. The hydroxyl radical is capable of abstracting hydrogen from the deoxyribose giving rise to sugar radicals that can fragment in many ways (Fig 1.11) [Halliwell and Aruoma, 1991]. {*In the scheme shown in fig 1.11, [1] reacts with a second molecule of oxygen to produce a new radical species [2], which undergoes further reduction by Fe(11)n or other reducing agents to the hydroperoxy compound [3]. Cleavage of the (C-3)-(C4) bond would occur readily under neutral or slightly acidic conditions to give acyl hemiaminacetal [4]. Subsequent fragmentation of the phosphodiester bonds ultimately yields the base-propenal [7]; the 5'- and 3'-terminal groups on DNA become a free phosphate ester [6], and the phosphate ester of glycolic acid [8], respectively. Giloni et al, 1981*} . Reactions with the deoxyribose-derived radicals can also give rise to the release of purine and pyrimidine bases producing abasic sites and strand breaks as well as alkali labile sites [Von Sonntag, 1987].

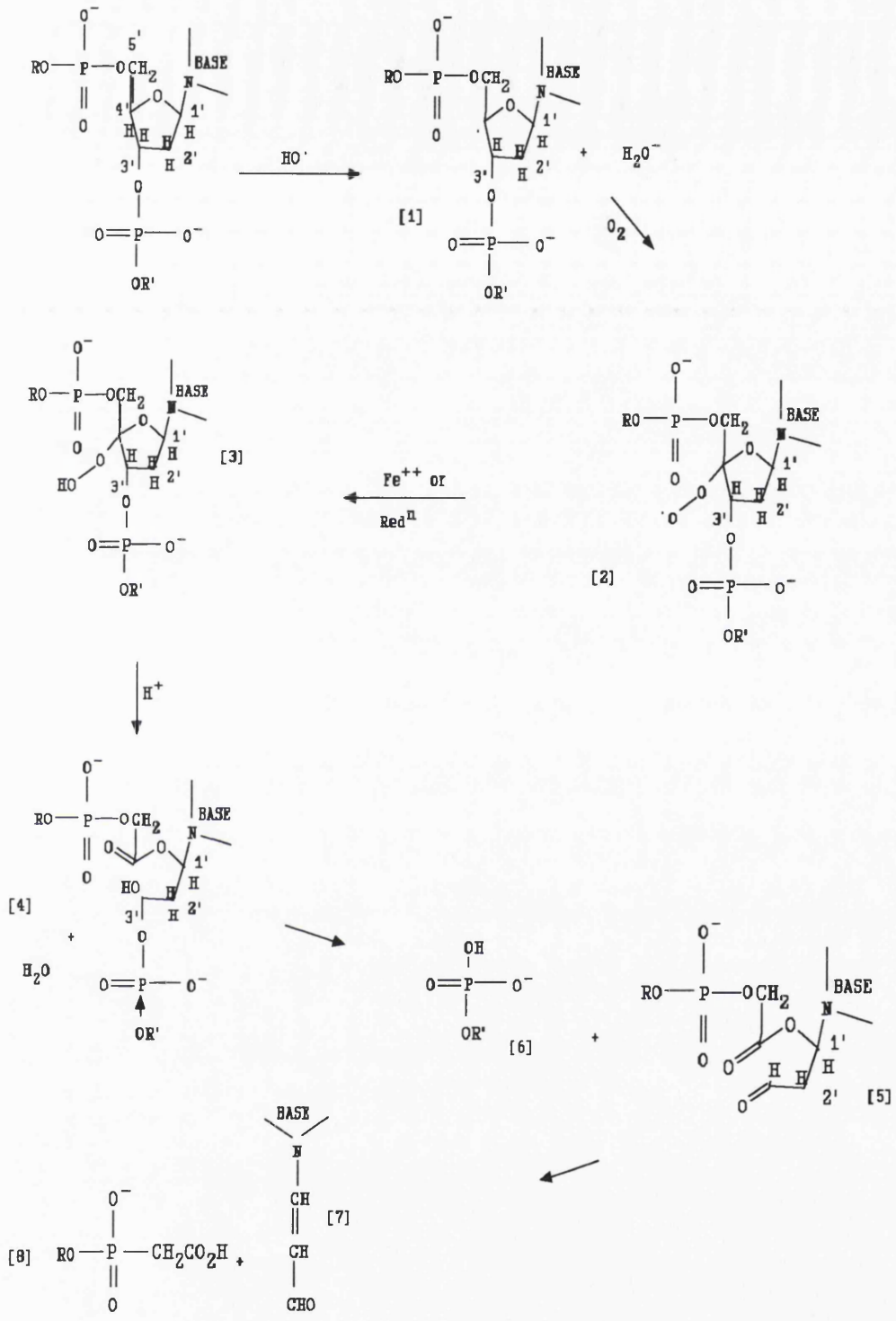

Fig. 1.11 Proposed reaction mechanism for the cleavage of deoxyribose by the hydroxyl radical (Section 1.8.6).

The hydroxyl radical may add to guanine at the C4,C5 and C8 positions. Addition at the C8 position results in a radical that can have several fates of which 8-hydroxyguanine is just one (Fig. 1.12). Similar additions to adenine are also possible. Pyrimidines are also attacked by the hydroxyl radical resulting in multiple products. Thymine can form *cis* and *trans* thymine glycols, while cytosine can form several products including cytosine glycols (Fig 1.12) [Halliwell and Aruoma, 1991; Steenken, 1898, Teoule, 1987]. The long term result of oxidant induced DNA lesions includes cross-links between DNA bases and between DNA bases and amino acids of nuclear proteins. Furthermore such lesions may ultimately lead to mutations.

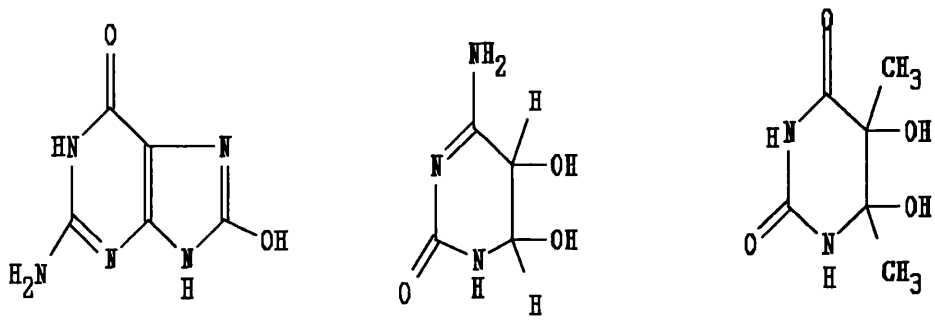

Fig. 1.12 Some of the end products that result from the attack of hydroxly radicals upon DNA bases.

CHAPTER 2

MATERIALS AND METHODS

2.1. The determination of pyridine nucleotides

2.1.1 Materials

NAD^+, $NADP^+$, NADH, NADPH, Phenazine ethanosulphate (PES), 3-(4,5-dimethylthiazol-2-yl)-2,5-diphenyltetrazolium bromide (MTT), glucose-6-phosphate, glucose-6-phosphate dehydrogenase, nicotinamide, EDTA, glycylglycine and alcohol dehydrogenase were obtained from Sigma chemical Co. (Poole, Dorset, U.K.). potassium hydroxide, ethanol, chloroform, ammonium phosphate, perchloric acid and dipotassium hydrogen orthophosphate were obtained from BDH Ltd (Poole, Dorset). HPLC grade methanol was obtained from Rathburns (Walkerburn, Borders, Scotland). Tributylamine was purchased from Aldrich Chemical Co. Ltd (Poole, Dorset).

2.1.2 Determination of NAD^+ and $NADP^+$.

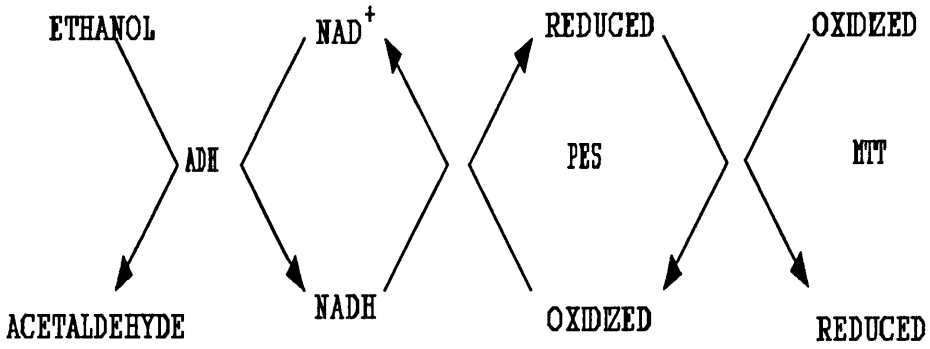

Fig. 2.1 Schematic representation of the recycling of NAD^+.
ADH; Alcohol dehydrogenase, PES; Phenazine ethanosulphate, MTT; 3-(4,5-dimethylthiazol-2-yl)-2,5-diphenyltetrazolium bromide.

2.1.3 Principle

The method used to determine NAD^+ and $NADP^+$ is based on the enzyme-linked recycling assay described by Bernofsky and Swan (1973). The enzyme-mediated reduction of $NAD(P)^+$ to NAD(P)H is linked to 3-(4,5-dimethylthiazol-2-yl)-2,5-diphenyltetrazolium bromide (MTT, thiazolyl blue) via phenazine ethosulphate (PES). NAD(P)H reduces PES which in turn reduces MTT (Fig. 2.1). Reduced MTT absorbs at 570 nm, therefore the rate of increase in absorbance at this wavelength is proportional to the amount of NAD^+ present. The amount of NAD^+ in an unknown can be compared to a series of standard concentrations.

2.1.4 Extraction of nucleotides and sample preparation

2.1.5 NAD^+ and $NADP^+$

The method exploits the fact that the reduced form of the pyridine nucleotides is destroyed by acidic conditions whilst the oxidized form may be stored in acid for up to 7 days without significant loss [Kalhorn et al 1985].

A 1.0 ml aliquot of cell suspension (10^6 cell/ml) was removed and placed in a plastic test tube (75x12mm) and centrifuged (Denley BR 401 refrigerated centrifuge) for 1 min at 300 rpm, the supernatant was then aspirated and the pellet resuspended in 1.0 ml ice-cold perchloric acid (PCA) 0.5M. The suspension was allowed to precipitate for 15 min on ice after which the sediment was removed by centrifugation at 2500 rpm for 10 min. A 0.8 ml sample of the supernatant was then transferred to a 1.5 ml plastic Eppendorf tube.

The standard nucleotide solutions were made by dissolving a known amount of the

nucleotide in PCA. The samples/standard were neutralized prior to assay by the addition of 0.1 ml dipotassium orthophosphate (0.1M) to 0.8 ml of the PCA (sample/standard) solution, pH was then adjusted to 7.2-7.6 by the addition of 230-260 µl KOH (3M). The salt precipitate was removed by centrifugation in an Eppendorf microcentrifuge (centrifuge 5413) and the supernatant used in the nucleotide assay.

2.1.6 NAD^+ assay

The assay was carried out on a Shimadzu MPS 200 recording spectrophotometer (from V.A. Howe and Co. Ltd, London,SW6 3EP) at room temperature. The NAD^+ assay mixture consisted of 1.6 mls 0.1M phosphate buffer (pH 7.6), 100 µl PES, 100 µl MTT, 15 µl ethanol and 300 µl sample/standard. The reaction was started with the addition of 20 µl alcohol dehydrogenase (1250U/ml) and thorough mixing of reactants. After a lag of 60 seconds the change in absorbance at 570 nm was determined for a further 60 seconds.

2.1.7 $NADP^+$ assay

The $NADP^+$ assay was essentially the same as the NAD^+ assay except that alcohol dehydrogenase/ethanol was replaced by glucose-6-phosphate dehydrogenase/glucose-6-phosphate. The assay mixture consisted of 1.3 ml glycylglycine buffer (0.1M gylcylglycine, 0.1M nicotinamide and 12.5 mM EDTA pH 7.4), 100 µl PES, 100 µl MTT, 100 µl glucose-6-phosphate and 500 µl sample/standard. The reaction was started by the addition of 20 µl glucose-6-phosphate dehydrogenase and thorough mixing of the reactants.

2.1.8 Extraction of NADH and NADPH

The extraction and determination of NAD(P)H was based on the method described by Kalhorn et al 1985. This method relies on the stability of NAD(P)H under alkali conditions. A 1.0 ml aliquot of cell suspension was placed in a glass tube and spun for 1 min at 300 rpm, the supernatant was then aspirated and the pellet resuspended in 2 mls of ice-cold ethanolic KOH (99% ethanol, 1% KOH). The contents were mixed and allowed to stand on ice for at least 15 min to allow complete precipitation. After precipitation the ethanol was removed by centrifugation at 2500 rpm for 5 min and aspiration (it is important to remove the ethanol completely). The pellet was then resuspended in 1.0 ml chloroform and thoroughly mixed to disperse the pellet in the solvent, after which 0.4 ml of KOH (0.01M) was added. The tube was further agitated to mix the two phases before separation by centrifugation (3500 rpm, 10 min). After centrifugation the upper phase was then removed and stored at -80°C before analysis. Recovery (> 90%) was determined by comparing the difference between the amount of the nucleotide recovered when 3 µM of standard nucleotide was added to an aliquot of cell suspension before and after the extraction stage.

2.1.9 Determination of NADH and NADPH

Both NADH and NADPH strongly absorb at 340 nm, this makes the analysis of either nucleotide in the presence of the other difficult. To overcome this problem, the nucleotides were first separated before quantification. Separation was achieved by reversed phase HPLC using a C18 column (Bechman Ltd) attached to a Beckman HPLC system (Beckman 110A pumps, a Beckman 421 system controller, Hitachi 100-10 spectrophotometer and an attex C-R1A integrator). The mobile phase consisted of

ammonium phosphate pH 6.0 (82%) , methanol (17.85-17.87%) and tributylamine (0.13-0.15%) (the changes in the proportion of methanol and tributylamine were necessary as the column became less efficient). Tributylamine is immiscible in aqueous solutions therefore in preparing the mobile phase it is important to first dissolve the tributylamine in the methanol before adding the ammonium phosphate.

The aqueous extract was loaded on the column via a 50 µl loop and the eluent monitored at 340 nm at a flow rate of 0.8-1.0 ml/min. Retention times varied between 5-7 min and 8-10 min for NADH and NADPH respectively (depending on the exact proportion of methanol and tributylamine), while interference from unknown peaks was minimal.

2.2. Determination of reduced glutathione

2.2.1 Materials

GSH, o-phthaldialdehyde and EDTA were purchased from Sigma Chemical Co. Ltd (Poole, Dorset, U.K.). Potassium dihydrogen phosphate (KH_2PO_4) was obtained from BDH Ltd (Poole, Dorset, U.K.).

2.2.2 Glutathione assay

The method employed to determine intracellular reduced glutathione (GSH) was based on the method of Hissin and Hilf (1976). The reaction product of GSH and o-phthaldialdehyde (o-PT) fluoresces at 350/420 nm (excitation/emission). The extraction of GSH was identical to the method used to extract the oxidized pyridine nucleotides. The reaction mixture consists of 2.775 ml KH_2PO_4 (0.1M), 75 µl sample/standard (in PCA). The reaction was started by the addition of 150 µl o-PT (1.0 mg/ml in

methanol) with vigorous mixing. The reactants were left in the dark at room temperature for 20 min before fluorescence was determined on a Perkin-Elmer 300 Fluorescence spectrophotometer. Samples were quantified by comparison with a series of standard GSH solutions (0-40 µM).

2.3. Determination of cellular protein

2.3.1 Materials

Bovine serum albumin (BSA) was obtained from Sigma Chemical Co. (Poole, Dorset, U.K.), Copper sulphate ($CuSO_4$), sodium carbonate ($NaCO_3$), sodium potassium tartrate (NaKtartrate) and Folin & Ciocalteau's reagent was purchased from BDH Ltd (Poole, Dorset, U.K.)

2.3.2 Solutions

Solution A : 2% $NaCO_3$

Solution B : 1% $CuSO_4$

Solution C : 2% NaKTartrate

Solution D : 50% solution B (v/v) + 50% solution C (v/v)

Solution E : 98% solution A (v/v) + 2% solution D (v/v)

Solution F : 50% Folin reagent (v/v) + 50% distilled water (v/v)

2.3.3 Sample preparation

Cellular protein was determined by the method of Lowry et al (1951). A 1.0 ml aliquot of cell suspension (10^6 cell/ml) was removed and placed in a plastic test tube

and centrifuged for 1 min at 300 rpm, the supernatant was then aspirated and the pellet resuspended in 1.0 ml ice-cold perchloric acid (PCA) 0.5M. The suspension was then allowed to precipitate for 15 min on ice after which the sediment was removed by centrifugation at 2500 rpm for 10 min. The pellet was then washed once with ice-cold PCA (0.5M), resuspended in 0.8 ml of NaOH (1M) and left overnight to digest. Prior to the assay a 1 : 40 dilution of the digested protein was made.

The protein content of the sample was determined by reference to a series of standards prepared from BSA in NaOH (0.5M). Once prepared the stock BSA can be stored for up to 6 weeks. The BSA standard curve was constructed from 0, 24, 48, 72, 96 and 120 µg/ml protein.

2.3.4 Protein assay

The success of this assay depends on the time the reagents are added and the thorough mixing of the reactants. A 0.5 ml aliquot of sample or standard was added to a glass test tube and to this 5 ml of solution E was added with mixing. The solution was then left at room temperature for 10 min after which 0.5 ml of solution F was added immediately followed by a 2 second vortex. The reactants were then allowed to stand for 30 min at room temperature before absorbance was determined at 750 nm.

2.4. The determination of intracellular ATP

This method relies on the detection of bioluminescence produced by the luciferase extract of firefly tails in the presence of ATP [Lemasters and Hackenbrock 1978; Strehler 1968; Stanley and Williams 1969].

The reaction;

Luciferase (E) + Luciferin (LH_2) + ATP ----> $E.LH_2AMP$ + PPi

$E.LH_2AMP$ + O_2 -----> E + CO_2 + oxyluciferin + light

Since the amount of light produced is proportional to the amount of ATP present, a photon detection system can be calibrated for the estimation of ATP levels in samples of tissue and cells.

2.4.1 Materials

ATP and firefly lantern extract were purchased from Sigma chemical Co. (Poole, Dorset, U.K.). Perchloric acid, potassium dihydrogen orthophosphate (KH_2PO_4), magnesium sulphate heptahydrate ($MgSO_4.7H_2O$) and disodium arsenate heptahydrate ($Na_2AsO_4.7H_2O$) were purchased from BDH Ltd (Poole, Dorset, U,K.).

2.4.2 Sample and standard preparation

A 1.0 ml aliquot of cell suspension (10^6 cell/ml) was removed and placed in a plastic test tube and centrifuged for 1 min at 300 rpm, the supernatant was then aspirated and the pellet resuspended in 1.0 ml ice-cold perchloric acid (PCA) 0.5M. The suspension was allowed to precipitate for 15 min on ice after which the sediment was removed by centrifugation at 2500 rpm for 10 min. A 100 µl aliquot was then removed and stored at -80°C prior to analysis. The normal level of ATP in rat hepatocytes is 20-30 nmol/10^6 cells, as 10^6 cells were extracted in 1.0 ml the concentration range of the standard curve was 0-40 µM ATP in 0.5M PCA.

2.4.3 ATP assay

The assay was performed in plastic test tubes to prevent variation in luminescence due to differing internal diameter of glass test tubes. The assay mixture contained 2.0 ml of $MgSO_4$ buffer (80 mM $MgSO_4.7H_2O$, 10 mM KH_2PO_4 and 100 mM $Na_2AsO_4.7H_2O$ adjusted to pH 7.4.) and 10 µl sample or standard. The reaction was started by the addition of the lantern extract followed by a 2 second vortex. The firefly lantern extract was provided as a powder with its buffer. On the day of the assay it was prepared by resuspension in distilled water and the sediment removed by centrifugation at 1000 rpm for 5 min at 0°C. Bioluminescence was measured 15 seconds after the start of the reaction on a Thorn EMI detector linked to a Amstrad PC1512 computer.

2.5. Preparation of isolated rat hepatocytes

2.5.1 Materials

Collagenase Type 1V, EGTA, Bovine serum albumin, HEPES, Haematocytometer and trypan blue were all purchased from Sigma Chemical Co. (Poole, Dorset, U.K.). All other chemicals were purchased from BDH Ltd, (Poole, Dorset, U.K.).

2.5.2 Buffers

Hank I

NaCl 137 mM, KCl 5.4 mM, $MgSO_4$ 0.81 mM, $NaHPO_4$ 0.34 mM, KH_2PO_4 0.44 mM, HEPES 12.6 mM, BSA 0.67% (w/v) $NaHCO_3$ 25 mM and EGTA 0.5 mM at pH 7.4.

Hank II

Hank II is essentially the same Hank 1 minus BSA and EGTA but with Collagenase 0.025% (w/v).

Krebs Henseleit buffer (KH):

NaCl 119.2 mM, KCl 4.8 mM, KH_2PO_4 1.2 mM, $MgSO_4$ 1.2 mM, $CaCl_2$ 3.6 mM, $NaHCO_3$ 25 mM and HEPES 12.6 mM at pH 7.4.

Krebs Henseleit + Albumin

Krebs Henseleit buffer + 1% BSA (w/v) at pH7.4.

Both Hanks and KH buffers were made up and stored as concentrated solutions.

Hanks was made up as a 10x concentrated solution and diluted on the day of isolation after which the $NaHCO_3$ and HEPES, were added. The buffer was then gassed for 10 min with Carbogen after which the BSA, EGTA or $CaCl_2$ were added before the pH was set at 7.4.

KH was made as a 2x concentrated solution in which all the constituents are added minus $NaHCO_3$. This solution was gassed with Carbogen for 10 min after which the

$NaHCO_3$ is added and stored until use.

The working solution consist of a 1:1 dilution of stock KH in distilled water after which the HEPES (and BSA) were added and pH set at 7.4.

2.5.3 Hepatocyte isolation

Hepatocytes were prepared from male Wistars rats weighing approximately 200-230g as previously described by Moldeus et al (1978). The rat was sedated with ether anaesthesia and placed on the operating table (ventral side up) and secured with clips. A plastic beaker containing ether-soaked tissue was placed over the animal's nose. The thoracic and abdominal fur was then wetted with 70% ethanol and the abdominal cavity opened with a longitudinal incision avoiding the diaphragm. Two further lateral incisions were made just below the liver. The viscera and lower lobes of the liver were displaced to the right to expose the hepatic portal vein and then two 15cm ligatures passed under the vein and tied using fine curved forceps. To facilitate cannulation a small incision was made in the hepatic portal vein just below the ligatures using sprung scissors (it is important that the point where the incision is made is not too close to the liver as this may result in a failure to perfuse some of the lobes). The canula was then inserted in the vein and the two ligatures tied. The hepatic vein and artery were then cut. This facilitates the perfusion of the liver and as blood is flushed out the liver appears blanched. At this point the diaphragm is cut to kill the animal. The perfusion flow rate was set at 1-2 drops/sec, the liver rapidly dissected out and placed in the perfusion apparatus.

Following successful cannulation the liver was first perfused for 5 minutes with Hank 1 buffer (during this time the collagenase (50 mg) was added to the Hank II buffer), to remove the blood and free calcium. After 5 minutes perfusion the Hank I buffer was replaced by Hank II buffer with collagenase. The collagenase perfusion lasts approximately 12 minutes. Digestion is complete when the texture of the liver becomes spongy. After digestion the liver is cut from the cannula and placed in a shallow beaker containing 50 ml of Krebs Henseleit plus albumin buffer. The hepatocytes were then teased out of the liver using round end forceps to break up the capsula whilst swirling the liver gently for 1-2 minutes. The cell suspension was filtered to remove debris and clumped cells using a nylon gauze (or tea strainer). Smaller cell debris was removed by centrifugation for 1 min at 250 rpm, the supernatant was removed by aspiration and the pellet was resuspended in Krebs Henseleit buffer. The hepatocytes were washed three times by resuspension in Krebs Henseleit buffer followed by centrifugation and aspiration of the supernatant. After the final wash the cells were resuspended in approximately 30 ml of Krebs Henseleit buffer.

2.6. Determination of cell number and viability

Cell number and viability were determined by trypan blue exclusion. A 50 µl aliquot of cell suspension was added to 450 µl of trypan blue solution (0.4%, w/v), a sample of this solution was then loaded on a haemocytometer (Sigma) and cell number determined as follows

a) $\frac{\text{live cells}}{\text{total cells}} \times 100 = \%$ viability

b) yield = total live cells

normal yield for a 200-230g Wistar was 200-300 x 10^6 cells.

After the determination of cell number the hepatocytes were diluted to 10^6 cells/ml in Krebs Henseleit buffer before treatment. Cells were normally incubated in round bottomed flasks at 37°C and continually gassed with 95% O_2/5%CO_2.

2.7. Determination of NAD^+ hydrolysis

Poly(ADP-ribose)polymerase hydrolyses NAD^+ to ADP-ribose and nicotinamide. By radiolabelling NAD^+ at the nicotinamide moiety, NAD^+ hydrolysis would result in the formation of radiolabelled nicotinamide.

2.7.1 Radiolabelling of intracellular NAD^+

The radiolabelling of intracellular NAD^+ was as described by [Richter et al, 1990; Purvis and Lowenstein, 1961], by injecting (intraperitoneal) a male wistar rat with (0.227 µmol) 12.5 µCi [carbonyl-^{14}C]-nicotinamide (Amersham International), the animal was returned to its cage and allowed food and water ad libitum. After 4-5 hours the animal was anaesthetized and the hepatocytes isolated as described above.

2.7.2 Sample preparation

The isolated hepatocytes were preincubated as described above before exposure to the appropriate compound. At the designated time points intracellular nucleotides (NAD^+,$NADP^+$ and nicotinamide) were extracted by removing and centrifuging a 1.0 ml aliquot of cell suspension (10^6 cells/ml) for 1 min at 300 rpm. The pellet was resuspended in 1.0 ml PCA (0.5M). After 10 min the sediment was removed by centrifugation at 2500 rpm for 10 min and the supernatant removed and stored at -80°C before assay. Prior to HPLC separation the sample was neutralized by adding 50 µl of KOH (3M) and 10 µl KH_2PO_4 (0.1M) to 200 µl sample. The precipitate was removed by centrifugation (Eppendorf centrifuge 5413) for 1 min and the supernatant removed and later injected on the HPLC column.

2.7.3 Separation of NAD^+, $NADP^+$ and nicotinamide by HLPC

The nucleotides were separated by ion-exchange HPLC using a partisil SAX ion-exchanger attached to a precolumn and both protected by a guard column (Millipore). The columns were linked to the System Gold HPLC system (Beckman Ltd.) connected to a Waters 484 u.v. detector (Waters, Millipore) set at 254 nm. The samples were injected via a 50 µl loop.

2.7.4 Mobile phase

Buffer A: 0.01M ammonium phosphate pH 4.9

Buffer B: 0.2M ammonium phosphate pH 4.8

2.7.5 HPLC separation

Before chromatography the column was washed for 30 min with buffer B. The following program was used to separate the nucleotides on the System Gold HPLC system.

1. Equilibrate for 60 min with 100% buffer A.
2. Inject 50 µl sample.
3. 0 min to 10 min 100% buffer A.
4. 10 min to 20 min 100% buffer B
5. 20 min to 45 min 100% buffer A
6. Return to step 2.

Samples were collected manually to ensure that each peak was represented by a single fraction. Fractions were stored at 4°C until radioactivity was determined.

2.7.6 Detection of radiolabelled NAD^+, $NADP^+$ and nicotinamide by liquid scintillation counting

The fraction volume varied according to peak size, therefore all fractions were made up to 2.0ml with mobile phase buffer. Fractions were the mixed with 4.0ml of scintillation fluid (Aquasol, Aquasol Ltd) and disintegrations per minute (dpm) determined on a Beckman scintillation counter. The peaks containing NAD^+, $NADP^+$ and nicotinamide were identified by injecting the unlabelled nucleotides and noting their retention times.

2.8. The determination of DNA strand breakage by alkaline elution

2.8.1 Principle

The technique of alkaline elution introduced by Kohn et al 1981, has been rapidly accepted as an exceptional technique for detecting DNA damage. The technique utilizes filters to discriminate DNA-single strand sizes in mammalian cells with sensitivity in the order of one lesion per 10^7 nucleotides. The filters mechanically impede the passage of long DNA strands whilst reducing mechanical fragmentation as the cells are deposited on the filter prior to lysis by a detergent. Following lysis the cell proteins and RNA are washed away leaving double stranded DNA on the filter. The protein bound to the filter can then be removed by exposure to enzymes. An alkaline solution can then be pumped through the filter and the rate of elution of the DNA, now single stranded is measured. Single strand breaks are measured on the basis of an increase in DNA elution rate when compared to untreated controls.

2.8.2 Apparatus

The filtration funnel consisted of a Swinnex type 25 mm polyethylene filter holder (Swinnex, Millipore) connected to a 50 ml polyethylene Luer-Lok syringe. The junction between the filter holder and the syringe was strengthened with epoxy cement. The orifice of the syringe was enlarged to 1/8 in by drilling as this facilitates the filling of the upper chamber of the filter holder. The filter holder was connected at the bottom to a 14 gauge stainless steel needle which was soldered into a metal sleeve which is inserted through a rubber stopper (Fig. 2.2).

A peristaltic pump (Gilson Multiplus) provides a slow non-pulsating outflow through the filter. The pump was connected to 0.89 mm (i.d.) solvent flexible manifold pump tubing and to the fraction collector by 0.86 mm (i.d.) polyethylene tubing.

2.8.3 Lysis buffer

The Sarcosyl-NaCl-EDTA lysis buffer consisted of 0.2% sodium dodecylsarcosine, 2.0M NaCl and 0.04M EDTA with pH adjusted to 10.0.

2.8.4 Phosphate-buffered saline (PBS)

Phosphate-buffered saline was purchased as tablets from Flow/ICN Ltd and consisted of 0.15M NaCl, 0.86M K_2HPO_4 and 0.014M KH_2PO_4.

2.8.5 Eluting Solution

The acid form of ethylenediaminetetraacetic acid (EDTA) (5.84g) was dissolved in 40 ml of tetraethyl ammonium hydroxide (Aldrich), this was made up to 1 litre with distilled water once the EDTA had dissolved and the pH adjusted to 12.1 with the tetraethyl ammonium hydroxide.

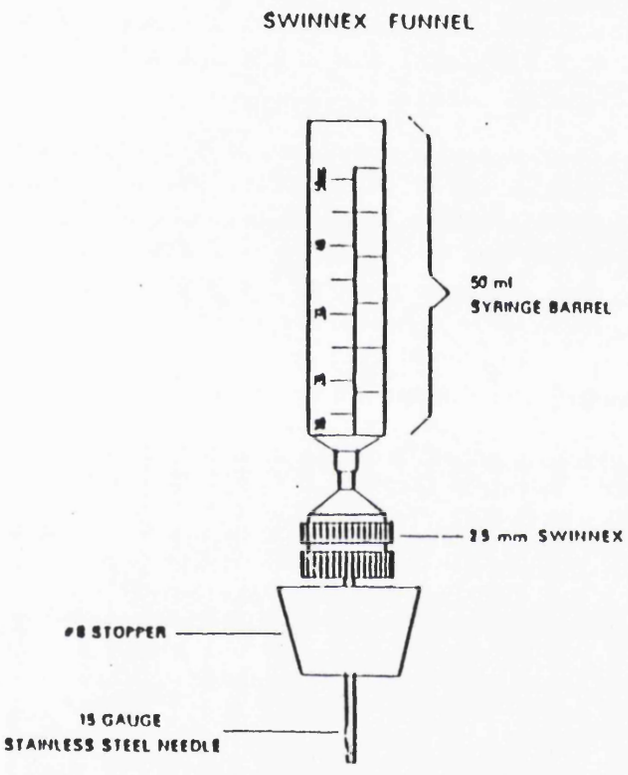

Fig. 2.2. Apparatus for Alkaline elution

2.8.6 Hoechst dye solution

A stock solution of Hoechst 33258 (Sigma Chemical Co.) was prepared in 10% saline. On the day of the assay the solution was diluted to 2.25 μM in distilled water.

2.8.7 Cell culture and Treatment.

Human myeloid leukaemia cells (K562) [Lozzio and Lozzio, 1975] were obtained from the Department of Oncology, University College and Middlesex School of Medicine. The cells were cultured in RPMI 1640 supplemented with 5% heat-inactivated foetal calf serum and L-glutamine (2mM) at 37°C. In order to determine damage to DNA, cells in exponential growth phase were labelled with 0.015 μCi/ml [^{14}C]-thymidine (Amersham International) for 20 hours. The cells were then incubated in the absence of radiolabel for 1 hour to chase all the radioactivity into high molecular weight DNA prior to treatment. Cells (10^6/ml) were then exposed to the quinones (in DMSO 0.1% v/v) and incubated for various times at 37°C. Aliquots (0.8 ml) of the cell suspension were removed and made up to 10 ml with ice-cold phosphate-buffered saline and immediately assayed for DNA damage as described below.

2.8.9 Alkaline Elution

Prior to loading the cells onto the filter, 5ml of PBS was added to the elution funnel. This was used to fill the upper chamber of the filter holder with a 1 ml Gilson pipette fitted with a plastic tip that passes through the orifice at the top of the chamber. The PBS was allowed to pass through the filter by gravity until the level was just above the neck of the filter holder. At this point the outlet of the filter holder

was blocked until the cell suspension was loaded on the filter.

Following treatment the diluted cell suspension was gently poured into the elution funnel, and the outlet at the base of the filter holder opened. The solution was allowed to drip through the filter by gravity. As soon as the flow stopped the chamber was filled with 7 ml of lysis buffer this was allowed to drip through the filter under gravity (protected from light) and collected in scintillation vials. Once the lysis buffer had passed through the filter, the funnel was attached to the pump and 2ml of lysis buffer containing 0.5mg/ml protinease K (Sigma Chemical Co.) was gently pipetted into the upper chamber of the filter holder then 40 ml of eluting buffer added. The filter holder and funnel were then protected from light and the peristaltic pump and fraction collector (LKB, ultrarac 2070) switched on. The pump was set at 2.0 ml/ hour and 3 hour fractions collected for 15 hours.

After 15 hours the pump and fraction collector were switched off and the excess elution buffer decanted. The pump was then set to five times its eluting rate and the buffer remaining in the filter holder chamber and line tubing were pumped into plastic test tubes. The filter was then removed and placed in a glass scintillation vial before determination of DNA. The filter holder and line tubing were washed by pumping 10 ml of eluting buffer at high speed through the system, a 2.5 ml aliquot of this solution was transferred to a scintillation vial for DNA determination.

2.8.10 Determination of DNA by liquid scintillation counting.

The filter was removed and placed in a glass vial to which 400 µl 1M HCL was added, the vial was sealed and placed in a oven for 1 hour at 60°C to depurinate the

DNA. After removing the vial from the oven, 2.5 ml of 0.4 M NaOH was added to the vial. The vial was resealed and left for one hour at room temperature where the NaOH converts the apurinic sites to strand breaks thus fragmentating the DNA. Before scintillation the elution fractions (approximately 6.0 ml) were transferred to scintillation vials and the 2.5 ml aliquot of wash solution was made up to 6.0 ml with eluting buffer. The fractions in the scintillation vials were then mixed with 10 ml of scintillation fluid (Aquasol containing 0.7% glacial acetic acid as this prevents chemiluminescence of the alkali solutions). Finally the radioactivity was determined.

2.8.11 Determination of DNA by Fluorimetry

The development of sensitive fluorimetric techniques for assaying DNA made alkaline elution quantifiable in cells such rat hepatocytes whose DNA cannot be radioactively labelled. The method employed here was as described by Stout and Becker (1982). The method relies on the enhanced fluorescence of Hoechst dye 33258 when bound to DNA. The lysis stage was similar to that described for the radiolabelled cells. This was followed by an additional wash stage in which 10 ml of buffer (lysis buffer minus the detergent) was gently pipetted into the filter holder and allowed to drip through the filter under gravity. The additional wash is required as the detergent interfers with the fluorimetric assay.

Before the assay, the DNA remaining on the filter was removed by placing the filter in a glass vial containing 6.0 ml of eluting buffer. This was placed in a oven for 1 hour at 70°C. The vial was then vigorously vortexed for 1 min and an aliquot assayed for DNA as follows. The assay components were added to a 5.0 ml plastic test tube in the following order, 0.25 ml KH_2PO_4 (17 mM) (to adjust the filtrate pH to 6.8-7.0),

3.0 ml of filtrate and 0.8 ml Hoechst 33258 (2.25 μM) in saline. Fluorescence was then determined on a Perkin Elmmer LS-2-B fluorometer at 360/450 nm excitation/emission.

2.9. Determination of DNA strand breakage by alkaline unwinding.

2.9.1 Principle

The method of fluorescence analysis of the rate of unwinding was first described by Birnboim and Jevcak (1981). When double stranded DNA is exposed to moderately alkaline solutions, hydrogen bonds are broken and the two strands unwind. Whereas small DNA molecules rapidly unwind, the very large DNA molecules of mammalian cells may require hours of exposure to alkali for complete unwinding. However the rate of unwinding may be increased by prior exposure to ionizing radiation and the increased rate could be used as a sensitive measure of the rate of DNA strand breaks. Previously, methods which measured the rate of DNA unwinding required a physical separation of the double and single strands of DNA, additionally radiolabelling was necessary to detect the small amount of DNA involved. This method uses a dye as a direct probe of DNA structure. The detection relies on the ability of the fluorescent dye, ethidium bromide, to bind selectively to double stranded DNA in the presence of single stranded DNA when short duplex regions in "single stranded" DNA molecule are destabilized by alkali. The method is applicable to crude mammalian cell extracts with little interference from RNA or other cell components.

The fluorescence contribution of other cell components is estimated from the blank sample (B) in which the cell extract is first lightly sonicated before treatment with the

alkali. This procedure will lead to the unwinding of low molecular weight DNA. A second sample is used to estimate total fluorescence (T). The difference (T-B) provides an estimate of the amount of double stranded DNA in the extract. A third sample (P) is used to estimate the rate of unwinding. The crude extract is then exposed to alkaline conditions such that only partial unwinding take place, where the degree of unwinding is related to the size of the DNA. The fluorescence of the sample less the fluorescence of the blank (P-B) provides an estimate of the amount of double stranded DNA remaining, expressed as percentage D by relationship:

$$\text{Percentage D} = (P-B) \div (T-B) \times 100$$

2.9.2 Fluorescence analysis of unwinding

An aliquot of cell suspension (K562 cells) 2.5 x 10^6 cells was washed once in HEPES buffer (0.14M NaCl, 6.7 mM KCl, 1.2 mM $CaCl_2$, and 2.4 mM HEPES, pH 7.4) and resuspended in 1.95 ml of buffer containing 0.25 mM mesoinositol, 10 mM sodium phosphate and 1.0 mM $MgCl_2$ (pH 7.2). The cells were then distributed in 200 µl aliquots into nine tubes (T. to measure total double stranded DNA; P. to measure double stranded DNA after unwinding; and B. to measure background fluorescence). To each tube was added 200 µl of a solution containing 9 M urea, 10 mM NaOH, 2.5 mM cyclohexanediaminetetraacetate and 0.5% Triton X-100. The cells were then placed on ice for 10 min to lyse and disrupt the chromatin. Immediately a 400 µl aliquot of a solution containing 1 M glucose and 14 mM mercaptoethanol was added to the tubes labelled T, to prevent any unwinding of the DNA. Then a solution containing 0.45 volumes of the urea solution in 0.55 volumes of 0.2M NaOH was added to each tube. The DNA was allowed to unwind for 30 min at 0°C, after which

the tubes containing the blank sample were sonicated for 3 sec to allow complete unwinding. The DNA was then allowed to unwind for a further 15 min at 15°C and unwinding was stopped by the addition of 400 µl of the glucose-mercaptoethanol solution and the tubes placed on ice. The amount of double stranded DNA remaining was assayed by the addition of ethidium bromide (6.7 µg/ ml final solution) and fluorescence measured (emission,590 nm: excitation, 520 nm). The assay was performed in reduced lighting. The ratio of double stranded fluorescence to background fluorescence was between 2.0 to 2.5.

2.10. Quantification of DNA fragmentation

The method used to quantify DNA fragmentation is partly based on that previously reported by McConkey et al 1988. At the appropriate times, cells (3 x 10^6) were resuspended in a lysis buffer containing Tris (5 mM), EDTA (20 mM) and 1% Triton X-100 (v/v), pH 8.0. The cell suspension was allowed to lyse for 30 min on ice before centrifugation (13,000g) for 40 min in an Eppendorf microcentrifuge (centrifuge 5413) to separate the intact chromatin (pellet) from DNA fragments (supernatant).

DNA was quantified by measuring the increased fluorescence induced by Hoechst 33258 when the dye is complexed with DNA [Stout and Becker, 1982]. DNA was calibrated by preparing a stock solution of calf thymus DNA (0.5 mg/ml) dissolved in NaCl (0.154 M), Na_3citrate (0.015 M) pH 7.0. A DNA standard curve (0-7µg/ml) was made by further dissolving the DNA stock solution in the lysate solution. The assay mixture contained 1.30ml sample/standard, 0.7ml KH_2PO_4 (17 mM) to adjust the pH to 6.8-7.0. and 0.75ml Hoechst 33258. Fluorescence was determined on a Perkin-

Elmer model LS-3 spectrophotometer at 450 nm during 360 nm excitation.

As it proved difficult to resuspend the chromatin pellet, DNA fragmentation was quantified by determining the amount of DNA in the supernatant as well as in the lysate solution prior to centrifugation (Total DNA). % DNA fragmentation was then quantified using the following formula:

$$\% \text{ DNA fragmentation} = \frac{\text{DNA in supernatant}}{\text{Total DNA}} \times 100$$

2.11. Determination of Growth inhibition.

K562 cells (10^6 cells/ml) were exposed to various concentrations of the quinones for 15 min after which they were resuspended in fresh medium and diluted to 10^5 cells/ml. The cells were then incubated for 72 hours at 37°C during which time cell number was determined at 24 hour intervals with a haemocytometer.

2.12. Statistical analysis

Results were generally expressed as mean ± SEM. Where appropriate statistical significance was tested by Student's *t*-test with the accepted significance level of $P < 0.05$.

CHAPTER 3

PYRIDINE NUCLEOTIDE CHANGES INDUCED BY BIS(AZIRIDINYL)BENZOQUINONES IN RAT HEPATOCYTES

Abstract- Quinone containing compounds may be toxic by a number of mechanisms, including oxidative stress caused by redox cycling, interaction with cellular thiols and arylation of DNA. Using rat hepatocytes, the cytotoxicity of three di-substituted 2,5-bis(1-aziridinyl)-1,4-benzoquinones (BABQ) was examined. These quinones differed in their ability to redox cycle and in their reaction with cellular GSH. High concentrations of 2,5-bis(1-aziridinyl)-1,4-benzoquinone (TW13) (arylates and redox cycles) and 2,5-bis(1-aziridinyl)-3-bromo-6-ethyl-1,4-benzoquinone (TW25) (arylates and redox cycles) caused a prolonged increase in the level of $NADP^+$ which was accompanied by extensive plasma membrane blebbing and preceded a loss of membrane integrity. In cells exposed to 2,5-bis(1-aziridinyl)-3-{ 2-(carbamoyloxy)-1-(methoxyethyl)}-1-6-methyl-1,4-benzoquinone (carboquone) which neither arylates or redox cycles the increase in $NADP^+$ was not accompanied by plasma membrane blebbing or the a loss of membrane integrity. The exposure of rat hepatocytes to either the BABQ or 2,3-dimethoxy-1,4-naphthoquinone (2,3-diOMe-1,4-NQ) resulted in an early depletion in the level of NAD^+. At non-toxic concentrations of 2,3-diOMe-1,4-NQ intracellular NAD^+ slowly recovered to control levels, while no recovery in the level of NAD^+ was observed in hepatocytes exposed to the BABQ. The changes in the pyridine nucleotides suggests two distinct modes of cell killing during 2,5-bis(1-aziridinyl)-1,4-benzoquinone-induced oxidative stress. Whereas acute cytotoxicity may result from the extensive oxidation of NADPH, the prolonged depletion of NAD^+ may result in a delayed cytotoxicity.

3.1. INTRODUCTION

The cytotoxicity of quinones as diverse as adriamycin, menadione and diaziquone (AZQ) has been attributed to their ability to bind directly to DNA [Dzielenziak et al, 1990; Tewey et al 1984], to cause oxidative stress by redox cycling [Kappus and Sies 1981] and to arylate intracellular thiols [Gant et al, 1988; Driebergen et al, 1986]. Quinone cytotoxicity has also been attributed to their ability to inhibit mitochondrial electron transport [Phelps and Crane, 1985].

Several reactions involving quinone containing compounds are either mediated by or alter the level of cellular pyridine nucleotides. The one electron reduction of quinones to the semiquinone is mediated by enzymes such as microsomal NADPH-cytochrome P-450 reductase, microsomal NADH-cytochrome b_5 reductase or mitochondrial NADH-ubiquinone oxidoreductase [Kappus and Sies, 1981; Kappus, 1986; Powis et al, 1981]. Where the semiquinone is auto-oxidized back to the parent quinone in a futile redox cycle, oxidative stress results from the disproportionate consumption of reducing equivalents (NAD(P)H, GSH) and the generation of active oxygen species ($O_2^{\cdot-}$, H_2O_2 and $OH^{\cdot}$) [Cohen and d'Arcy Docherty, 1987]. The two electron reduction of quinones to the hydroquinone is thought to be mediated by DT-diaphorase, a NADPH dependent enzyme [Lind et al, 1982]. In addition to the loss of pyridine nucleotides by a one or two electron reduction of quinones, NADPH loss may also result from the removal of H_2O_2 through the GSH peroxidase/GSSG reductase cycle [Kappus and Sies, 1981].

DNA damage results in the activation of poly(ADP-ribose)polymerase which consumes NAD^+ as a source of ADP-ribose [Schraufstatter et al, 1986b; Berger et al

1979]. Quinone containing compounds may cause DNA damage either by direct interaction with DNA or as a result of the generation of active oxygen species during redox cycling [Dorr et al 1985; Tewey et al 1984; Cantoni et al 1991; Coleman et al 1989]. Under circumstances where the DNA damage is rapidly repaired, there is a concurrent recovery in the NAD^+ level [Marks and Fox, 1991]. However where DNA repair is impaired or delayed, the prolonged depletion of intracellular NAD^+ may result in the depletion of cellular ATP and ultimately cell death, in a form of suicide response [Gaal et al, 1987]. In addition to their role as coenzymes, pyridine nucleotides play a significant role in other cellular activities, including the maintenance of cellular redox status and cellular energy level [Reed, 1986; Thurman and Kauffman 1980]. The oxidation and hydrolysis of NADPH has been associated with the release of calcium from intracellular stores [Frei et al, 1986]. The elevation of intracellular free calcium may cause cytotoxicity by a number of mechanisms including activation of proteases, phospholipases or endonucleases [Nicotera et al, 1986; Glende et al, 1986; Orrenius, 1985].

Aziridinylbenzoquinones such as AZQ are increasingly used in cancer chemotherapy [Gutierrez et al 1986; Silva and O'Brien 1989]. They are thought to be metabolized to their active moieties by bioreductive activation [Gutierrez, 1985]. The presence of two active groups, the quinone moiety and the alkylating aziridinyl groups, suggests that these compounds may exert their effects by more than one mechanism. In addition to the activation of the aziridinyl groups, cytotoxicity may be linked to the reduction of the quinone moiety or to their interaction with cellular thiols [Szmigiero et al, 1984; Lusthof et al, 1989; Lusthof et al, 1990].

This study investigates intracellular, ATP and pyridine nucleotide changes induced

by three 3,6-disubstituted 2,5-bis(1-aziridinyl)-1,4-benzoquinones (BABQ), with varying abilities to redox cycle and to interact with glutathione [Prins et al, 1989] (Fig. 3.1). The bromo-ethyl-substituted BABQ (TW 25) has previously been shown to rapidly deplete glutathione and is inactivated by glutathione substitution, while the non-substituted BABQ (TW 13) causes a slower depletion of glutathione (Prins et al 1989; Driebergen et al 1986). Both compounds are good redox cyclers. The third compound, carboquone is a cytostatic agent which does not react with glutathione and is a poor redox cycler. The pyridine nucleotide changes induced by two concentrations of the BABQ were compared to the changes induced by 2,3-dimethoxy-1,4-naphthoquinone (2,3-diOMe-1,4-NQ), a pure redox cycling quinone [Stubberfield and Cohen, 1989].

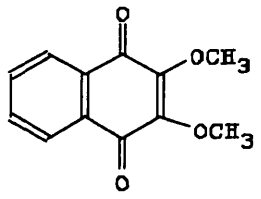

(a)

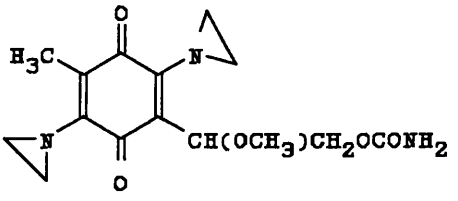

(b)

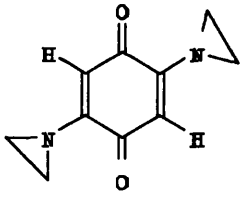

(c)

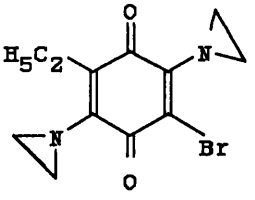

(d)

Fig. 3.1 Structural formulae of the quinones. a; 2-3,dimethoxy-1,4-naphthoquinone b; carboquone, c; TW13 and d; TW25.

3.2 Methods and Materials

3.2.1 Materials

Collagenase, HEPES, GSH, ATP, firefly lantern extract, thiazolyl blue, phenazine ethosulphate, alcohol dehydrogenase, glucose-6-phosphate, glucose-6-phosphate dehydrogenase and all nucleotides were purchased from Sigma Chemical Co Ltd (Poole, U.K.). Tributylamine was purchased from Aldrich Chemical Co. (Gillingham, U.K.). The BABQ were synthesised as previously described [Prins et al, 1989]. 2,3-Dimethoxy-1,4-naphthoquinone was synthesised as previously described [Stubberfield and Cohen, 1989]. All other chemicals were purchased from BDH Ltd (Poole, Dorset, U.K.)

3.2.2 Isolation and Incubation of Rat Hepatocytes.

Rat hepatocytes were prepared as previously described (chapter 2), by collagenase perfusion of the livers of adult male wistar rats (220-260g). The isolated cells (10^6 cell/ml) were suspended in Krebs Henseleit buffer containing 12.5 mM HEPES under an atmosphere of 95% O_2/5% CO_2 (pH 7.4) and were incubated in continuously rotating round bottom flasks at 37°C. Following isolation and prior to treatment the cells were preincubated at 37°C for 30 min. Cell viability was determined by trypan blue exclusion in a 0.4% solution and samples were prepared as previously described [Stubberfield and Cohen, 1988]. Protein was measured by the method of Lowry et al, (1951)

3.2.3 Determination of Pyridine Nucleotides ATP and GSH.

Oxidized pyridine nucleotides (NAD^+, $NADP^+$) were determined using the spectrophotometric recycling assay of Bernofsky and Swan, (1973) as previously described in chapter 2. Reduced pyridine nucleotides were first separated by HPLC on a C18 reverse-phase Bondapak column using isocratic gradient with 82% 0.2 mM ammonium phosphate pH 6.0/17.85% methanol/ 0.15% tributylamine as described previously in chapter 2. The eluent was monitored at 340 nm and the concentration determined by peak height. Intracellular ATP was determined using the luciferase-linked luminescence method as previously described by Stubberfield and Cohen, (1988). GSH was measured by the o-PT method described earlier.

3.2.5 Estimation of Plasma Membrane Blebbing.

The amount of plasma membrane blebbing was assessed by counting the cells using the following criteria.

Stage (1): Formation of a limited number of small blebs on the surface of some (< 50%) of the cells.

Stage (2): Numerous small blebs are formed and most cells (> 75%) are affected.

Stage (3): Growth and coalescence of blebs into larger blebs.

3.3. RESULTS

3.3.1 Effects of Quinones on Cellular Viability and Intracellular ATP

The two redox cycling BABQ (TW25 and TW13) caused a concentration dependent cytotoxicity to freshly isolated hepatocytes (Table 3.1). No cell death was observed in hepatocytes exposed for 180 min to carboquone (100-200 μM), TW13 (100 μM), TW25 (50 μM) or 2,3-diOMe-1,4-NQ (50 μM) (Table 3.1).

A small decrease in the level of ATP was observed in hepatocytes exposed to carboquone (100-200 μM), TW25 (50 μM) and 2,3-diOMe-1,4-NQ (50 μM). In cells exposed to TW25 (100 μM) the decrease in ATP accompanied the loss in membrane integrity (Table 3.1). In hepatocytes exposed to TW13 a significant decrease in ATP was observed at 100 and 200 μM. Whereas no cell death was observed in hepatocytes exposed to 100 μM, at 200 μM the loss of ATP preceded cell death by 60 min.

3.3.2 The Effect of the Quinones on Plasma Membrane Blebbing.

In hepatocytes exposed to high concentrations of TW25 (100 μM) and TW13 (200 μM), cytotoxicity was preceded by extensive plasma membrane blebbing (Fig. 3.2A and 3.2B). At lower concentrations of TW25 (50 μM) and TW13 (100 μM) only minor blebbing was observed (Fig. 3.2A and 3.2B). In cells exposed to carboquone (100-200 μM) and 2,3-diOMe-1,4-NQ (50 μM) no blebbing was observed.

3.3.3 Effects of the Quinones on Pyridine Nucleotide Changes.

Within 60 min of exposure to the quinones, intracellular NAD^+ decreased to approximately 1.0 nmol/mg (Fig. 3.3 and 3.4). Whereas a recovery to control NAD^+

levels was observed in hepatocytes exposed to 2,3-diOMe-1,4-NQ (50 μM) (Fig. 3.3A), no recovery was observed in the BABQ treated hepatocytes. In the hepatocytes exposed to the BABQ at concentrations where cell viability remained at the control level, the intracellular NAD^+ level was maintained just above 1.0 nmol/mg (Fig. 3.3 and 3.4). At toxic concentrations of TW25 intracellular NAD^+ remained below 1.0 nmol/mg from 30 min (Fig. 3.4A and 3.4B).

Although all the quinones induced a rapid increase in intracellular $NADP^+$ (Fig 3.5 and 3.6), the greatest elevation (> 1.5 nmol/mg) was observed in hepatocytes exposed to cytotoxic concentrations of the BABQ (Fig. 3.6A and 3.6B), the $NADP^+$ level remained elevated throughout the incubation. At non-toxic concentrations of TW13, TW25 and carboquone (100-200 μM), the magnitude of the $NADP^+$ elevation (> 0.5 < 1.25 nmol/mg) was less than that caused by the cytotoxic BABQ. In contrast to the BABQ, the early elevation in $NADP^+$ observed in hepatocytes exposed to 2,3-diOMe-1,4-NQ (50 μM) decreased to control levels by 90 min (Fig. 3.5A).

The quinones were less effective in altering the reduced pyridine nucleotides (NADH, NADPH) (Fig. 3.7 and 3.10). No change was observed in the NADH level except where the decrease coincided with the loss of membrane integrity (Fig 3.8A and 3.8B) (Table 3.1). In hepatocytes exposed to the redox cycling BABQ, there was a slight increase in NADPH within the first 30 min (Fig. 3.9 and 3.10), this was followed by a later decrease which matched the $NADP^+$ increase. In hepatocytes exposed to carboquone, a dose dependent decrease in NADPH was observed which reflected the increase in $NADP^+$, suggesting oxidation of NADPH (Fig. 3.9B). As observed in hepatocytes exposed to the redox cycling BABQ, and previously reported by Stubberfield and Cohen (1989) there was a slight early increase in NADPH in 2,3-

diOMe-1,4-NQ treated cells, which lasted until 60 min. By 90 min the NADPH level returned to the control value (Fig. 3.9A)

3.3.4 The Effect of the Quinones on Intracellular GSH

The BABQ caused a rapid depletion of GSH, although differences in the rate and extent were observed (Fig. 3.11 and 3.12). Whereas TW13 and Carboquone caused a gradual depletion of GSH over 60 min (Fig. 3.11 B and 3.12A), TW25 caused a rapid initial depletion (85% in 30 min) after which no further decrease was observed (Fig.3.12B).

TABLE 3.1. Effects of the BABQ on cellular ATP and Viability.

Compound	Concentration (μM)	ATP (nmol/mg)	% Viability
Control	-	20.7 ± 2.8	79 ± 4
2,3-diOMe-1,4-NQ	50	15.9 ± 3.2	72 ± 2
Carboquone	100	19.1 ± 4.1	74 ± 3
Carboquone	200	15.4 ± 4.0	72 ± 4
TW13	100	12.1 ± 3.0*	77 ± 2
TW13	200	1.6 ± 1.4**	22 ± 8*
TW25	50	16.8 ± 2.5	75 ± 5
TW25	100	8.0 ± 3.0*	53 ± 11*

ATP (nmoles/mg protein) and viability measurements were made after 180 min incubation as described in methods and materials. The values represent mean ± SEM from three separate incubations.

* significantly different from controls ($p < 0.05$).

** significantly different from controls ($p < 0.01$).

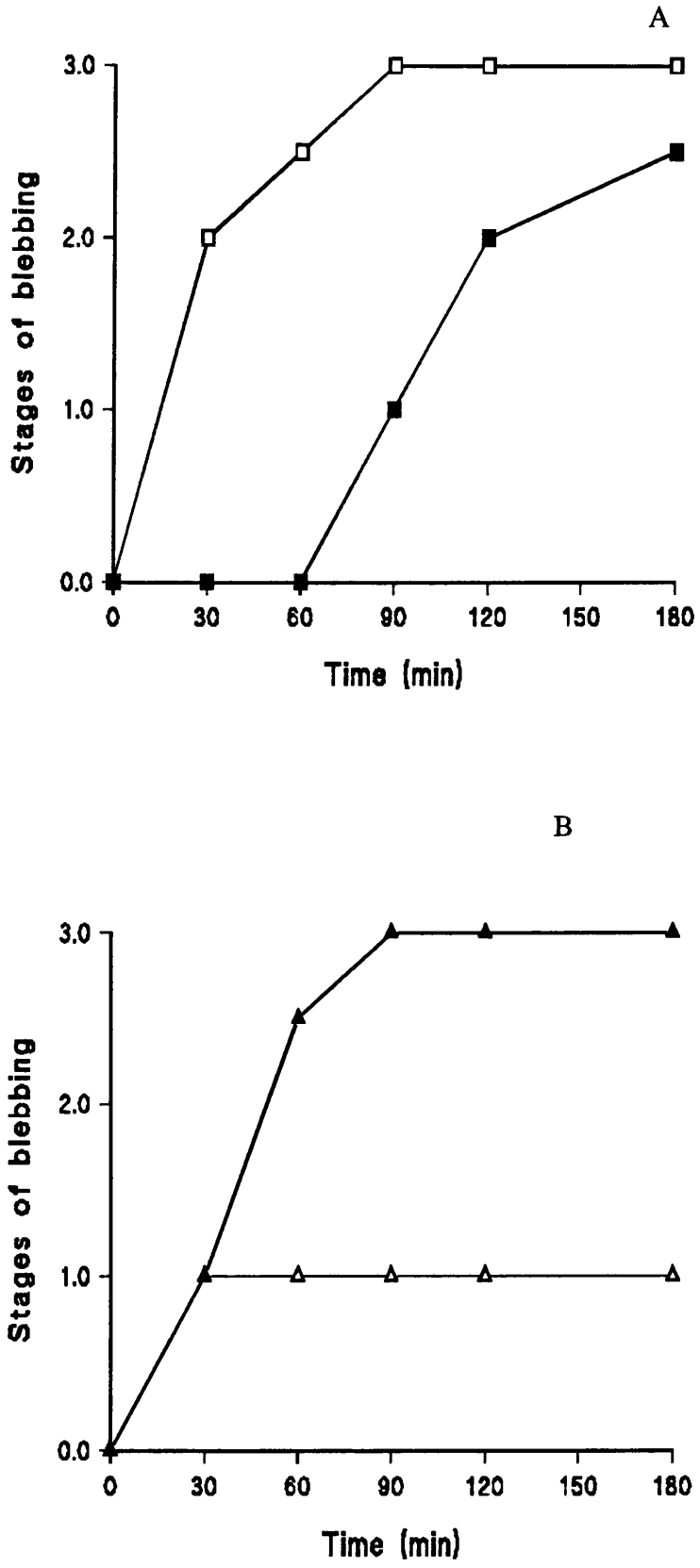

Fig. 3.2 The effect of quinones on plasma membrane blebbing. Cells were incubated either with (A) TW13 (100 (■) and 200 (□) μM) or (B) TW25 (50 (△) and 100 (▲) μM). At the times indicated plasma membrane blebbing was assessed as described in the methods and materials. Values represent the mean of three individual incubations.

A

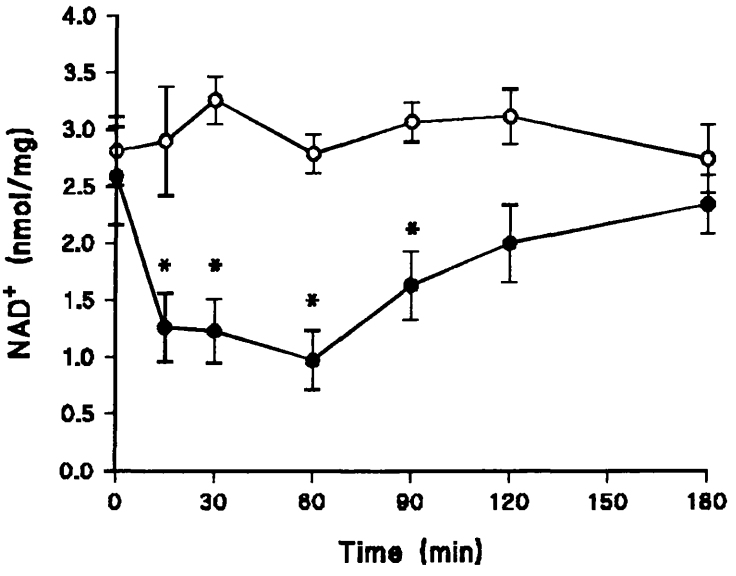

B

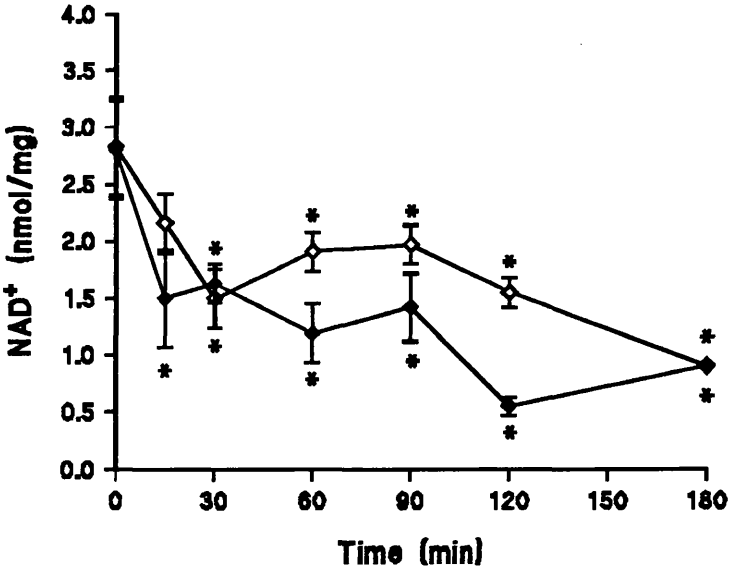

Fig. 3.3 The effect of quinones on the level of NAD^+ in hepatocytes. Cells were incubated either (A) alone (O) or with 2,3-diOMe-1,4-NQ (50 µM) (●), (B) carboquone (100 (◊) and 200 (♦) µM). At the indicated time points NAD^+ (nmoles/mg protein) was determined as described in materials and methods. Values represent the mean ± SEM of three individual incubations.* Significantly ($P < 0.05$) different from control (Fig. 3.3 A, O).

A

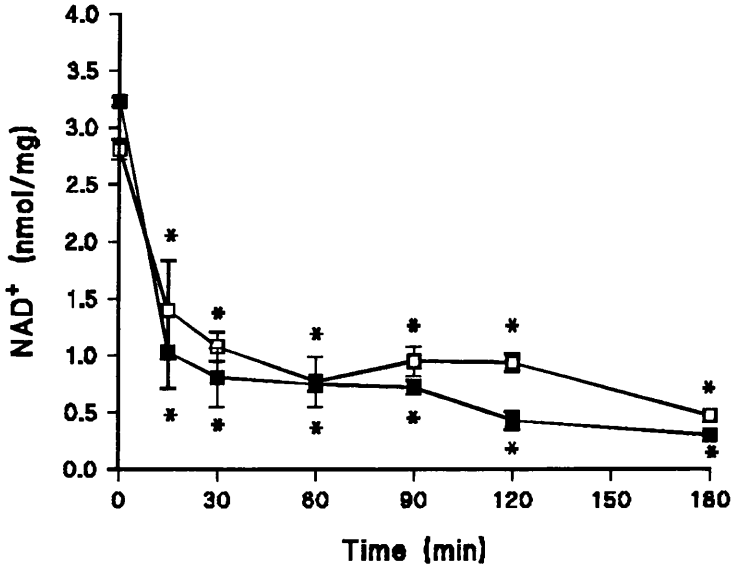

B

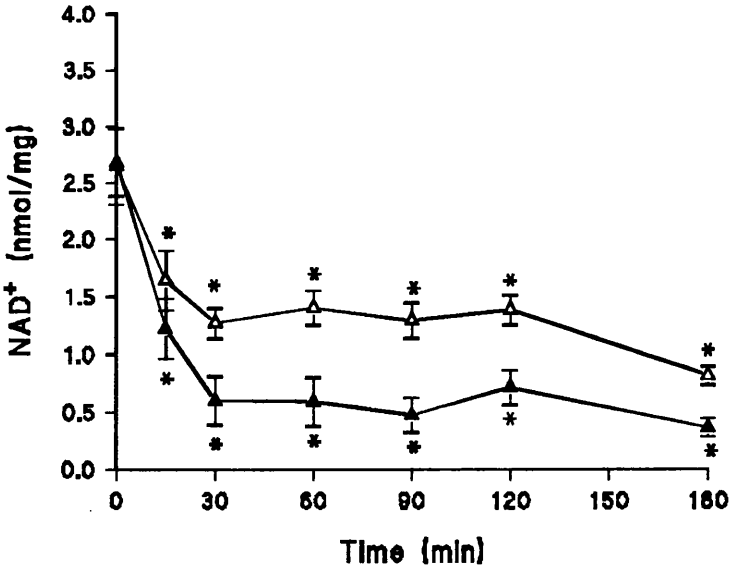

Fig. 3.4 The effect of quinones on the level of NAD^+ in hepatocytes. Cells were incubated either (A) TW13 (100 (□) and 200 (■) μM) or (B) TW25 (50 (△) and 100 (▲) μM). At the indicated time points NAD^+ (nmoles/mg protein) was determined as described in materials and methods. Values represent the mean ± SEM of three individual incubations. Significantly ($P < 0.05$) different from control (Fig. 3.3A, O).

A

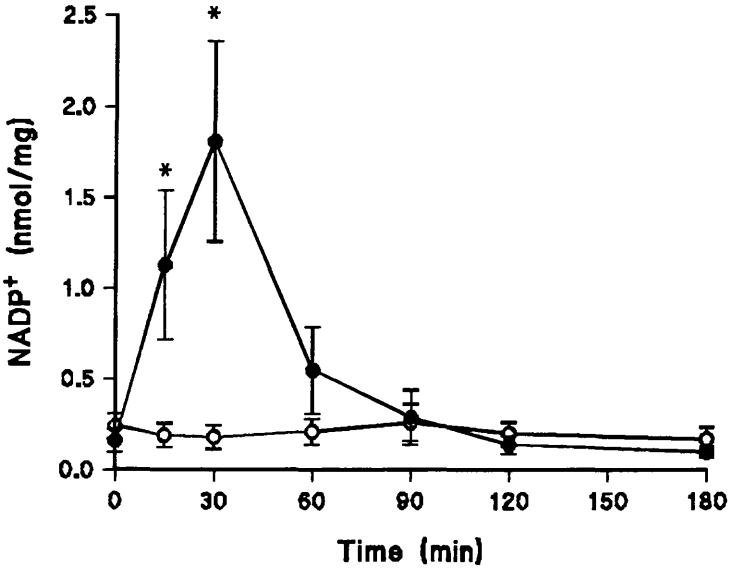

B

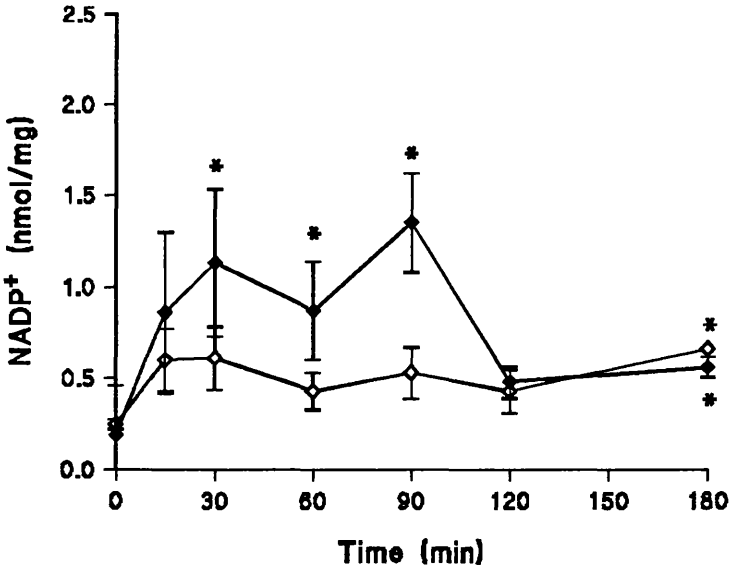

Fig. 3.5 The effect of quinones on the level of $NADP^+$ in hepatocytes. Cells were incubated either (A) alone (O) or with 2,3-diOMe-1,4-NQ (50 µM) (●), (B) carboquone (100 (◊) and 200 (♦) µM). At the indicated time points $NADP^+$ (nmoles/mg protein) was determined as described in materials and methods. Values represent the mean ± SEM of three individual incubations. Significantly ($P < 0.05$) different from control (Fig. 3.5A, O)

A

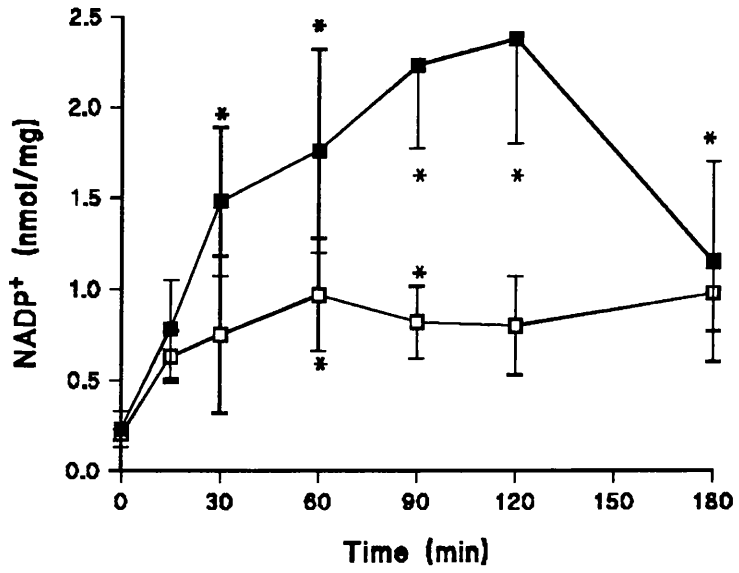

B

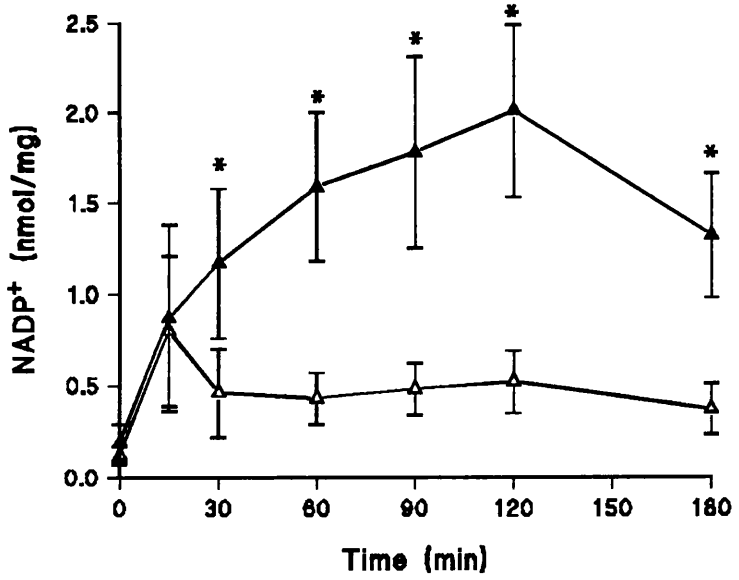

Fig. 3.6 The effect of quinones on the level of $NADP^+$ in hepatocytes. Cells were incubated with either (A) TW13 (100 (□) and 200 (■) μM) or (B) TW25 (50 (△) and 100 (▲) μM). At the indicated time points $NADP^+$ (nmoles/mg protein) was determined as described in materials and methods. Values represent the mean ± SEM of three individual incubations. Significantly ($P < 0.05$) different from control (Fig. 3.5A, ○).

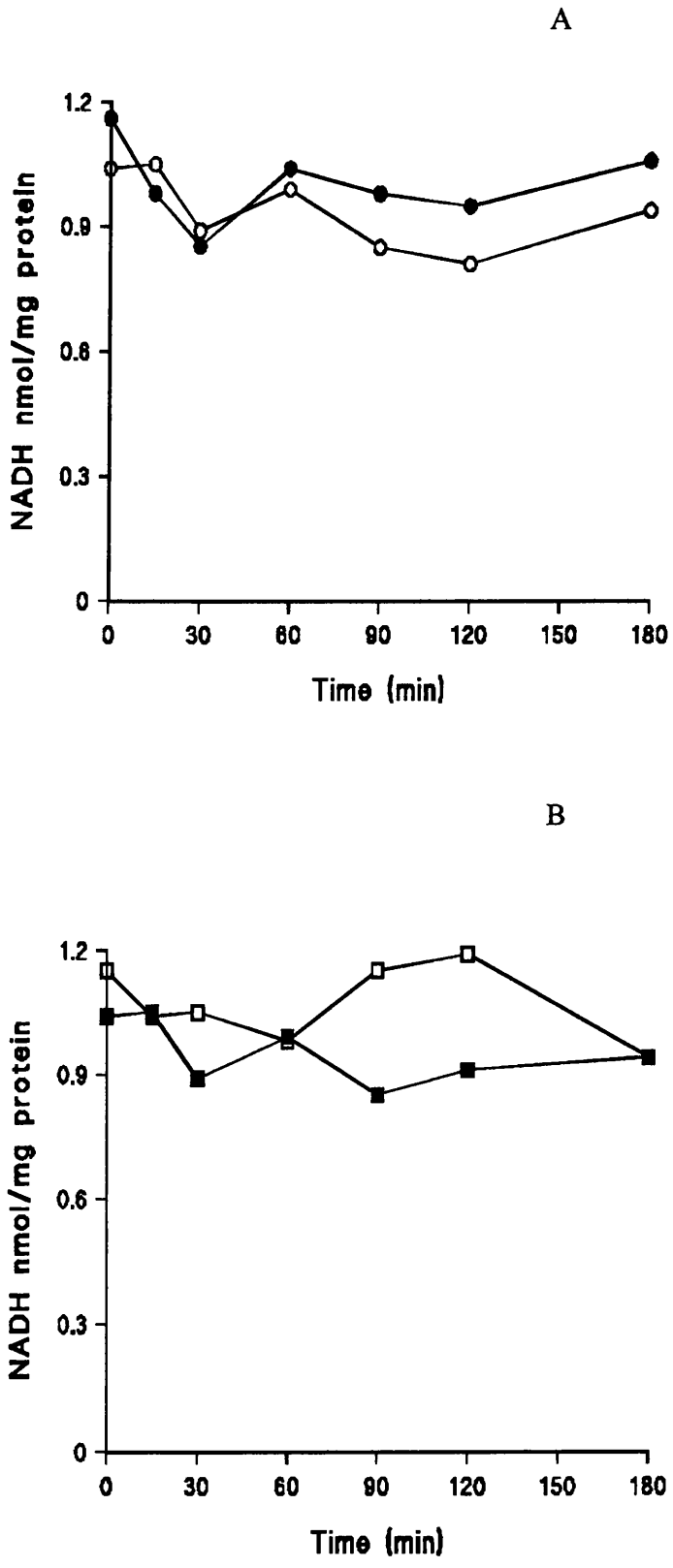

Fig. 3.7 The effect of quinones on the level of NADH in hepatocytes. Cells were incubated either (A) alone (O) or with 2,3-diOMe-1,4-NQ (50 μM) (●), (B) carboquone (100 (□) and 200 (■) μM). At the indicated time points NADH (nmoles/mg protein) was determined as described in the materials and methods. Values represent the mean of three individual incubations.

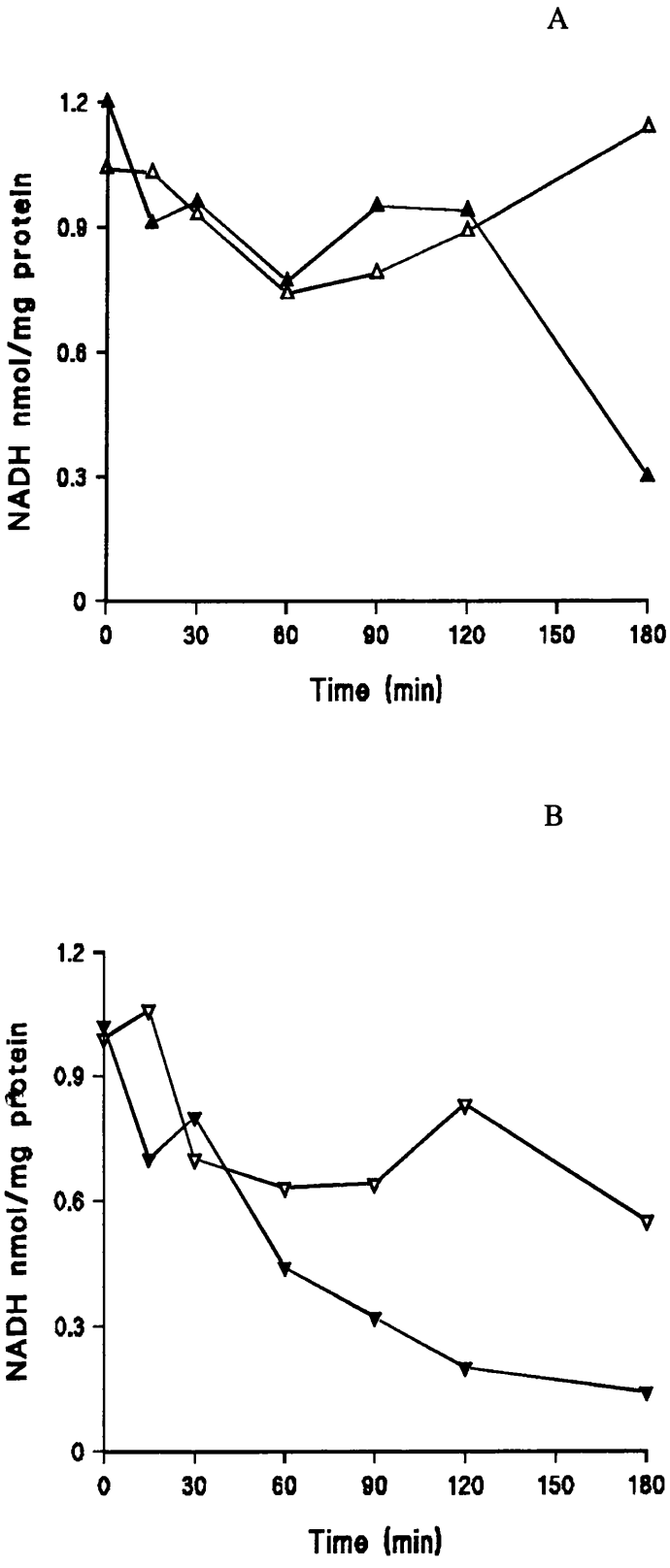

Fig. 3.8 The effect of quinones on the level of NADH in hepatocytes. Cells were incubated either (A) TW13 (50 (▵) and 100 (▲) μM) or (B) TW25 (100 (▽) and 200 (▼) μM). At the indicated time points NADH (nmoles/mg protein) was determined as described in the materials and methods. Values represent the mean of three individual incubations.

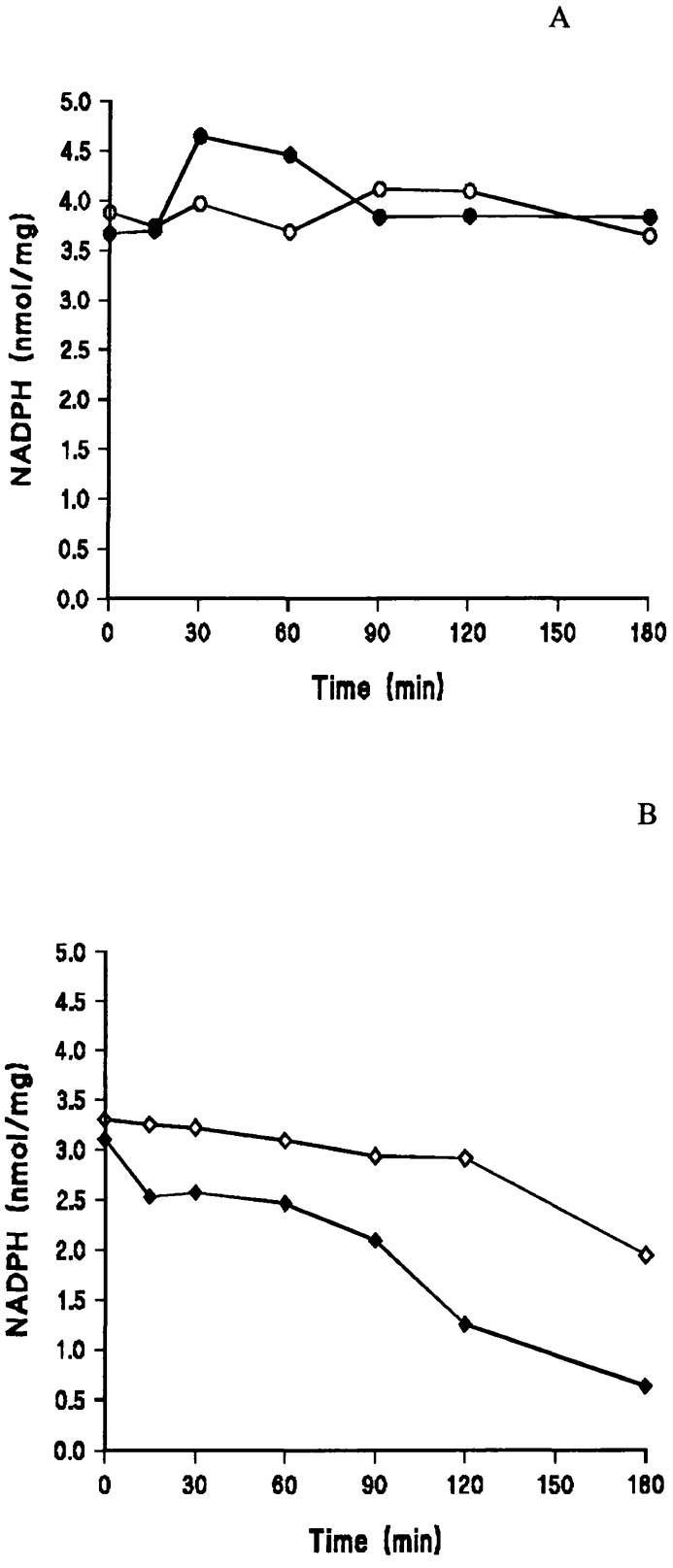

Fig. 3.9 The effect of quinones on the level of NADPH in hepatocytes. Cells were incubated either (A) alone (O) or with 2,3-diOMe-1,4-NQ (50 µM) (●), (B) carboquone (100 (◊) and 200 (♦) µM). At the indicated time points NADPH (nmoles/mg protein) was determined as described in the materials and methods. Values represent the mean of three individual incubations.

A

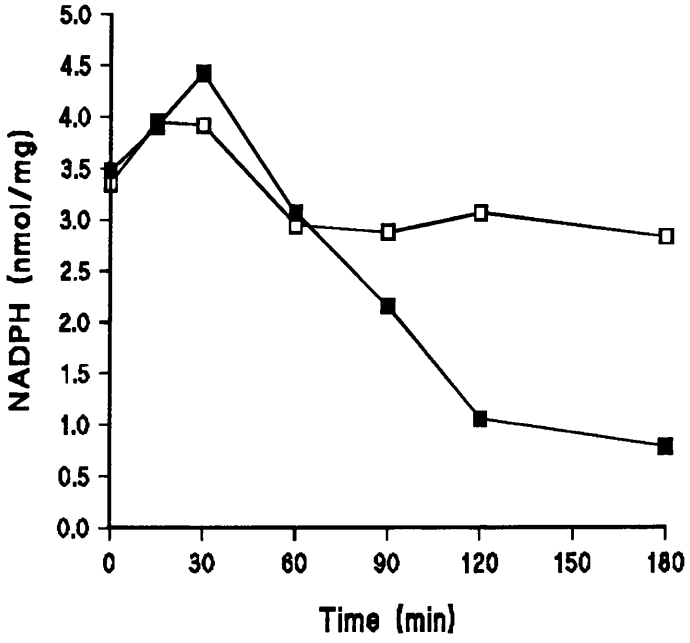

B

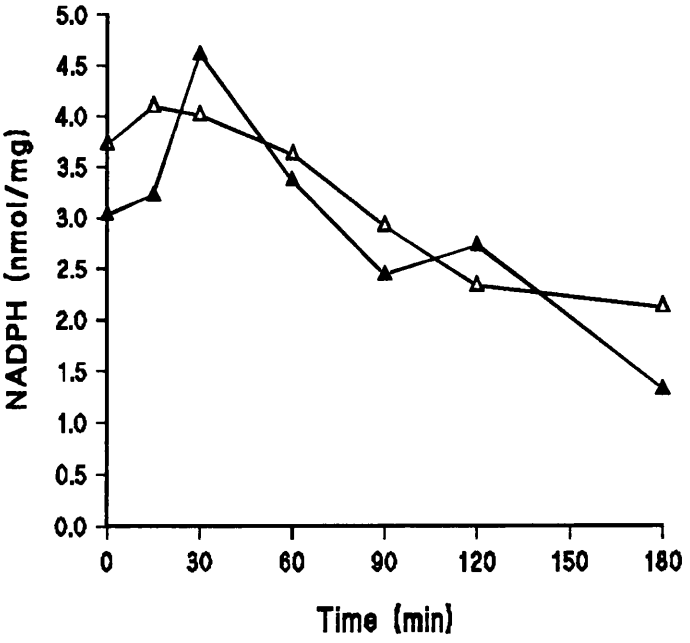

Fig. 3.10 The effect of quinones on the level of NADPH in hepatocytes. Cells were incubated either (A) TW13 (100 (□) and 200 (■) μM) or (B) TW25 (50 (△) and 100 (▲) μM). At the indicated time points NADPH (nmoles/mg protein) was determined as described in the materials and methods. Values represent the mean of three individual incubations.

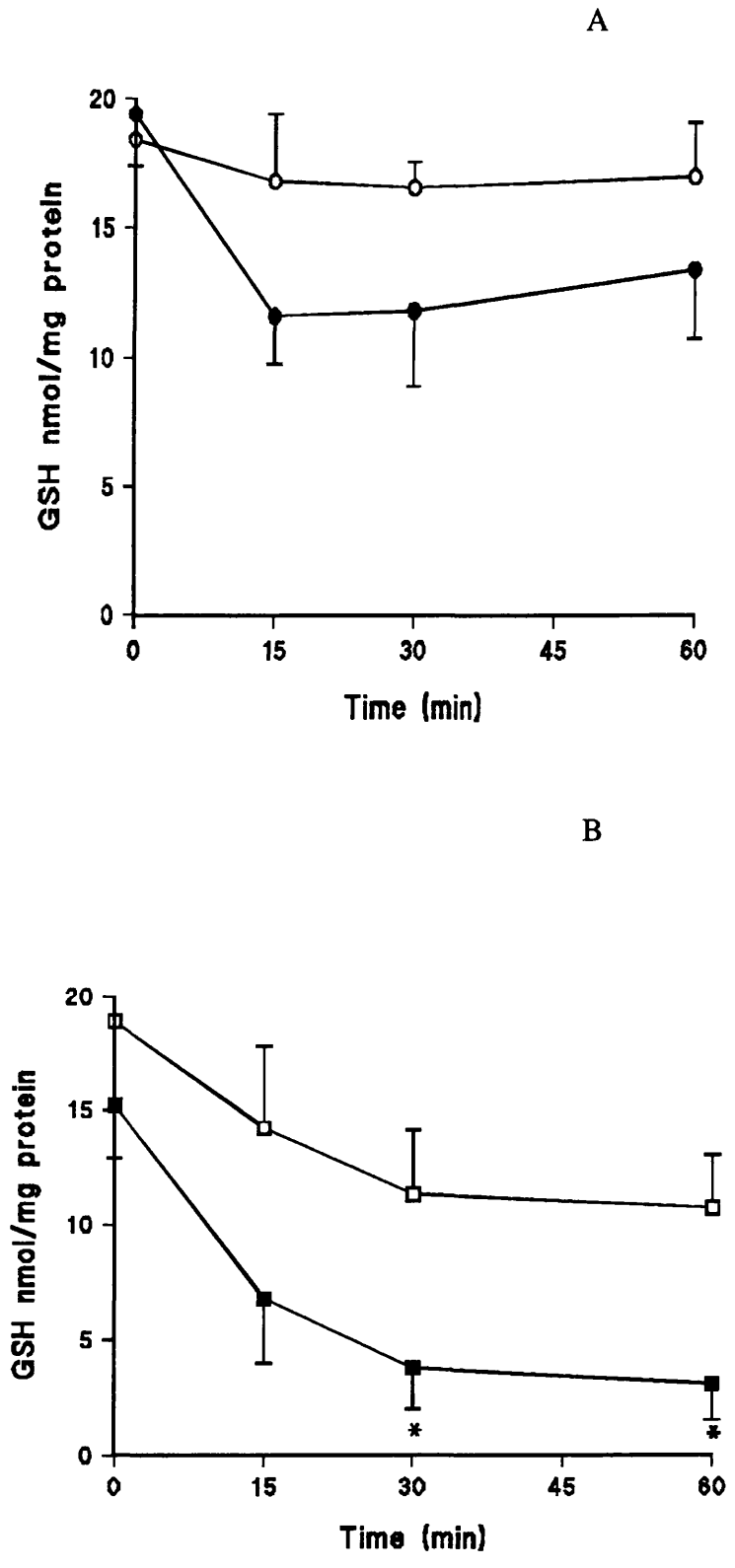

Fig. 3.11 The effect of quinones on the level of GSH in hepatocytes. Cells were incubated either (A) alone (O) or with 2,3-diOMe-1,4-NQ (50 µM) (●), (B) carboquone (100 (□) and 200 (■) µM). At the indicated time points GSH (nmoles/mg protein) was determined as described in the materials and methods. Values represent the mean ± SEM of three individual incubations. Significantly ($P < 0.05$) different from control (Fig. 3.11A, O)

A

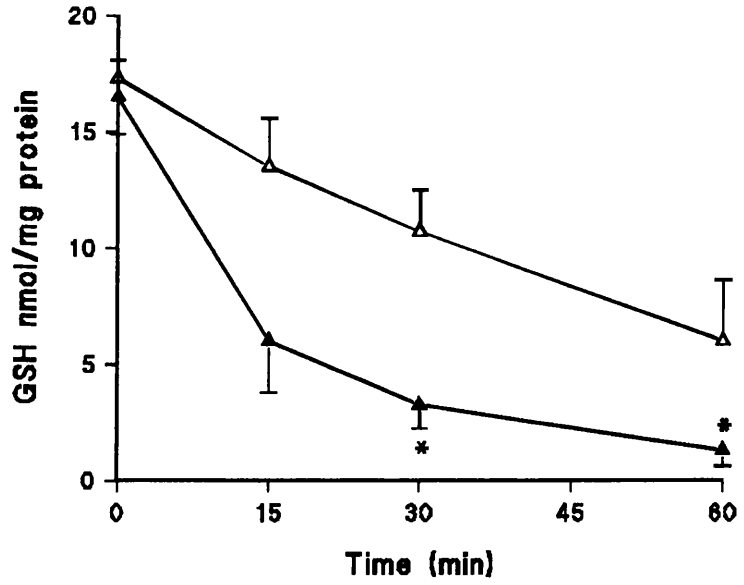

B

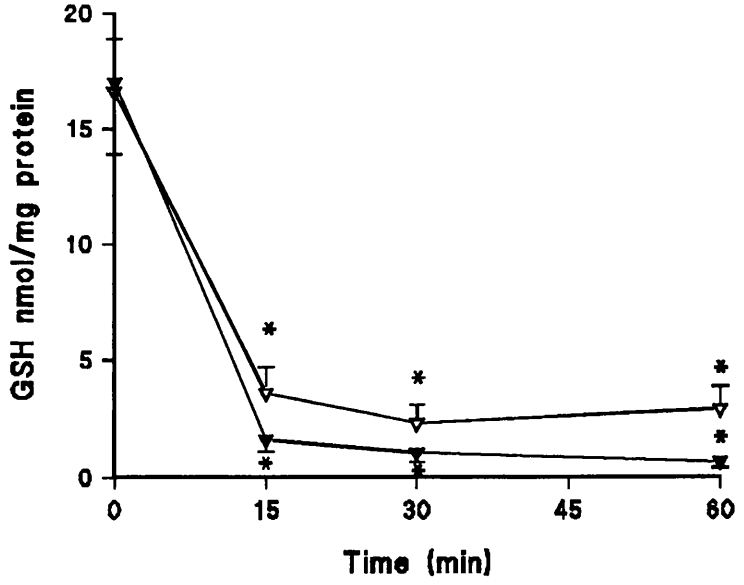

Fig. 3.12 The effect of quinones on the level of GSH in hepatocytes. Cells were incubated either (A) TW13 (50 (△) and 100 (▲) μM) or (B) TW25 (100 (▽) and 200 (▼) μM). At the indicated time points GSH (nmoles/mg protein) was determined as described in the materials and methods. Values represent the mean ± SEM of three individual incubations. Significantly ($P < 0.05$) different from control (Fig. 3.11A, O).

3.4. DISCUSSION

In previous studies with hepatocytes, naphthoquinones were shown to significantly alter the level of pyridine nucleotides [Cohen and Stubberfield, 1990]. It was suggested that these changes may play a role in quinone-induced cell death. This study examines the pyridine nucleotide changes induced by three BABQ with differing abilities to redox cycle and to deplete intracellular GSH [Prins et al, 1989]. Previously it was demonstrated that the cytotoxicity of the BABQ correlated well with their ability to deplete GSH. However compounds with the same ability to deplete GSH differed significantly in the time of onset of cell death, suggesting the involvement of additional mechanisms.

The pyridine nucleotide changes induced by the BABQ were similar to the changes induced by cytotoxic concentrations of naphthoquinones [Stubberfield and Cohen 1989]. The two major changes were a prolonged oxidation of NADPH and a rapid early depletion of NAD^+. In hepatocytes exposed to TW13 and TW25 the large and prolonged increase in $NADP^+$ was accompanied by an equivalent decrease in NADPH. The oxidation of NADPH reduced the NADPH/$NADP^+$ ratio from 10 to less than 1 and could be explained by the effects of extensive redox cycling [Smith et al, 1987]. At toxic concentrations, the elevated $NADP^+$ was accompanied by extensive plasma membrane blebbing which preceded cell death.

The mitochondrion has the largest pool of NADPH (> 75%) [Sies, 1982]. Any change in the cellular NADPH/$NADP^+$ ratio will alter the mitochondrial redox status. A decrease in the mitochondrial NADPH/$NADP^+$ ratio has been reported to stimulate the release of Ca^{2+} from mitochondria [Lehninger et al, 1978; Vercesi, 1987; Bellomo et al, 1987]. Redox cycling also results in the generation of H_2O_2, which precipitates

the depletion of GSH in the GSH peroxidase/GSSG reductase cycle, and may contribute to the elevation of oxidized protein sulphydryls [Di Monte et al, 1984a; Thor et al, 1982; Di Monte et al, 1984b]. These changes in intracellular redox status are also known to increase intracellular Ca^{2+} and may contribute to the subsequent activation of Ca^{2+} dependent proteases, phospholipases and endonuclease [Orrenius, 1985].

At non-toxic concentrations of TW13, TW25 and carboquone, some oxidation of NADPH was seen. However this was less than at toxic concentrations and was accompanied by minor plasma membrane blebbing. In hepatocytes exposed to 2,3-diOMe-1,4-NQ, a massive early elevation of $NADP^+$ was observed which rapidly returned to control levels. The absence of plasma membrane blebbing in 2,3-diOMe-1,4-NQ treated cells may be explained by the transient nature of the $NADP^+$ elevation, possibly due to the activation of the hexose monophosphate shunt [Smith et al, 1987]. The extensive oxidation of NADPH combined with the inability to reduce $NADP^+$ appears to be involved in the cytotoxicity of BABQ.

In this study a rapid early depletion of NAD^+ was observed in hepatocytes exposed to all the quinones. Cytotoxicity was preceded by a prolonged depletion of NAD^+ below 1.0 nmol/mg. In hepatocytes exposed to 2,3-diOMe-1,4-NQ, as well as at non-toxic concentrations of the BABQ, the NAD^+ level remained above 1.0 nmol/mg for most of the incubation. Where the NAD^+ level remained below 1.0 nmol/mg for long periods, a significant loss of ATP is observed. This suggests that the maintenance of NAD^+ above a critical level may contribute to the maintenance of intracellular ATP [Redegeld et al, 1989].

A rapid depletion of NAD^+ is indicative of the activation of poly(ADP-

ribose)polymerase following DNA damage [Berger, 1985]. The most likely cause of the 2,3-diOMe-1,4-NQ-induced NAD^+ depletion is single strand breaks, resulting from the generation of active oxygen species. This form of DNA damage is usually rapidly repaired [McWilliams et al, 1983], and may explain the recovery of NAD^+ seen in the hepatocytes exposed to 2,3-diOMe-1,4-NQ. Although BABQ are known to generate active oxygen species, they may also cause DNA damage by the activation of the aziridinyl groups. In contrast to single strand breaks, the repair of DNA damage resulting from arylation is slow and may explain the prolonged depletion of NAD^+ seen at both concentrations of carboquone and the lower concentrations of the redox cycling BABQ.

These results suggests that BABQ may cause cell death by two separate mechanisms manifested by two distinct changes in cellular pyridine nucleotides. The first change results from redox cycling and oxidative stress. This causes extensive oxidation of NADPH resulting in the elevation of cytoplasmic Ca^{2+} and the early loss of membrane integrity. The second pyridine nucleotide change, the depletion of NAD^+, results from DNA damage and may precipitate ATP depletion and a delayed cytotoxicity.

CHAPTER 4

REDOX CYCLING, OXIDATIVE STRESS AND PYRIDINE NUCLEOTIDE INTERCONVERSION

Abstract- Oxidant-induced cell injury is often preceded by alterations in intracellular pyridine nucleotides. Recently the depletion of NAD^+ has been attributed to the interconversion of NAD(H) to NADP(H). Pyridine nucleotide interconversion was investigated using hepatocytes exposed to 2,3-diOMe-1,4-NQ which causes oxidative stress by redox cycling as well as tert-butyl hydroperoxide which causes oxidative stress without redox cycling. Both tert-butyl hydroperoxide (250-750 μM) and 2,3-dimethoxy-1,4-naphthoquinone (50 μM) induce a rapid depletion of NAD^+, while no change in the level of NADH was observed. In cells exposed to 2,3-diOMe-1,4-NQ (50 μM), extensive oxidation of NADPH to $NADP^+$ was also observed and this was followed by an increase in the level of $NADP^+$ + NADPH {NADP(H)}. However, no change in the total pyridine nucleotide { NAD(H) + NADP(H) } pool was detected. In cells exposed to tert-butyl hydroperoxide, only a slight oxidation of NADPH to $NADP^+$ was observed, accompanied by a decrease in total pyridine nucleotide pool. These results suggest that during oxidative stress, the increase in $NADP^+$ probably results solely from the oxidation of NADPH and that the depletion of NAD^+ is independent of the increase in $NADP^+$. No evidence of an interconversion of NAD^+ to $NADP^+$ was found.

4.1 INTRODUCTION

The mechanisms underlying the changes in cellular pyridine nucleotides observed during oxidative stress has been extensively reported [Berger et al, 1979; Kappus and Seis, 1981; Lind et al, 1982; Reed, 1986; Schraufstatter et al, 1986a]. However, in a recent study Yamamoto and Farber (1992), observed that in rat hepatocytes, tert-butyl hydroperoxide (tBH) caused a decrease in intracellular NAD^+, NADH and NADPH and a simultaneous increase in $NADP^+$. In an earlier study, Stubberfield and Cohen (1989), reported that certain redox cycling quinones caused a coincidental decrease in NAD^+ and an increase in $NADP^+$. In both studies, the depletion of NAD^+ could not be prevented by 3-aminobenzamide, a potent inhibitor of poly(ADP-ribose)polymerase, while no change in total pyridine nucleotides {NAD(H) + NADP(H)} was detected. In an attempt to explain the nucleotide changes, Stubberfield and Cohen (1989) proposed that during oxidative stress intracelluar NAD^+ was interconverted to NADP(H). This was suggested as a cellular response to combat oxidative stress. The proposed mechanism of nucleotide interconversion involved the activation of an NAD^+ kinase found in a number of tissues including rat liver [Kaplan, 1985]. It is envisaged that the activation of the kinase is mediated by calmodulin [Eppel et al, 1981]. During oxidative stress the increase in cytosolic Ca^{2+} results in the activation of calmodulin which leads to the activation of the NAD^+ kinase [Stubberfield and Cohen, 1989]. Furthermore, during oxidative stress, activation of the NAD^+ kinase is also thought to be enhanced by the decrease in NADPH which has previously been shown to inhibit NAD^+ kinase (Oka and Field, 1968) .

However, the alteration of pyridine nucleotides by the interconversion of NAD^+ to

NADP(H) is incompatible with the pyridine nucleotide change induced by cellular reductases as well as the activation of poly(ADP-ribose)polymerase. In an attempt to determine the fate of the pyridine nucleotides during oxidative stress, the changes in pyridine nucleotides induced by the redox cycling quinone 2,3-diOMe-1,4-NQ were compared to those induced by tBH which causes oxidative stress without redox cycling.

4.2. Methods and Materials

4.2.1 Materials

Collagenase Type 1, HEPES, thiazolyl blue, phenazine ethosulphate, alcohol dehydrogenase, glucose-6-phosphate, glucose-6-phosphate dehydrogenase, 3-aminobenzamide, nicotinamide, theophylline and all nucleotides were purchased from Sigma Chemical Co Ltd (Poole, U.K.). Tributylamine was purchased from Aldrich Chemical Co. (Gillingham, U.K.). 2,3-Dimethoxy-1,4-naphthoquinone was synthesised as previously described [Stubberfield and Cohen 1989]. The bis-aziridinylbenzoquinones were obtained as in chapter 3. All other chemicals were purchased from BDH Ltd (Poole, Dorset, U.K.)

4.2.2 Isolation and Incubation of Rat Hepatocytes.

Rat hepatocytes were prepared as previously described (chapter 2) by collagenase perfusion of the livers of adult male Wistar rats (220-260g). The isolated cells (10^6 cell/ml) were suspended in Krebs Henseleit buffer containing 12.5 mM HEPES under an atmosphere of 95% O_2/5% CO_2 (pH 7.4) and were incubated in continuously rotating round bottom flasks at 37°C. Following isolation and prior to treatment the cells were preincubated at 37°C for 30 min. Cell viability was determined by trypan blue exclusion {0.4% (w/v) solution}. Protein was measured by the method of Lowry et al (1951)

4.2.3 Determination of Pyridine Nucleotides.

Oxidized pyridine nucleotides (NAD^+, $NADP^+$) were determined using the spectrophotometric recycling assay of Bernofsky and Swan (1973) as previously

described in chapter 2. Reduced pyridine nucleotides were first separated by HPLC on a C18 reverse-phase Bondapak column (Millipore Ltd) using an isocratic gradient with 82% 0.2 mM ammonium phosphate pH 6.0/17.85% methanol/ 0.15% tributylamine as described previously [Kalhorn et al, 1985]. The eluent was monitored at 340 nm and concentration determined by peak height.

4.2.4 Statistical Analysis.

The results were expressed as mean ± SEM. Where appropriate statistical significance was tested by Student's *t*-test with the accepted significance level of $P < 0.05$.

4.3 Results

4.3.1 Effect of tert-Butyl Hydroperoxide on Cellular Viability

Previously, redox cycling quinones were shown to cause a concentration dependent cytotoxicity in rat hepatocytes (Chapter 3; Stubberfield and Cohen 1989). In the present study, hepatocytes were exposed to increasing concentrations of tBH (250-750 μM) which resulted in cell death as was determined by the cell's inability to exclude trypan blue. No loss in cell viability was observed in cells exposed to the lower concentrations of tBH (250-500 μM) (Fig. 4.1). However, at the higher concentration (750 μM) a loss of membrane integrity was detected within 60 min of exposure to the hydroperoxide (Fig. 4.1).

4.3.2 The Effect of tert-Butyl Hydroperoxide on the Pyridine Nucleotides

The pyridine nucleotide levels in untreated hepatocytes (Fig. 4.2) was similar to that observed previously [Stubberfield and Cohen 1989]. An examination of the pyridine nucleotides changes induced by tBH revealed a similar pattern of change in hepatocytes exposed to toxic and non-toxic concentrations (Fig. 4.3-5). Within the first 30 min exposure to tBH (250-750 μM), a concentration dependent increase in the level of $NADP^+$ was detected (Fig.4.3-5). However no change in the level of NADPH was observed (Fig 4.3-5). tBH induced no change in the level of NADH, whereas a rapid concentration dependent depletion of NAD^+ was observed within 10 minutes of exposure to the hydroperoxide (Fig. 4.3-5). After 30 min the NAD^+ level begins to recover to control values.

4.3.3 The Effect of 2,3-diOMe-1,4-NQ on the Pyridine Nucleotides

As previously reported [Stubberfield and Cohen 1989], 2,3-diOMe-1,4-NQ (50 μM)

caused an initial decrease in NAD^+ and a transient increase in $NADP^+$, followed by a prolonged increase in NADP(H) (Fig. 4.6). No change in NADH was detected. By measuring the nucleotides at very early time points i.e after 3 min exposure, an initial decrease in NADPH was observed. This is in agreement with the previously reported early decrease in NADPH in hepatocytes exposed to menadione [Smith et al, 1987] and may account for the early increase in $NADP^+$.

4.3.4 Pyridine Nucleotide Interconversion Induced by t-BH and 2,3-diOMe-1,4-NQ

The interconversion of pyridine nucleotides requires the transfer of nucleotides from NAD(H) to NADP(H) without a loss of total nucleotides. In hepatocytes exposed to tBH, the depletion of NAD(H) was not compensated for by an increase in the level of NADP(H) (Table 4.1 and 4.2). Furthermore the depletion of NAD^+ was accompanied by a decrease in total pyridine nucleotides (Table 4.1 and 4.2). In contrast, the decrease in NAD(H) induced by 2,3-diOMe-1,4-NQ was approximately equal to the increase in NADP(H) while no significant change in the total pyridine nucleotide pool was observed, in agreement with Stubberfield and Cohen (1989).

4.3.5 Pyridine Nucleotide Interconversion Induced by Aziridinylbenzoquinones

As pyridine nucleotide interconversion was originally suggested as a response of hepatocytes to quinone-induced oxidative stress, the net change in pyridine nucleotides induced by several bis-aziridinylbenzoquinones was also investigated. The BABQ induced a rapid decrease in NAD(H) which was not matched by an increase in NADP(H), instead a decrease in total pyridine nucleotides was detected (Table 4.3).

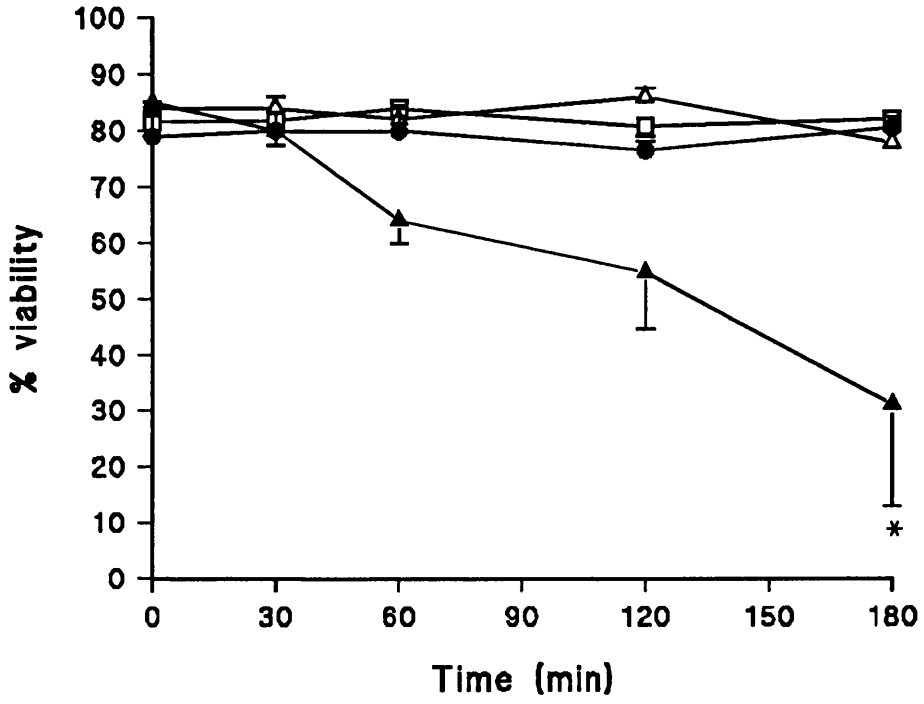

Fig. 4.1 The effects of tBH on the viability of rat hepatocytes. Cells were incubated either alone (△) or with tBH: 250 μM (□), 500 μM (●) or 750 μM (▲). Cell viability was determined by trypan blue exclusion as described in the Materials and Methods. Values represent Mean ± SEM of three separate incubations.

* Significantly ($P < 0.05$) different from control.

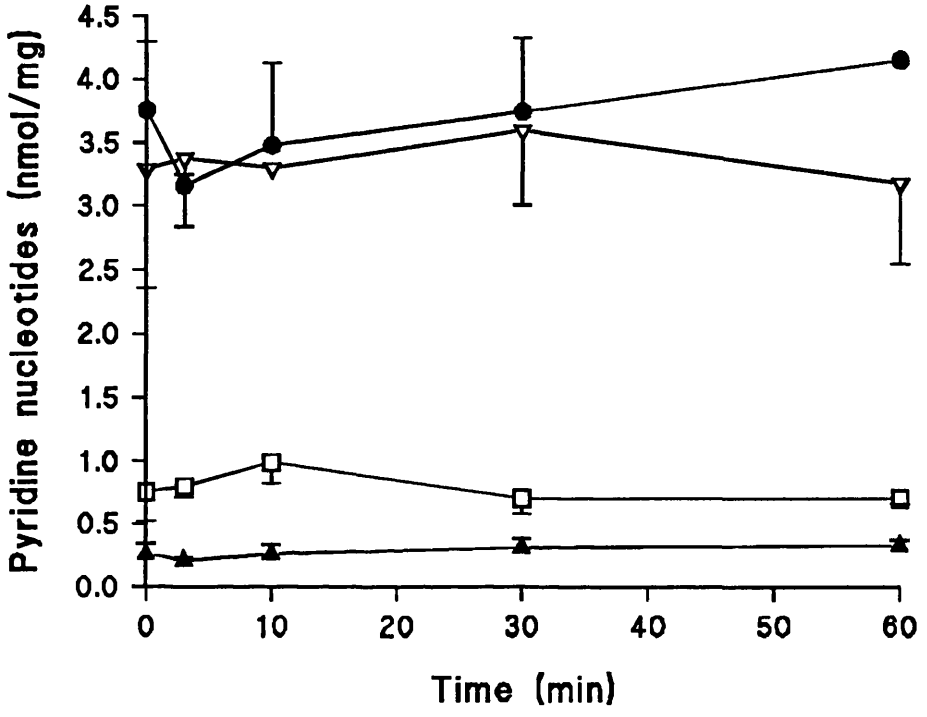

Fig. 4.2 Intracellular pyridine nucleotides levels in untreated hepatocytes. Cells were incubated with DMSO alone. At the times indicated intracellular NAD^+ (●), NADH (□), $NADP^+$ (▲) and NADPH (▽) were determined as in the Materials and Methods. Values represent Mean ± SEM of three separate incubations.

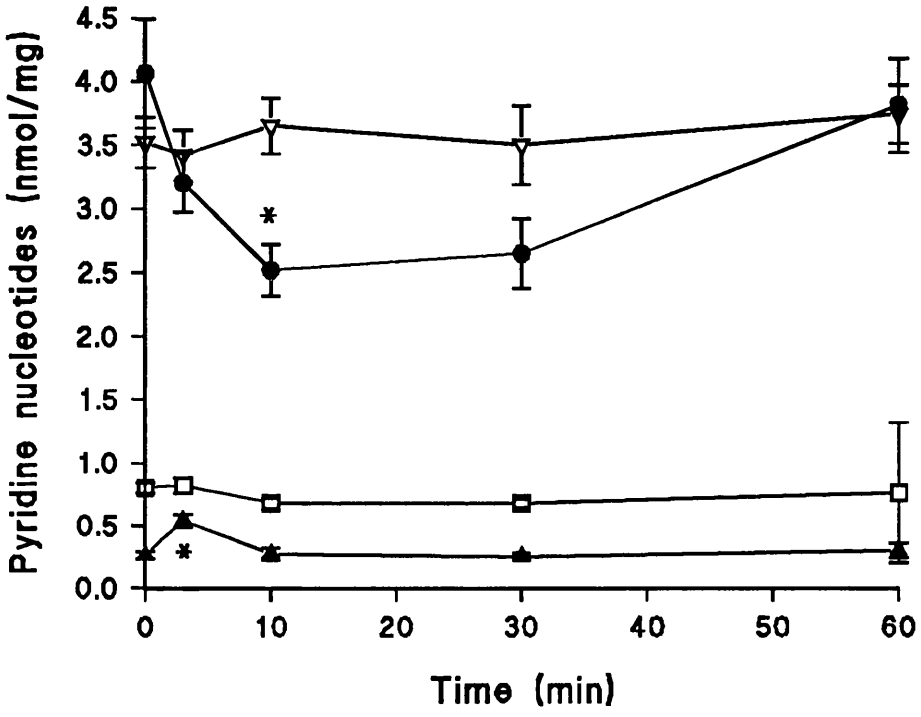

Fig. 4.3 The effects of tBH on cellular pyridine nucleotides. Hepatocytes were incubated with tBH (250 μM). At the times indicated intracellular NAD^+ (●), NADH (□), $NADP^+$ (▲) and NADPH (▽) were determined as in the Materials and Methods. Values represent Mean ± SEM of three separate incubations.

* Significantly ($P < 0.05$) different from control (Fig. 4.2).

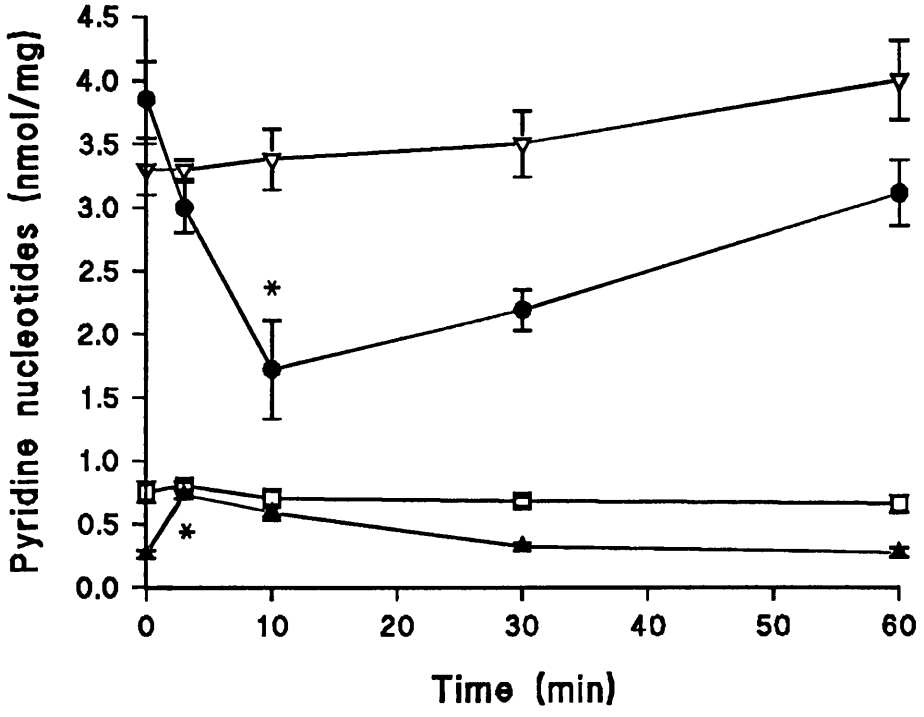

Fig. 4.4 The effects of tBH on cellular pyridine nucleotides. Hepatocytes were incubated with tBH (500 μM). At the times indicated intracellular NAD^+ (●), NADH (□), $NADP^+$ (▲) and NADPH (▽) were determined as in the Materials and Methods. Values represent Mean ± SEM of three separate incubations.

* Significantly ($P < 0.05$) different from control (Fig. 4.2).

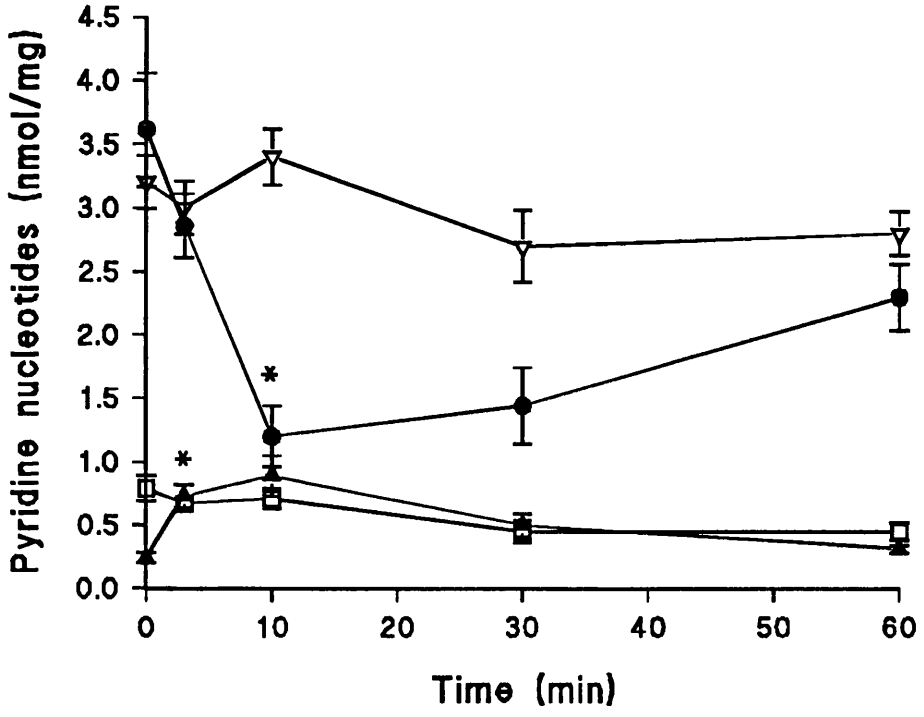

Fig. 4.5 The effects of tBH on cellular pyridine nucleotides. Hepatocytes were incubated either tBH (750 µM). At the times indicated intracellular NAD^+ (●), NADH (□), $NADP^+$ (▲) and NADPH (▽) were determined as in the Materials and Methods. Values represent Mean ± SEM of three separate incubations.

* Significantly ($P < 0.05$) different from control (Fig. 4.2).

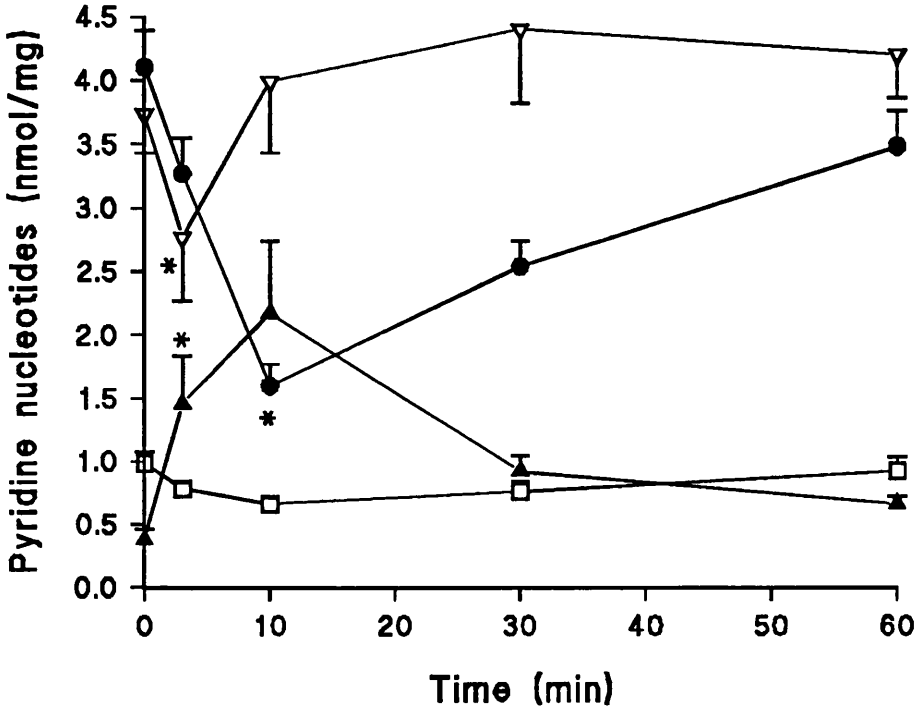

Fig. 4.6 The effects of 2,3-d-OMe-1,4-NQ on cellular pyridine nucleotides. Hepatocytes were exposed to the quinone (50 μM) and at the times indicated intracellular NAD^+ (●), NADH (□), $NADP^+$ (▲) and NADPH (▽) were determined as in the Materials and Methods. Values represent Mean ± SEM of three separate incubations. * Significantly ($P < 0.05$) different from control (Fig. 4.2).

Table 4.1. Effect of 2,3-diOMe-1,4-NQ and tBH on total pyridine nucleotide levels (3 min)

	NAD^+ + NADH { NAD(H) }	$NADP^+$ + NADPH { NADP(H) }	total pyridine nucleotides
Control	3.96 ± 0.02	3.60 ± 0.52	7.60 ± 0.52
2,3-diOMe-1,4NQ (50 µM)	4.05 ± 0.20	4.23 ± 0.21	8.24 ± 0.11
tBH (250 µM)	4.11 ± 0.26	3.95 ± 0.19	8.00 ± 0.43
tBH (500 µM)	3.75 ± 0.33	4.00 ± 0.07	7.60 ± 0.34
tBH (750 µM)	3.54 ± 0.23	3.70 ± 0.20	7.22 ± 0.37

Nucleotides measurements (nmol/mg protein) were made after 3 min incubation in the presence of either 2,3-diOMe-1,4-NQ or tBH as described in the Material and Methods. The values represent mean ± SEM from three separate hepatocyte preparations.

Table 4.2. Effect of 2,3-diOMe-1,4-NQ and tBH on total pyridine nucleotide levels (30 min)

	NAD^+ + NADH { NAD(H) }	$NADP^+$ + NADPH { NADP(H) }	total pyridine nucleotides
Control	4.45 ± 0.57	3.95 ± 0.59	8.60 ± 0.80
2,3-diOMe-1,4NQ (50 µM)	3.30 ± 0.16*	5.32 ± 0.66	8.63 ± 0.78
tBH (250 µM)	3.34 ± 0.26	3.76 ± 0.30	7.10 ± 0.53
tBH (500 µM)	2.77 ± 0.16*	3.80 ± 0.26	6.59 ± 0.41*
tBH (750 µM)	1.92 ± 0.28*	3.27 ± 0.23	5.19 ± 0.38*

Nucleotides measurements (nmol/mg protein) were made after 30 min incubation in the presence of either 2,3-diOMe-1,4-NQ or tBH as described in the Material and Methods. The values represent mean ± SEM from three separate hepatocyte preparations. * Significantly ($P < 0.05$) different from control.

Table 4.3 Effect of BABQ on total Pyridine nucleotide levels (30 min)

Compound	NAD^+ + NADH {NAD(H)}	$NADP^+$ + NADPH {NADP(H)}	Total pyridine nucleotides
Control	4.41 ± 0.86	4.15 ± 0.86	8.56 ± 1.26
CQ (100 µM)	2.55 ± 0.25*	3.48 ± 0.40	6.03 ± 0.40*
CQ (200 µM)	2.36 ± 0.36*	3.70 ± 0.21	6.07 ± 0.55*
TW13 (100 µM)	1.96 ± 0.27*	4.68 ± 0.04	6.64 ± 0.52*
TW13 (200 µM)	1.76 ± 0.26*	5.91 ± 0.31*	7.67 ± 0.4
TW25 (50 µM)	1.97 ± 0.28*	4.58 ± 0.72	6.55 ± 0.99*
TW25 (100 µM)	1.25 ± 0.23*	5.97 ± 0.47*	7.18 ± 0.60

Nucleotide measurements (nmol/mg protein) were made after 30 min incubation in the presence of either DMSO alone or the quinone as described in the Material and Methods. the values represent Mean ± SEM from three separate hepatocyte preparations. * Significantly ($P < 0.05$) different from control.

4.4. DISCUSSION

4.4.1 Pyridine Nucleotide Changes and the Cytotoxicity of tert-Butyl Hydroperoxide

Redox cycling quinones and tBH induce oxidative stress in mammalian cells by a different mechanisms [Kappus and Sies, 1981; Richter and Kass, 1991; Jewell et al 1986]. An examination of the two forms of the pyridine nucleotides NAD(H) and NADP(H) provides a good indicator of the biochemical processes involved. Redox cycling results in a disproportionate consumption of reducing equivalents such as NADPH, whereas NADPH is consumed in a stoichiometric manner during the metabolism of tBH. Hence even at cytotoxic concentrations of tBH, far less NADPH is oxidized when compared to that previously reported during the metabolism of the redox cycling quinones. A number of studies suggest that tBH-induced cytotoxicity results from the oxidation and hydrolysis of NADP(H) and the subsequent increase in cytosolic Ca^{2+}. Although there may be some NADPH oxidation in the present study, the most pronounced nucleotide change is the depletion of NAD^+, which indicates DNA damage and the activation of poly(ADP-ribose)polymerase. The metabolism of tBH is known to result in the generation of radical species which cause DNA damage [Coleman et al, 1989]. However, the early onset of cell death is more likely to result from the radical-induced peroxidation of membrane lipid and the subsequent loss of membrane integrity [Jewell et al, 1986].

4.4.2 Interconversion Induced by 2,3-diOMe-1,4-NQ

Stubberfield and Cohen (1989), observed that in hepatocytes exposed to 2,3-diOMe-1,4-NQ, the increase in $NADP^+$ was greater than the decrease in NADPH, this suggested that oxidation of NADPH could not account for the increase in $NADP^+$. They proposed that the early increase in $NADP^+$ induced by 2,3-OMe-1,4-NQ may be the result of the activation of an NAD^+ kinase, which converts NAD^+ to $NADP^+$.

Although an increase in NAD^+ phosphorylation cannot be ruled out, an increase in $NADP^+$ is most likely to result from the activation of NADPH dependent reductases, which generate $NADP^+$ during the metabolism of quinones [Kappus, 1986; Smith et al, 1987]. By measuring intracellular pyridine nucleotides at a very early time point i.e. 3 min after the exposure to 2,3-diOMe-1,4-NQ (50 μM), a simultaneous decrease in the level of NADPH and an increase in $NADP^+$ was observed. Furthermore, no change in total NADP(H) was detected (Fig. 4.6).

Although these early changes in NADP(H) were consistent with the oxidation of NADPH, they were not detected in the studies of Stubberfield and Cohen (1989) or Cohen and Stubberfield (1990), as the earliest time point in their studies was 10 min. In the present study, between 3 and 10 min, there is an increase in the level of $NADP^+$ and an increase in total NADP(H) (Fig. 4.6), (Table 4.1), which coincided with the extensive oxidation of NADPH and may reflect a greater recovery of NADP(H) when the nucleotide is in the oxidized ($NADP^+$) form [Yamamoto and Farber, 1992]. After 10 min incubation, there is an increase in the level of NADPH and NADP(H), while the level of $NADP^+$ decreased to control values (Fig. 4.6), (Table 4.2). The increase in NADPH may be the result of the activation of the hexose monophosphate shunt which converts $NADP^+$ to NADPH. A decrease in the NADPH/$NADP^+$ ratio, such as following a 3 min exposure to 2,3-diOMe-1,4-NQ may activate the shunt [Kappus, 1986; Smith et al 1987]. Following the activation of the shunt, a significant proportion of the cellular NADPH may remain outside the mitochondrial compartment, thus facilitating the recovery of NADPH and contributing to the increase in total NADP(H). After 60 min, the decrease in NADPH and NADP(H) probably reflects the movement of NADPH into the mitochondria.

4.4.3 Interconversion Induced by tert-Butyl Hydroperoxide ?

In a recent study, Yamamoto and Farber (1992) reported a tBH induced interconversion of pyridine nucleotides in rat hepatocytes. The proposed mechanism

involves not only the conversion of NAD^+, but also NADH and NADPH to $NADP^+$. They suggested that the increase in $NADP^+$ was at least due in part to the oxidation of NADPH. However as the increase in $NADP^+$ was greater than the decrease in NADPH they concluded that an interconversion of NAD^+ may have occurred. In this study no evidence of a tBH induced an interconversion of NAD(H) to $NADP^+$ was detected. These results suggest that tBH induced a concentration dependent oxidation of NADPH. At both non-toxic and toxic concentrations the depletion of NAD^+ was accompanied by a decrease in the total pyridine nucleotide pool (Table 4.2) suggesting the hydrolysis of NAD^+. As was suggested for the changes induced by 2,3-diOMe-1,4-NQ, the recovery of NADP(H) may be enhanced when the nucleotide is in its oxidized form, hence as less oxidation of NADPH was observed during the metabolism of tBH, no increase in NADP(H) was detected (Table 4.1 and 4.2).

4.4.4 Interconversion Induced by the Aziridinylbenzoquinones ?

In the previous chapter the pyridine nucleotide changes induced by the BABQ were discussed in relation to cytotoxicity, here the possibility of BABQ-induced interconversion is examined. Although the BABQ induced extensive oxidation of NADPH, the increase in NADP(H) could not compensate for the loss in NAD^+. At the higher concentrations where the greater oxidation of NADPH was observed, the difference between the loss of NAD^+ and the increase in NADP(H) became less. This further supports the suggestion that a greater recovery of NADP(H) may occur when the nucleotide is in oxidized form. However, as was demonstrated with the 2,3-diOMe-1,4-NQ and tBH the increase in $NADP^+$ probably reflects the activation of cellular reductases whereas the depletion of NAD^+ suggest the hydrolysis of the nucleotide.

The possibility of pyridine nucleotide interconversion represented a novel cellular response to oxidative stress and was originally proposed as a mechanism whereby intracellular NAD(H) may be interconverted to NADP(H) in an attempt to combat the

effects of quinone-induced oxidative stress [Stubberfield and Cohen, 1989]. The results of the present study suggest that the early increase in the level of $NADP^+$ is due to oxidation of NADPH, while the depletion of NAD^+ is probably the result of hydrolysis, mediated either by poly(ADP-ribose)polymerase or a related enzyme.

CHAPTER 5

THE INHIBITION OF POLY(ADP-RIBOSE)POLYMERASE AND THE HYDROLYSIS OF NAD^+ DURING OXIDATIVE STRESS

Abstract- A characteristic feature of many types of chemically induced oxidative stress is a depletion of the pyridine nucleotide NAD^+. This has been attributed to either its hydrolysis to nicotinamide and ADP-ribose or to its phosphorylation (interconversion) to $NADP^+$. Preincubation of hepatocytes for one hour with either 3-aminobenzamide (20mM), nicotinamide (10 mM) or theophylline (7.5 mM), caused a reduction in rate of NAD^+ depletion induced by tert-butyl hydroperoxide (500 μM), 2,3-dimethoxy-1,4-naphthoquinone (50 μM), dimethyl sulphate (DMS) (800 μM) and N-methyl-N-nitro-N-nitrosoguanidine (NMNG) (280 μM). The depletion of NAD^+ was accompanied by a simultaneous increase in nicotinamide which was approximately equivalent to the decrease in NAD^+. Furthermore, in cells exposed to compounds which cause extensive oxidation of NADPH, an additional increase in the level of $NADP^+$ was also observed. These results suggest that during oxidative stress, the activation of poly(ADP-ribose)polymerase hydrolyses NAD^+ to nicotinamide and that the depletion of NAD^+ is independent of the increase in $NADP^+$.

5.1. INTRODUCTION

A reduction in the intracellular level of the pyridine nucleotide NAD^+ is usually associated with DNA damage and the activation of poly(ADP-ribose)polymerase [Berger et al, 1979]. Following DNA strand breakage, the chromatin-bound enzyme hydrolyses NAD^+, liberating free nicotinamide while transferring the ADP-ribose moiety to several nuclear proteins and to the ADP-ribose polymer [Althaus and Richter, 1987].

In numerous studies polymerase inhibitors have been shown to prevent the depletion of NAD^+ following DNA damage [Schraufstatter et al, 1986b; Skidmore et al, 1979]. However recently both Stubberfield and Cohen (1989), and Yamamoto and Farber (1992) reported that the depletion of NAD^+ induced by certain redox cycling quinones and tert-butyl hydroperoxide was independent of the activation of poly(ADP-ribose)polymerase. In both studies the depletion of NAD^+ was not prevented by 3-aminobenzamide, a potent inhibitor of poly(ADP-ribose)polymerase [Purnell and Whish, 1980].

In the present study, the role of poly(ADP-ribose)polymerase in the depletion of NAD^+ during oxidative stress is investigated. Two approaches were employed: The rate of NAD^+ depletion induced by a number of compounds which are known to cause DNA damage was determined in the absence and presence of several poly(ADP-ribose)polymerase inhibitors. Evidence of NAD^+ hydrolysis was found by measuring the simultaneous loss of NAD^+ and the formation of nicotinamide.

5.2. Methods and Materials

5.2.1 Materials

Collagenase Type 1, HEPES, thiazolyl blue, phenazine ethosulphate, alcohol dehydrogenase, glucose-6-phosphate, glucose-6-phosphate dehydrogenase, 3-aminobenzamide, nicotinamide, theophylline and all nucleotides were purchased from Sigma Chemical Co Ltd (Poole, U.K.). 2,3-Dimethoxy-1,4-naphthoquinone was synthesised as previously described [Stubberfield and Cohen, 1988]. All other chemicals were purchased from BDH Ltd (Poole, Dorset, U.K.).

5.2.2 Isolation and Incubation of Rat Hepatocytes.

Rat hepatocytes were prepared as previously described [Moldeus et al, 1978] by collagenase perfusion of the livers of adult male Wistar rats (220-260g). The isolated cells (10^6 cell/ml) were suspended in Krebs Henseleit buffer containing 12.5 mM HEPES under an atmosphere of 95% O_2/5% CO_2 (pH 7.4) and were incubated in continuously rotating round bottom flasks at 37°C. Following isolation and prior to treatment the cells were preincubated at 37°C for 30 min. Cell viability was determined by trypan blue exclusion {in a 0.4% (w/v) solution}. Protein was measured by the method of Lowry et al (1951)

5.2.3 Determination of Pyridine Nucleotides.

Oxidized pyridine nucleotides (NAD^+, $NADP^+$) were determined using the spectrophotometric recycling assay of Bernofsky and Swan (1973) as previously described in chapter 2.

5.2.4 Inhibition of Poly(ADP-ribose)polymerase.

The inhibition of poly(ADP-ribose)polymerase was achieved by preincubation of freshly isolated hepatocytes for one hour with either 3-aminobenzamide (20 mM), nicotinamide (10 mM) or theophylline (7.5 mM). The hepatocytes were preincubated for one hour with the inhibitors to increase the intracellular concentration of the inhibitors in the cells. The cells were then exposed to either tBH (500 µM), 2,3-diOMe-1,4-NQ (50 µM), DMS (800 µM) or NMNG (280 µM) and at various times aliquots of cell suspension removed for NAD^+ analysis.

5.2.5 Determination of NAD^+ Hydrolysis.

NAD^+ hydrolysis was determined by measuring the simultaneous depletion of NAD^+ and the increase in nicotinamide. Intracellular NAD^+ was radioactively labelled at the nicotinamide moiety by intrapertoneal injection of a male Wistar rat (200-230g) with 12.5 µCi (0.227 µmol) [Carbonyl-^{14}C]-nicotinamide (Amersham International Ltd) as described previously [Richter et al, 1990]. 4-5 hours after injection hepatocytes were isolated as described in chapter 2. Following a 30 min preincubation, the cells were exposed to either tBH (500 µM), 2,3-diOMe-1,4-NQ (50 µM) menadione (50 µM) or DMS (800 µM) and at various times aliquots of cell suspension were removed for analysis of NAD^+ and nicotinamide.

NAD^+ and nicotinamide were extracted by resuspension of 10^6 cells in 1.0 ml 0.5M perchloric acid as described previously [Stubberfield and Cohen, 1989]. Prior to analysis the acid extracts were partially neutralized by the addition of 50 µl KOH (3M) and 10 µl KH_2PO_4 (0.1M) to 200 µl of the perchloric acid extract. NAD^+ and nicotinamide were first separated by ion-exchange HPLC on a partisil SAX ion-

exchanger (Millipore) attached to the System Gold HPLC system (Beckman Ltd) and a Waters 484 u.v. detector (Waters, Millipore) set at 254 nm. Samples were injected via a 50 µl loop. Optimum separation was achieved using an isocratic gradient with 0.01M ammonium phosphate (pH 4.9) pumped at 1.0 ml/min for 10 min, followed by 0.2M ammonium phosphate (pH 4.8) at 1.0 ml/min for 10 min and finally 0.01M ammonium phosphate (pH 4.9) at 1.0 ml/min for 25 min. Peaks containing NAD^+ and nicotinamide were identified by injecting unlabelled NAD^+ and nicotinamide and comparing retention times. Radioactivity was determined by liquid scintillation counting using aquasol scintillation fluid (Aquasol Ltd) and disintegrations per minute determined.

5.2.6 Statistical Analysis.

The results were expressed as mean ± SEM. Where appropriate statistical significance was tested by Student's *t*-test with the accepted significance level of $P < 0.05$.

5.3. Results

5.3.1 The Effect of Poly(ADP-ribose)polymerase Inhibitors on Intracellular NAD^+

The evidence for nucleotide interconversion was partially based on the observation of a depletion of NAD^+ in the presence of the poly(ADP-ribose)polymerase inhibitor, 3-aminobenzamide [Stubberfield and Cohen 1988; Cohen and Stubberfield, 1990; Yamamoto and Farber, 1992]. In the present study, hepatocytes were preincubated for 1 hour with either 3-aminobenzamide (20 mM), nicotinamide (10 mM) or theophylline (7.5 mM) prior to exposure to the toxicant.

The three polymerase inhibitors had differing effects on the intracellular level of NAD^+ in hepatocytes. Incubation for 60 min with either nicotinamide or 3-aminobenzamide resulted in a rapid increase in NAD^+ when compared to untreated hepatocytes, whereas a 60 min incubation with theophylline had no effect on the NAD^+ level (Fig. 5.1). The level of NAD^+ remained unchanged after 75 min and 90 min of incubation (Fig. 5.1).

5.3.2 The Effect of the Poly(ADPribose)polymerase Inhibitors on 2,3-diOMe-1,4-NQ and t-BH Induced NAD^+ Depletion

In hepatocytes exposed to either 2,3-diOMe-1,4-NQ (50 µM) or tBH (500 µM), intracellular NAD^+ fell rapidly for 30 min, with the greatest rate of decrease observed within the first 15 min (Table 5.1). Following a 60 min preincubation with the polymerase inhibitors, the depletion of NAD^+ induced by both 2,3-diOMe-1,4-NQ and tBH was significantly reduced (Fig. 5.2 and 5.3).

5.3.3 The Effect of Poly(ADP-ribose)polymerase Inhibitors on Dimethyl Sulphate and NMNG Induced NAD^+ Depletion

The ability of the poly(ADP-ribose)polymerase inhibitors to prevent the depletion of NAD^+ induced by compounds which cause DNA damage has previously been used as evidence of the activation of the enzyme. In the studies of Stubberfield and Cohen, (1988) the ability of 3-aminobenzamide to prevent the depletion of NAD^+ induced by the alkylating agent dimethyl sulphate (DMS) is compared to its effects on quinone-induced NAD^+ depletion.

In this study, such a direct comparison could not be made as the initial rate of NAD^+ depletion induced by DMS was significantly less than that induced by 2,3-diOMe-1,4-NQ (50 μM) and tBH (500 μM) (Table 5.1). In the presence of the polymerase inhibitors, DMS-induced NAD^+ was significantly reduced (Fig. 5.4).

NMNG is also known to cause DNA damage and the depletion of NAD^+. In this study both 3-aminobenzamide and theophylline caused a reduction in NMMG-induced NAD^+ depletion. However nicotinamide had no effect on NMNG-induced NAD^+ depletion (Fig 5.5).

5.3.4 Radiolabelling of Intracellular Pyridine Nucleotides

The concept of nucleotide interconversion excludes the possibility of NAD^+ hydrolysis. However both redox cycling quinones and tert-butyl hydroperoxide have been reported to induce DNA damage [Cantoni *et al* 1991; Coleman *et al* 1989]. Following DNA damage poly(ADP-ribose)polymerase hydrolyses NAD^+ to nicotinamide and ADP-ribose [Skidmore et al, 1979]. In order to determine whether intracellular NAD+ is hydrolysed to nicotinamaide or phosphorolated to $NADP^+$

during oxidative stress, intracellular pyridine nucleotides were radiolabelled at the nicotinamide moiety as described in the Methods and Materials. Hepatocytes containing radiolabelled nucleotides were then exposed to a number of compounds which have previously been shown to cause a rapid depletion of NAD+ and intracellular nicotinamide NAD^+ and $NADP^+$ levels determined.

In untreated cells and in cells exposed to tBH and DMS, approximately 40-50% of the total cellular radioactivity was recovered by the acid extraction procedure of NAD^+, $NADP^+$ and nicotinamide. In cells exposed to the redox cycling quinones 2,3-diOMe-1,4-NQ (50 µM) and menadione (50 µM) this increased to approximately 70%. HPLC separation of the acid extract revealed radioactivity primarily in the peaks which coeluted with either nicotinamide, NAD^+ or $NADP^+$.

5.3.5 The Effect of Redox Cycling Quinones on Intracellular NAD^+ Radioactively Labelled in the Nicotinamide Moiety.

In untreated cells a greater proportion of the cells radioactivity was detected in NAD^+ than in nicotinamide (Fig 5.6). In cells exposed to the redox cycling quinones 2,3-diOMe-1,4-NQ (50 µM) and menadione (50 µM) for 15 and 30 min, a decrease in radioactivity associated with NAD^+ was accompanied by a simultaneous increase in radioactivity in the nicotinamide peak (Fig. 5.7 and Fig. 5.8) . The increase in nicotinamide radioactivity was approximately equal to that lost from NAD^+. Furthermore, in these cells an additional radioactive peak was found which co-eluted with $NADP^+$. As the radioactivity lost from NAD^+ could be accounted for by the increase in nicotinamide, the most likely source of the increase in radioactivity associated with $NADP^+$ is the oxidation of NADPH.

5.3.6. The Effect of tBH and Dimethyl Sulphate on Intracellular NAD^+ Radioactively Labelled in the Nicotinamide Moiety.

Cells containing the radiolabelled nucleotides were exposed to tBH as well as the alkylating agent dimethyl sulphate. Both compounds caused a simultaneous depletion of NAD+ and an increase in nicotinamide radioactivity (Fig. 5.9 and 5.10). No increase in radioactivity or in the peak associated with $NADP^+$ was observed in cells exposed to dimethyl sulphate and tBH.

Table 5.1 The effects of poly(ADP-ribose)polymerase inhibitors on the rate of NAD^+ depletion in rat hepatocytes.

	rate of NAD^+ depletion (pmol/min)			
	poly(ADP-ribose)polymerase inhibitors			
	-inhib	nico (10 mM)	3-ab (20 mM)	thp (7.5mM)
2,3-diOme (50 µM)	113 ± 19	83 ± 20@	82 ± 21@	84 ± 20
tBH (500 µM)	129 ± 21	92 ± 21@	72 ± 17@	61 ± 23@
DMS (800 µM)	59 ± 17*	13 ± 8@	24 ± 12@	32 ± 16@
NMNG (280 µM)	49 ± 42*	48 ± 42	37 ± 36	37 ± 30

Hepatocytes were incubated either in absence (-inhib) or in the presence of nicotinamide: 10 mM (nico), 3-aminobenzamide: 20 mM (3-ab) or theophylline: 7.5 mM (thp). After 1 hour the cells were then exposed to either 2,3-diOMe-1,4-NQ (2,3-diOme), t-BH, dimethyl sulphate (DMS) or NMNG for 15 min and intracellular NAD^+ determined as described in the Materials and Methods. Values represent the Mean ± SEM of at least 3 separate incubations. * Rate of hydrolysis significantly ($P < 0.05$) different from 2,3-diOMe-1,4-NQ-mediated (50 µM) hydrolysis. @ Rate of hydrolysis significantly different from the equivalent -inhib.

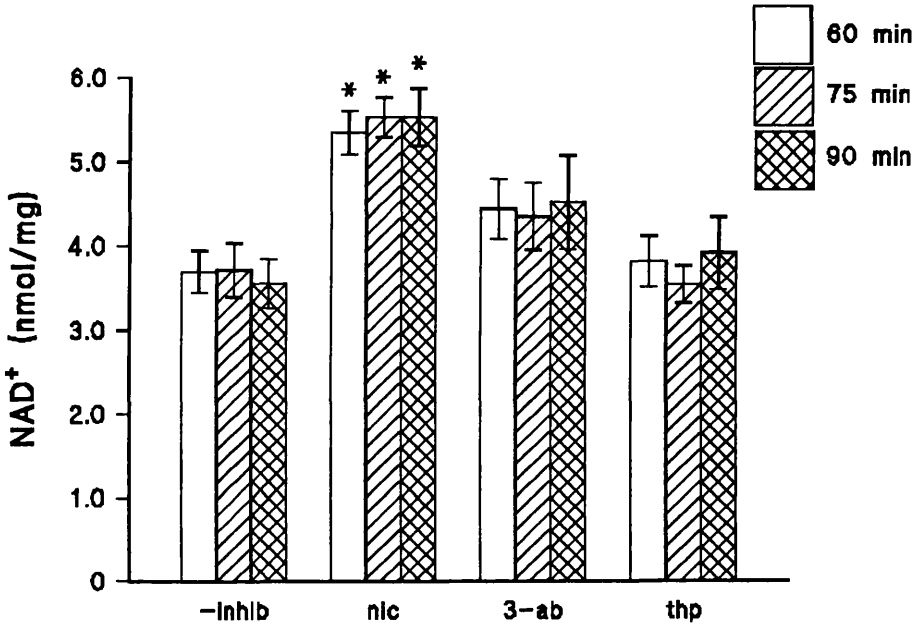

Fig. 5.1 The effect of poly(ADP-ribose)polymerase inhibitors on intracellular NAD^+. Hepatocytes were incubated either in the absence (-inhib) or in the presence of nicotinamide: 10 mM (nic), 3-aminobenzamide: 20 mM (3-ab) or theophylline: 7.5 mM (thp). At the designated times intracellular NAD^+ was determined as described in the Materials and Methods. Values represent the Mean ± SEM of at least 3 separate incubations. * Significantly different ($p < 0.05$) from the control (-inhib).

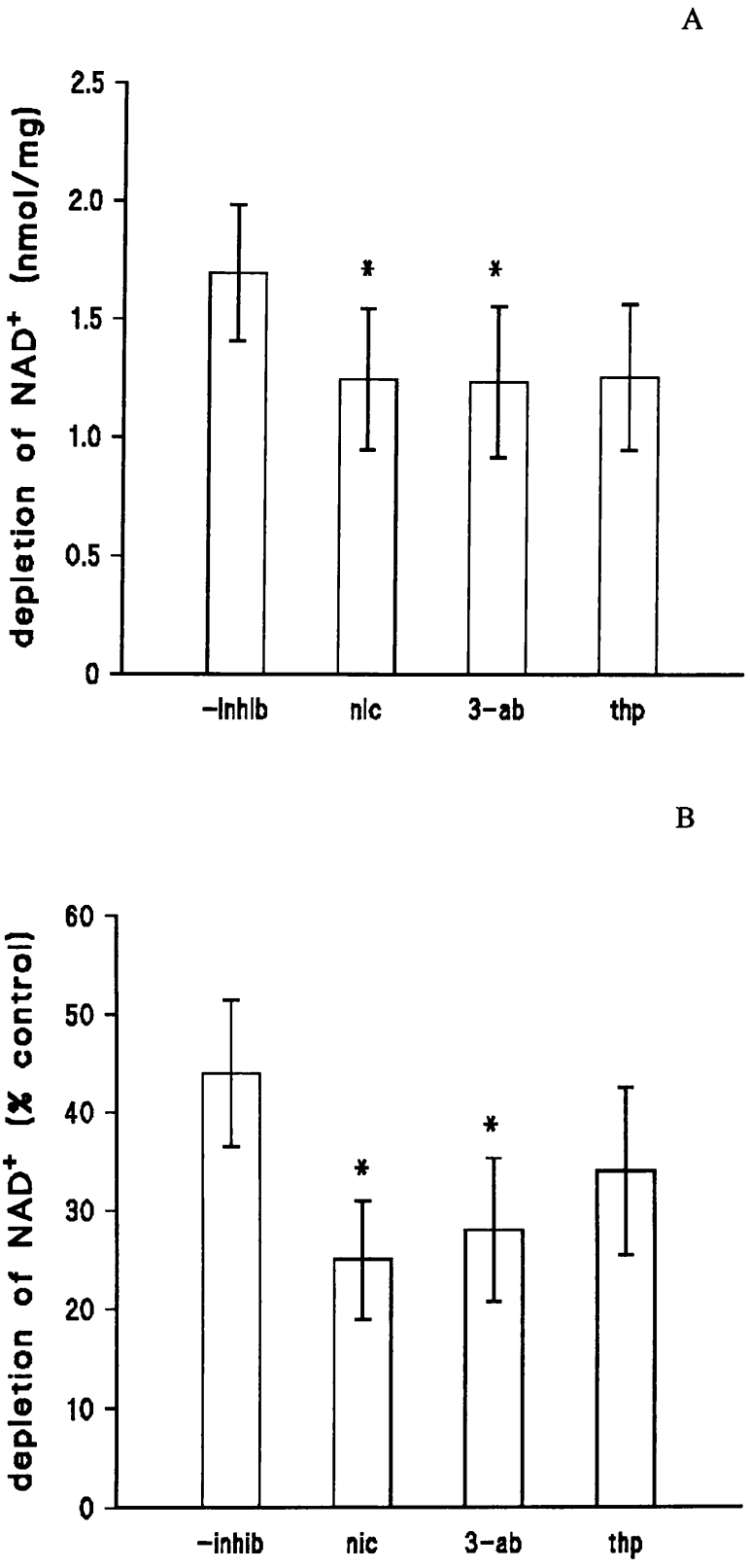

Fig. 5.2 The effects of poly(ADP-ribose)polymerase inhibitors on quinone-induced intracellular NAD^+ depletion. (A) The amount of NAD^+ depleted and (B) the percentage of initial NAD^+ lost. Hepatocytes were incubated either in the absence (-inhib) or in the presence of nicotinamide: 10 mM (nic), 3-aminobenzamide: 20 mM (3-ab) or theophylline: 7.5 mM (thp). After 1 hour the cells were exposed to 2,3-diOMe-1,4-NQ (50 µM) for 15 min and NAD^+ determined as described in the Materials and Methods. Values represent the Mean ± SEM of at least 3 separate incubations. * Significantly different ($p < 0.05$) from the control (-inhib).

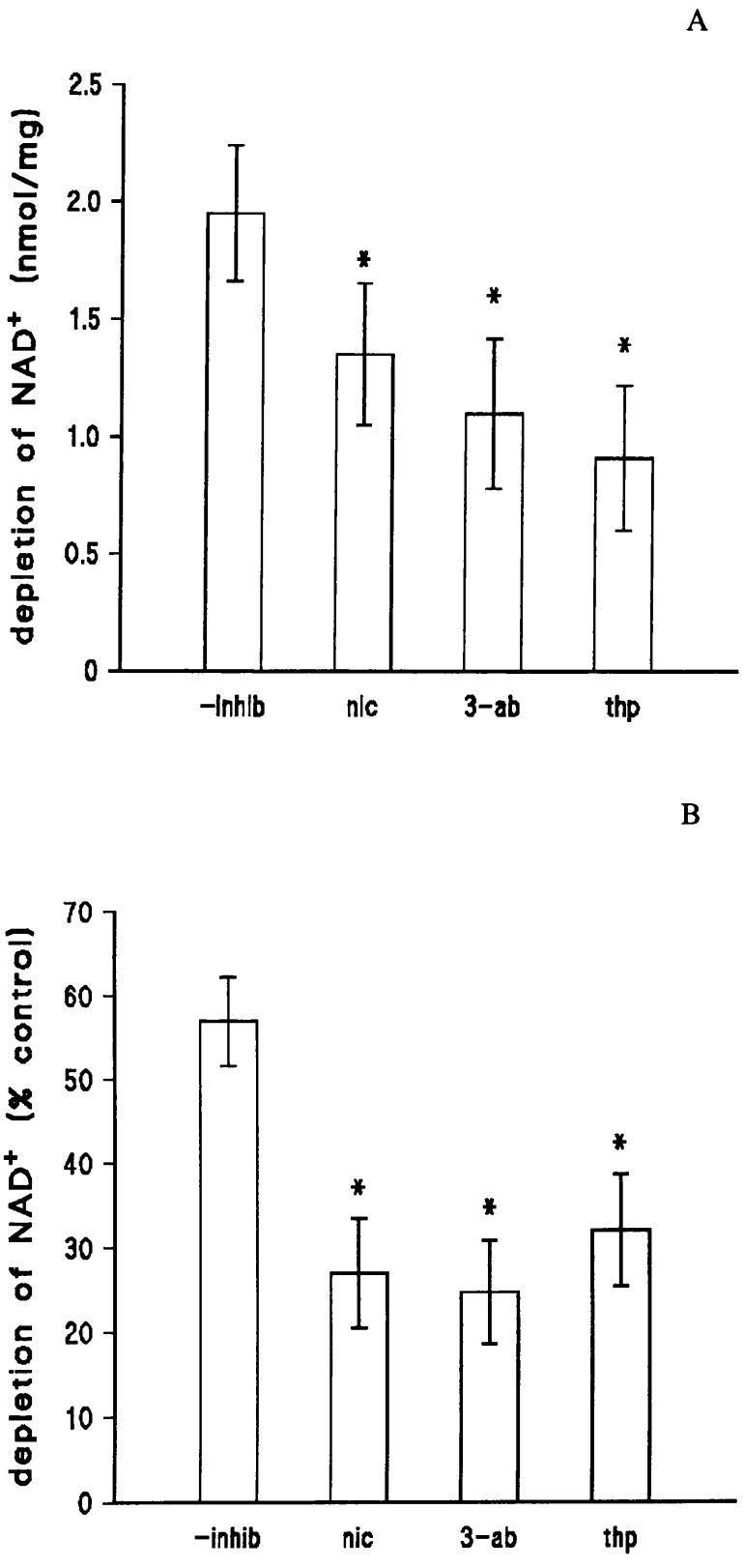

Fig. 5.3 The effects of poly(ADP-ribose)polymerase inhibitors on tBH-induced intracellular NAD^+ depletion. (A) The amount of NAD^+ depleted and (B) the percentage of initial NAD^+ lost. Hepatocytes were incubated either in the absence (-inhib) or in the presence of nicotinamide: 10 mM (nic), 3-aminobenzamide: 20 mM (3-ab) or theophylline: 7.5 mM (thp). After 1 hour the cells were exposed to tBH (500 μM) for 15 min and NAD^+ determined as described in the Materials and Methods. Values represent the Mean ± SEM of at least 3 separate incubations. * Significantly different ($p < 0.05$) from the control (-inhib).

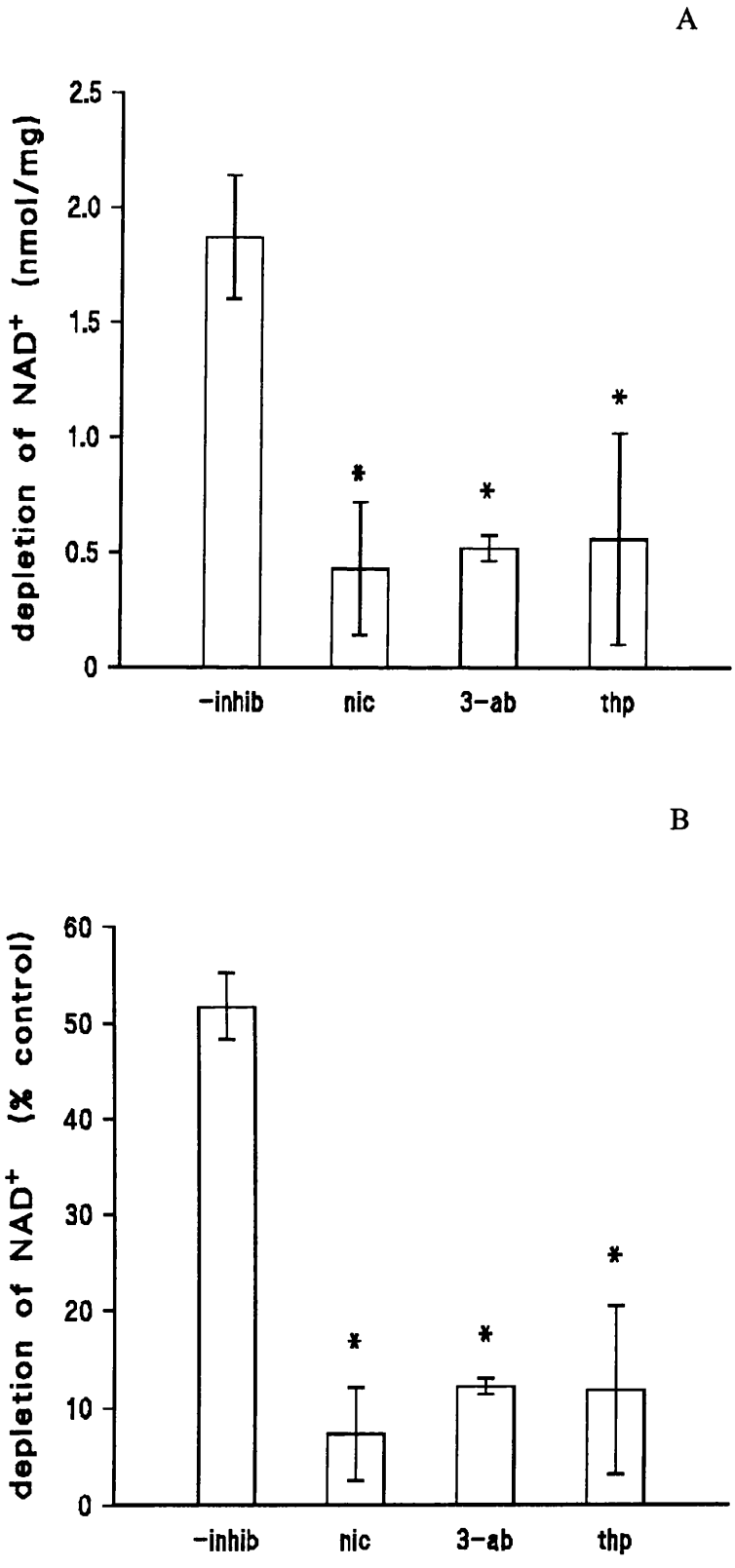

Fig. 5.4 The effects of poly(ADP-ribose)polymerase inhibitors on dimethyl sulphate-induced intracellular NAD^+ depletion. (A) The amount of NAD^+ depleted and (B) the percentage of initial NAD^+ lost. Hepatocytes were incubated either in the absence (-inhib) or in the presence of nicotinamide: 10 mM (nic), 3-aminobenzamide: 20 mM (3-ab) or theophylline: 7.5 mM (thp). After 1 hour the cells were exposed to DMS (800 µM) for 30 min and NAD^+ determined as described in the Materials and Methods. Values represent the Mean ± SEM of at least 3 separate incubations. * Significantly different ($p < 0.05$) from the control (-inhib).

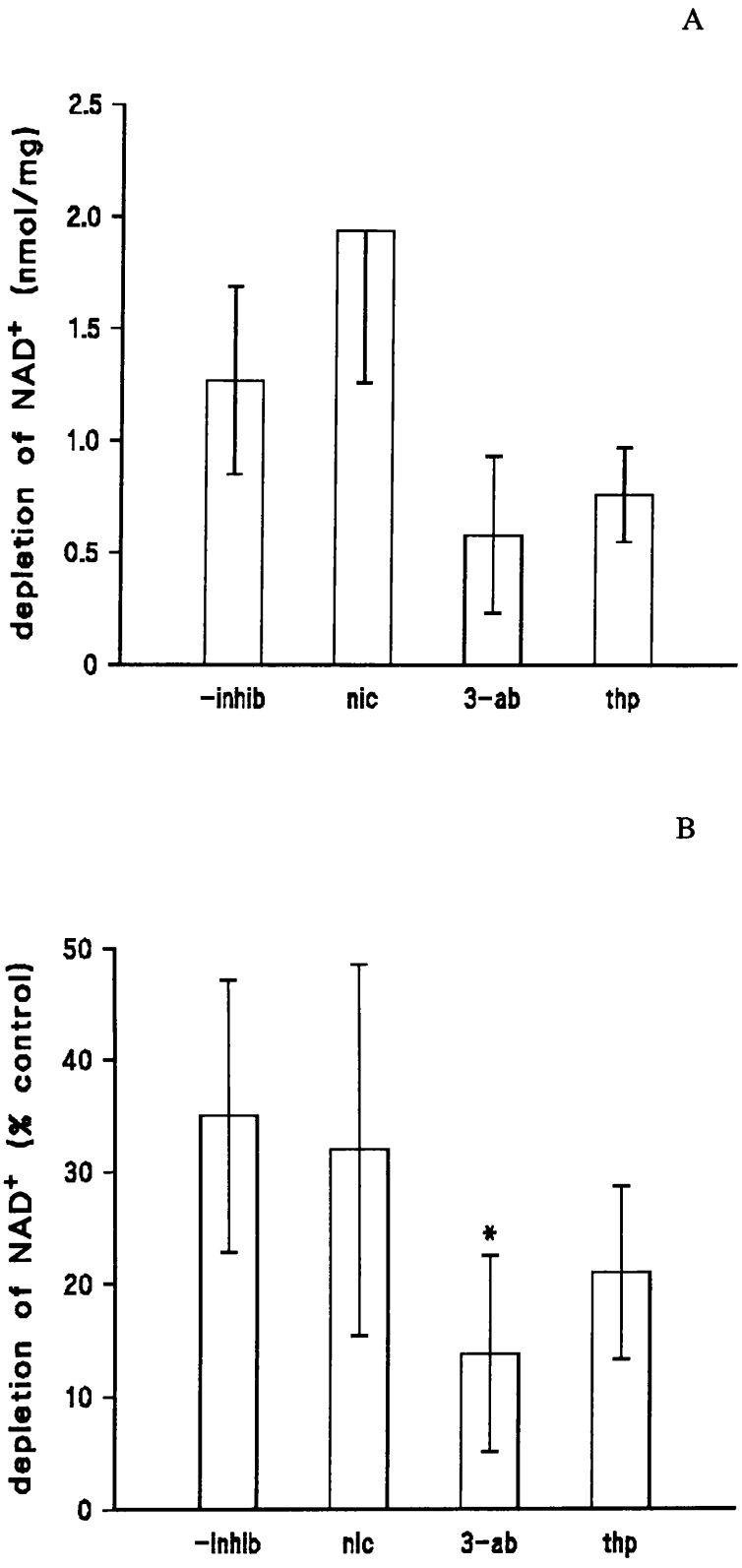

Fig. 5.5 The effects of poly(ADP-ribose)polymerase inhibitors on NMNG induced intracellular NAD^+ depletion. (A) The amount of NAD^+ depleted and (B) the percentage of initial NAD^+ lost. Hepatocytes were incubated either in the absence (-inhib) or in the presence of nicotinamide: 10 mM (nic), 3-aminobenzamide: 20 mM (3-ab) or theophylline: 7.5 mM (thp). After 1 hour the cells were exposed to NMNG (280 µM) for 30 min and NAD^+ determined as described in the Materials and Methods. Values represent the Mean ± SEM of at least 3 separate incubations. * Significantly different ($p < 0.05$) from the control (-inhib).

A

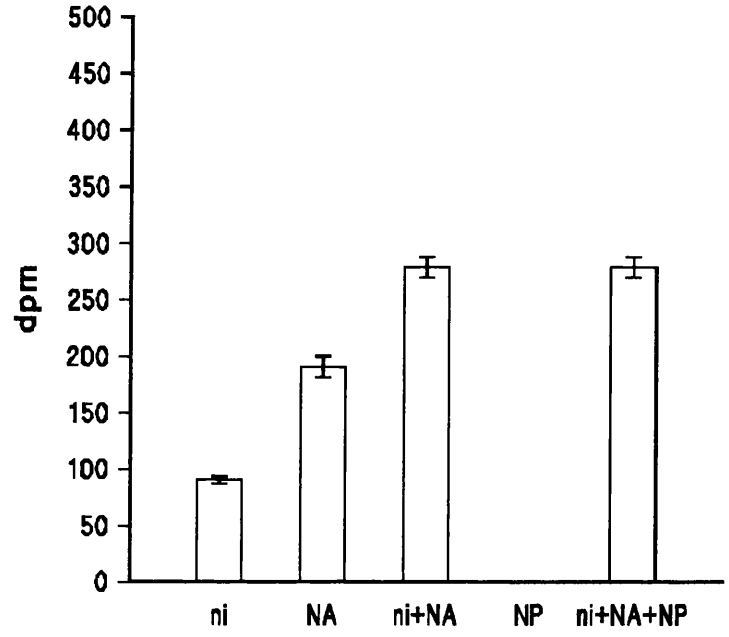

B

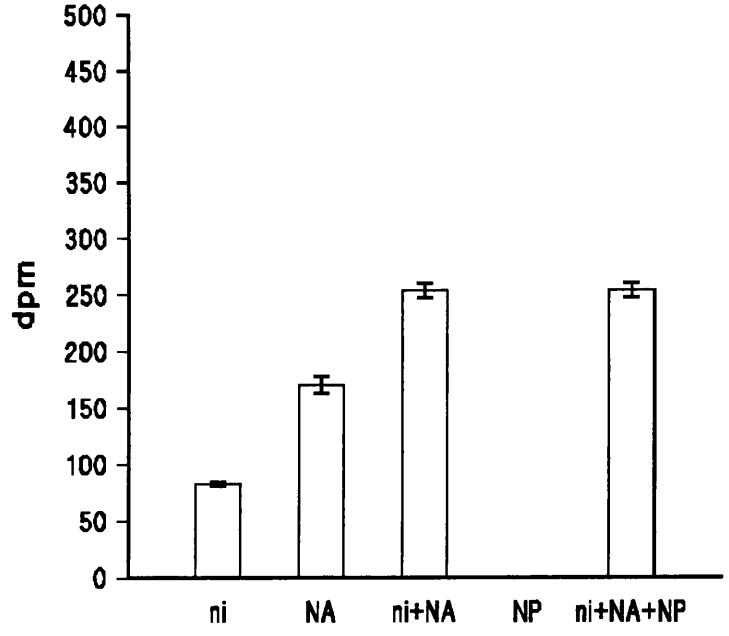

Fig. 5.6 The effect of DMSO on intracellular NAD^+ radiolabelled in the nicotinamide moiety. (A) after 15 min exposure and (B) after 30 min exposure. Hepatocytes were exposed to DMSO for the designated time, after which NAD^+ (NA), nicotinamide (ni) and $NADP^+$ (NP) were determined as described in the Materials and Methods. Values represent the Mean ± SEM of three separate incubations.

A

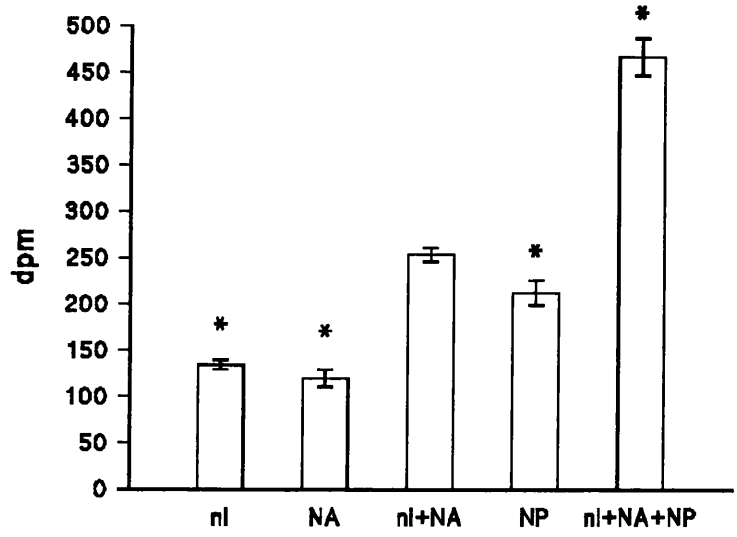

B

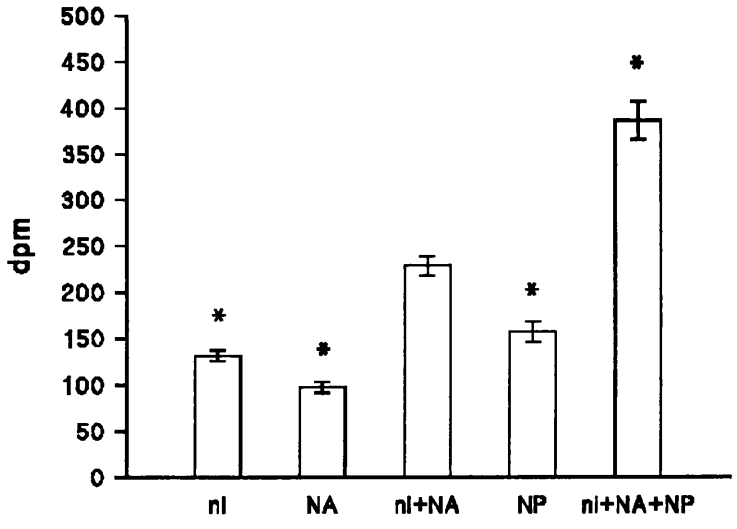

Fig. 5.7 The effects of 2,3-diOMe-1,4-NQ on the intracellular NAD^+ radiolabelled in the nicotinamide moiety. (A) after 15 min exposureand (B) after 30 min exposure. Hepatocytes were exposed to the quinone for the designated time, after which NAD^+ (NA), nicotinamide (ni) and $NADP^+$ (NP) were determined as described in the Materials and Methods. Values represent the Mean ± SEM of three separate incubations. * Significantly different ($p < 0.05$) from the control (Fig. 5.6).

A

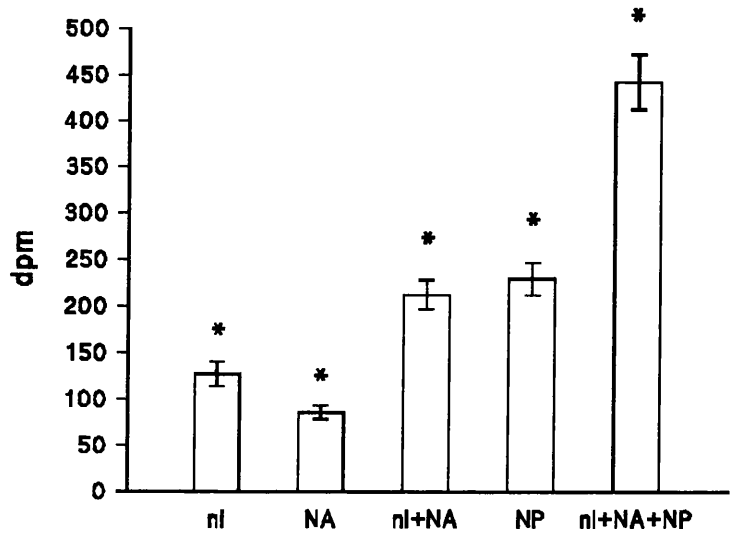

B

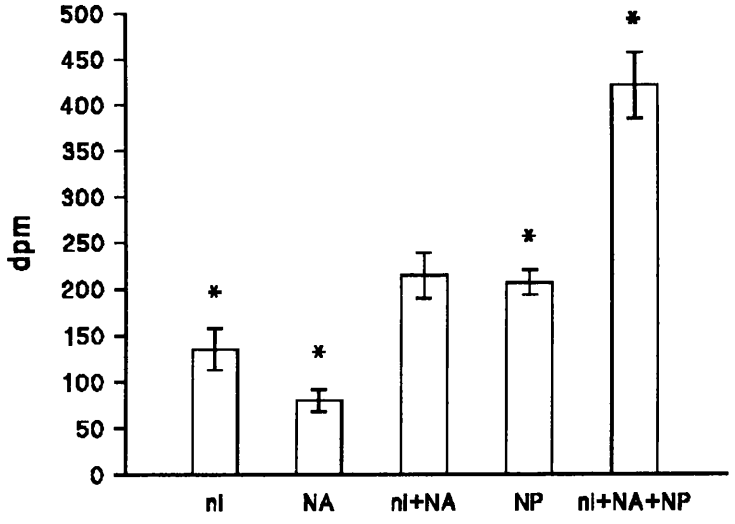

Fig. 5.8 The effects of menadione on the intracellular NAD^+ radiolabelled in the nicotinamide moiety. (A) after 15 min exposureand (B) after 30 min exposure. Hepatocytes were exposed to menadione for the designated time, after which NAD^+ (NA), nicotinamide (ni) and $NADP^+$ (NP) were determined as described in the Materials and Methods. Values represent the Mean ± SEM of three separate incubations. * Significantly different ($p < 0.05$) from the control (Fig. 5.6).

A

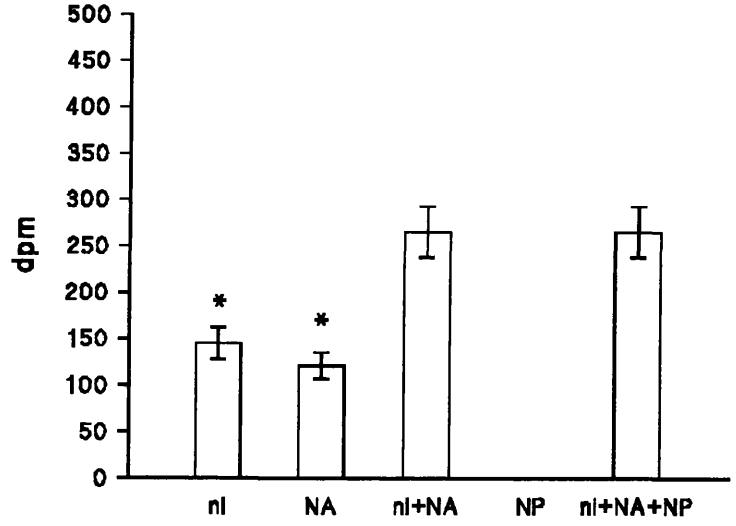

B

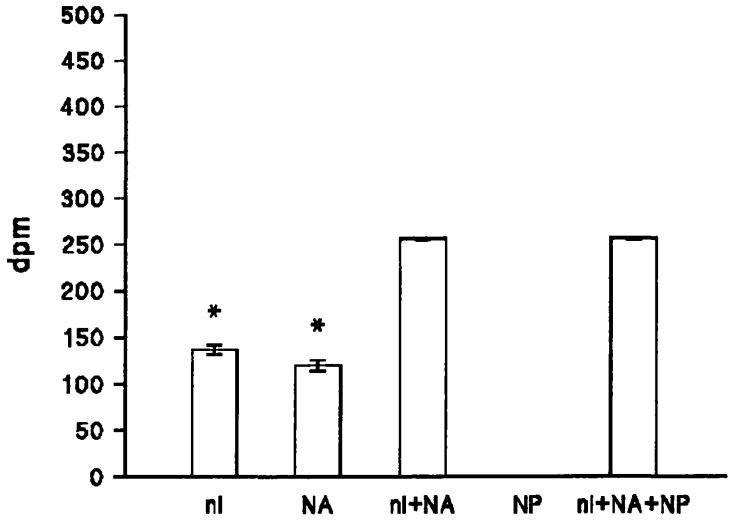

Fig. 5.9 The effects of tBH on the intracellular NAD^+ radiolabelled in the nicotinamide moiety. (A) after 15 min exposureand (B) after 30 min exposure. Hepatocytes were exposed to tBH for the designated time, after which NAD^+ (NA), nicotinamide (ni) and $NADP^+$ (NP) were determined as described in the Materials and Methods. Values represent the Mean ± SEM of three separate incubations. * Significantly different ($p < 0.05$) from the control (-inhib).

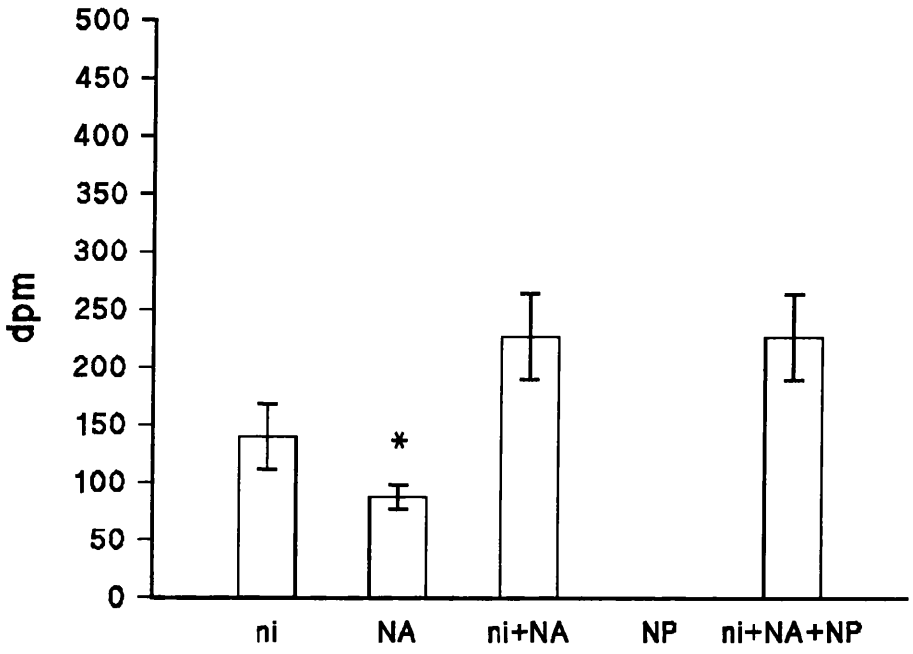

Fig. 5.10 The effects of dimethyl sulphate on the intracellular NAD^+ radiolabelled in the nicotinamide moiety. (A) after 15 min exposure and (B) after 30 min exposure. Hepatocytes were exposed to DMS for the designated time, after which NAD^+ (NA), nicotinamide (ni) and $NADP^+$ (NP) were determined as described in the Materials and Methods. Values represent the Mean ± SEM of three separate incubations. * Significantly different ($p < 0.05$) from the control (Fig. 5.6).

5.4. DISCUSSION

5.4.1 Poly(ADP-ribose)polymerase and Intracellular NAD^+

DNA strand breakage resulting from the exposure of mammalian cells to a variety of chemical agents has often been associated with the activation of poly(ADP-ribose)polymerase and the rapid depletion of intracellular NAD^+. In recent studies, Yamamoto and Farber (1992) found that the depletion of NAD^+ induced by tBH in rat hepatocytes was not prevented by 3-aminobenzamide while Stubberfield and Cohen (1988) reported a similar result in hepatocytes exposed to several redox cycling quinones. They suggested that during oxidative stress the depletion of NAD^+ was independent of the activation of poly(ADP-ribose)polymerase. Furthermore they proposed that the depletion of NAD^+ was due to an interconversion of pyridine nucleotides. However, results presented in the previous chapter suggest the depletion of NAD^+ is probably due to hydrolysis. In this chapter, data from two separate experiments provide evidence of poly(ADP-ribose)polymerase mediated hydrolysis of NAD^+.

The inhibition of Poly(ADP-ribose)polymerase in whole cell systems is particularly difficult as the enzyme is closely associated with the chromatin [Ueda and Hayaishi, 1985; Rankin et al, 1989]. Successful inhibitor studies of the enzyme are usually performed in either cell free systems, in permeabilized cells or following a long preincubation period in the presence of the inhibitor [Althaus and Richter 1987]. In this study three experimental changes were made to the previous studies of Stubberfield and Cohen (1988): cells were preincubated with the inhibitor for one hour prior to exposure to the toxicant; low concentrations of the toxicant were used and the

cells were exposed for a short time to the toxicant.

The increased intracellular NAD^+ observed in cells preincubated with either 3-aminobenzamide or nicotinamide provides evidence of the inhibition of NAD^+ hydrolysis within the cell (Fig. 5.1). In the studies of Stubberfield and Cohen (1988) the inhibitor was added just prior to the addition of the quinone, under these circumstances the inhibitor most probably could not enter the nucleus at the concentration necessary to inhibit the enzyme. In a recent study Rankin et al (1989) suggested that only 1% of the extracellular 3-aminobenzamide has entered the cell after 30 min.

5.4.2 The Effect of Poly(ADP-ribose)polymerase Inhibitors on Quinone and tBH Induced NAD^+ Depletion

In this study the poly(ADP-ribose)polymerase inhibitors nicotinamide, 3-aminobenzamide and theophylline significantly inhibited the rate of NAD^+ depletion induced by tBH and 2,3-diOMe-1,4-NQ (Fig 5.2 and 5.3). In the previous studies of Stubberfield and Cohen (1988) and Yamamoto and Farber (1992) the reported failure of poly(ADP-ribose)polymerase inhibitors to inhibit the depletion of NAD^+ was probably due to experimental design. In the studies of Stubberfield and Cohen (1988) the effect of the inhibitor was examined following 3 hours in the presence of the quinones. Furthermore, cytotoxic concentrations of the quinones were used. Under such circumstances no inhibition would be expected. The extent of activation of poly(ADP-ribose)polymerase is directly related to the number of DNA strand breaks. By using low non-toxic concentrations of a toxicant, the activation of the enzyme would be reduced, facilitating enzyme inhibition. Similarly, the rapid rate of reaction

of the enzyme means that shortly after activation most of the available NAD^+ is rapidly hydrolysed. Hence only by determining the rate of NAD^+ depletion after a short exposure to a toxicant can the effects of the polymerase inhibitors be seen.

5.4.3 The Effect of Poly(ADP-ribose)polymerase Inhibitors on Dimethyl Sulphate and NMNG Induced NAD^+ Depletion

The effects of the polymerase inhibitors on DMS induced NAD^+ depletion were also examined. As previously reported by Cohen and Stubberfield (1990), the polymerase inhibitor significantly inhibited the depletion of NAD^+ induced by dimethyl sulphate. Previously, when the effects of the polymerase inhibitors on dimethyl sulphate were compared to their effects on certain redox cycling quinones, the polymerase inhibitors completely inhibited dimethyl sulphate induced NAD^+ depletion, whereas the inhibitors had no effects on quinone induced NAD^+ depletion. However, these results suggest such direct comparisons could not be made as the initial rate of NAD^+ depletion induced by both tBH and 2,3-diOMe-1,4-NQ was nearly twice that induced by dimethyl sulphate (Table 5.1). This observation may partially explain the different effects of the inhibitors on dimethyl sulphate and the quinones previously reported [Stubberfield and Cohen, 1988].

In this study, the effects of the polymerase inhibitors on dimethyl sulphate induced NAD^+ depletion were compared to NMNG. Both are known to cause DNA damage by alkylation. An initial slow rate of NAD^+ depletion was observed in cells exposed to either compound. The rate of NAD^+ depletion increased to levels which were comparable to tBH and the quinones by 30 min. However, despite their similar initial rate of depletion, the inhibitors were far more effective in inhibiting dimethyl sulphate

induced NAD^+ depletion. NMNG was only partially inhibited by 3-aminobenzamide and theophylline while nicotinamide was less effective. These results suggest that the ability of polymerase inhibitors to completely inhibit dimethyl sulphate induced NAD^+ depletion may be due in part to a direct interaction between the inhibitor and dimethyl sulphate. This observation may account for the inhibition of DMS induced NAD^+ depletion and cytotoxicity reported previously, although only a short preincubation was used in those studies ['Stubberfield and Cohen 1988].

5.4.4 The Determination of NAD^+ Hydrolysis and Nicotinamide Formation

A further experiment was designed to determine the fate of NAD^+ during oxidative stress. The hydrolysis of NAD^+ by poly(ADP-ribose)polymerase would result in the simultaneous loss NAD^+ and increased nicotinamide formation. By radiolabelling the nucleotide at the nicotinamide moiety, a direct correlation could be made between the hydrolysis of NAD^+ and the formation of nicotinamide. Hepatocytes containing labelled pyridine nucleotides were exposed to a number of compounds which had previously been shown to cause a rapid depletion of NAD^+. In cells exposed to either 2,3-diOMe-1,4-NQ, menadione, tBH or dimethyl sulphate, the depletion of NAD^+ was accompanied by the simultaneous formation of nicotinamide. Furthermore the loss in NAD^+ was equivalent to the increase in nicotinamide. These results strongly suggest that during oxidative stress the depletion of NAD^+ is mediated by poly(ADP-ribose)polymerase or a related enzyme. These results clearly eliminate the possibility of an nucleotide interconversion as the explaination of the depletion of NAD^+ during oxidative stress.

CHAPTER 6

QUINONE-INDUCED DNA STRAND BREAKAGE IN RAT HEPATOCYTES AND HUMAN CHRONIC MYELOGENOUS LEUKAEMIC K562 CELLS

Abstract- In rat hepatocytes exposed to the quinones menadione or 2,3-dimethoxy-1,4-naphthoquinone (2,3-diOMe-1,4-NQ) a decrease in NAD^+ is observed. A decrease in NAD^+ is usually associated with DNA damage and activation of poly(ADP-ribose)polymerase. Using rat hepatocytes and human myeloid leukaemic cells (K562), this study examines the extent of DNA damage induced by these quinones at non-toxic concentrations i.e. at concentrations where all the cells exclude the dye trypan blue. Both quinones caused significant DNA damage at very low concentrations (5-100 μM). With 2,3-diOMe-1,4-NQ (15 μM) or menadione (15 μM) single strand breaks (SSB) as measured by alkaline elution were observed at very early time points (< 5 min), reaching a maximum between 20 and 30 min. Most SSB were repaired within 45 minutes of the removal of the quinones. Whilst complete repair was observed within 4 hours of the removal of 2,3-diOMe-1,4-NQ (15 μM), only partial repair was observed following exposure to menadione (15 μM). SSB induced by 2,3-diOMe-1,4-NQ (15 μM) were completely inhibited by the iron chelator 1,10-phenanthroline (25 μM), whereas in cells exposed to menadione (15 μM) they were only partially inhibited.

These results demonstrate that at very low concentrations the quinones induce extensive DNA damage possibly caused by hydroxyl radicals. The DNA damage was accompanied by an early cytostasis but not by a loss of membrane integrity.

6.1 INTRODUCTION

During oxidative stress, single strand breaks (SSB) in DNA may be induced by hydroxyl radicals generated during the metabolism of redox cycling quinones [Kappus and Sies, 1981; Starke and Farber, 1985]. This process involves the reduction of H_2O_2 by divalent metal ions, particularly Fe^{2+} in an iron catalysed Haber-Weiss reaction [Starke and Farber, 1985; Loeb et al, 1988]. During oxidative stress DNA damage may also result from the activation of Ca^{2+} dependent endonucleases possibly leading to DNA fragmentation and apoptosis [Cotter et al, 1990; McConkey et al, 1988].

Previously, in hepatocytes exposed to either 2,3-dimethoxy-1,4-naphthoquinone (2,3-diOMe-1,4-NQ) or menadione, Stubberfield and Cohen (1989) observed a decrease in the level of NAD^+, suggesting DNA damage and the activation of poly(ADPribose)polymerase. However in studies with inhibitors of poly(ADP-ribose)polymerase, Cohen and Stubberfield, 1990 found no evidence of the activation of the polymerase. Furthermore they inferred that in cells exposed to redox cycling quinones the depletion of NAD^+ was not due to DNA damage and the activation of poly(ADP-ribose)polymerase. The present study employs rat hepatocytes and human chronic myelogenous leukaemic cells (K562) [Lozzio and Lozzio, 1975](which possess NADPH-cytochrome c (cytochrome P-450) reductase [Trakshel et al, 1987] one of the major enzymes involved in the one electron reduction of redox cycling quinones) to investigate the extent of DNA damage induced by these quinones. The initial studies were carried out with isolated hepatocytes, which only remain viable for a short period of time (4-6h), thus making it difficult to perform long term studies. Additionally isolated hepatocytes have a high level of background strand breakage (Morrison et al

1984). In order to overcome this difficulty these studies were extended to K562 cells, which provide a more suitable model to assess the long term effects of DNA damage [Halliwell and Aruoma, 1991].

6.2. Materials and Methods

6.2.1 Materials.

Collagenase Type 1, HEPES and proteinase-K were obtained from Sigma Chemical Co. Ltd (Poole, U.K.). [^{14}C]-Thymidine (50-60mCi/mmol) was obtained from Amersham International (Rickmansworth, Herts, U.K.). Polyvinyl chloride filters were purchased from Millipore. Menadione (2-methyl-1,4-naphthoquinone) was obtained from Aldrich Chemical Co. (Gillingham, U.K.) and 2,3-diOMe-1,4-NQ was synthesized as previously described [Stubberfield and Cohen, 1989]. All other chemicals were obtained from BDH Ltd (Poole, Dorset, U.K.).

6.2.2 Isolation and Incubation of Rat Hepatocytes.

Hepatocytes were prepared as previously described [Stubberfield and Cohen, 1988] by collagenase perfusion of the livers of adult male Wistar rats (220-260g). Cell viability (85-95%) was determined by their ability to exclude trypan blue, 0.4% w/v final concentration. The isolated cells (10^6 cells/ml) were suspended in Krebs-Henseleit buffer containing 12.5 mM HEPES under an atmosphere of 95% O_2/5% CO_2 (pH 7.4) and incubated at 37°C in continuously rotating round bottom flasks. Following isolation the cells were allowed to equilibrate by preincubation at 37°C for 30 min prior to treatment.

The quinones were dissolved in DMSO and added at a final DMSO concentration of 0.1% v/v. The control incubations had a final DMSO concentration of 0.1% v/v alone. After exposure to the quinones, 0.8 ml aliquots of cell suspension (10^6 cells/ml) were

removed and spun at 500 rpm for 1 min in a bench centrifuge (4°C). The supernatant solution was removed by aspiration and the cells resuspended in 2 ml of ice cold Krebs-Henseleit buffer and kept on ice for 30 min prior to determination of DNA damage as described below.

6.2.3 Cell Culture and Treatment.

Human chronic myelogenous leukaemic cells (K562), from the Department of Oncology, University College and Middlesex School of Medicine, were cultured in RPMI 1640 supplemented with 5% heat inactivated foetal calf serum and L-glutamine(2mM) at 37°C. In order to determine damage to DNA, cells in exponential growth phase were labelled with 0.015 μCi/ml [^{14}C]-thymidine for 20 hours, then incubated in the absence of radiolabel for 1 hour to chase all the radioactivity into high molecular weight DNA prior to treatment. Cells (10^6/ml) were then exposed to the quinones (in DMSO 0.1% v/v) and incubated for various times at 37°C. Aliquots (0.8 ml) of the cell suspension were removed and made up to 10 ml with ice cold phosphate buffered saline and immediately assayed for DNA damage as described below.

6.2.4 Measurement of Single Strand Breaks (SSB) in DNA.

SSB were assayed by alkaline elution as described previously in chapter 2. Briefly, the cells (8×10^5) were lysed on 2 μm pore, 25 mm diameter polycarbonate filters with a sodium dodecylsarcosine-NaCl-EDTA lysis solution at pH 10. Elution was carried out at a rate of 2 ml/hour for 15 hours in a tetrapropylammonium hydroxide-

EDTA solution at pH 12.1. Samples were collected every three hours and assayed for ^{14}C radioactivity. As the DNA of isolated hepatocytes could not be radioactively labelled, the eluted DNA was determined fluorometrically using Hoechst 33258 as described by Stout and Becker (1982).

6.2.5 Determination of NAD^+ in K562 Cells

NAD^+ was assayed as described earlier. Briefly, following exposure to the quinones, 1.0 ml aliquots (10^6 cells/ml) of cell suspension were sedimented by bench centrifugation at 1000 rpm for 3 min and the supernatant fraction aspirated. NAD^+ was extracted by addition of 0.5M perchloric acid and the acid extract stored at -80°C prior to analysis.

6.3. RESULTS

6.3.1 Quinone-Induced Toxicity and SSB in Rat Hepatocytes.

Neither menadione (50 μM) nor 2,3-diOMe-1,4-NQ (50 μM) were toxic to isolated hepatocytes as assessed by trypan blue exclusion in agreement with previous studies [Stubberfield and Cohen, 1989]. In contrast, a brief exposure (15 min) of hepatocytes to either quinone caused significant SSB (Fig. 6.1) as assessed by alkaline elution [Kohn et al, 1981]. Under these conditions, the extent of SSB was greater in cells exposed to menadione than 2,3-diOMe-1,4-NQ (Fig. 6.1). A significant number of SSB was also observed in control hepatocytes incubated in the absence of the quinones. This was possibly related to the presence of approximately 15-20% dead cells in the incubation. In subsequent studies on quinone-induced DNA strand breakage, human chronic myelogenous K562 cells were employed. These cells provided two advantages over hepatocytes; they could be cultured for several generations and the background level of strand breakage was less than the hepatocytes.

6.3.2 Quinone-Induced SSB in K562 Cells.

In K562 cells exposed to either 2,3-diOMe-1,4-NQ or menadione (15 μM), SSB could be detected by 5 min and within 10 min DNA damage was extensive (Fig. 6.2 and 6.3). Within the first 10 min of exposure there was greater DNA damage in cells exposed to 2,3-diOMe-1,4-NQ (Fig. 6.2) than cells exposed to menadione (Fig. 6.3). Maximum DNA damage was observed between 30 and 60 min with no further

increase in SSB beyond 30 min. Both quinones induced a concentration dependent increase in SSB (Fig. 6.4 and 6.5). SSB were detected at concentrations as low as 5 μM. At concentration ≤10 μM, the extent of SSB induced by menadione was less than that induced by 2,3-diOMe-1,4-NQ (Fig. 6.4 and 6.5).

6.3.3 The Repair of Quinone-induced SSB

Redox cycling quinonesare thought to cause DNA strand breakage through the generation of hydroxyl radicals. SSB induced by hydroxyl radicals are usually not lethal as most are rapidly repaired. Within 45 minutes of the removal of the extracellular quinone extensive repair of SSB was detected (Fig. 6.6 and 6.7). Total repair was observed within four hours of the removal of 2,3-diOMe-1,4-NQ (15 μM) (Fig. 6.6). Although repair of SSB in menadione (15 μM) treated cells was extensive, total repair was not observed within four hours (Fig. 6.7).

6.3.4 The Effects of 1,10-Phenanthroline on Quinone-induced SSB

In preliminary experiments, the SSB induced by both quinones were partially inhibited by preincubating the hepatocytes for 10 min with the iron chelator 1,10-phenanthroline (25 μM) [Cantoni et al, 1989] before exposure to the quinone. The efficacy of 1,10-phenanthroline may be attributed to its ability to enter cells. Inside the cell it is capable of removing iron from the chromatin, reducing the damaging actions of H_2O_2 [Mello Filho et al, 1984]. In K562 cells preincubated for 30 min with 1,10-phenanthroline (25 μM) and then exposed to 2,3-diOMe-1,4-NQ (15 μM) for 15 min, no SSB were observed (Fig. 6.8) . In cells exposed to menadione (15 μM) for 15 min, the SSB were significantly reduced but were not completely inhibited (Fig.

6.9). Higher concentrations of 1,10-phenanthroline (50 μM) failed to further reduce the SSB in menadione treated cells suggesting an additional mechanism of DNA damage (Fig. 6.9).

6.3.5 The Effect of Quinones on Intracellular NAD^+ in K562 Cells

As reported in the earlier chapters and in previous studies, both 2,3-diOMe-1,4-NQ and menadione caused a decrease in the pyridine nucleotide NAD^+ in isolated hepatocytes [Stubberfield and Cohen, 1989]. In K562 cells exposed to either quinone (15 μM) for 15 min, a similar decrease in NAD^+ was also observed (Fig. 6.10).

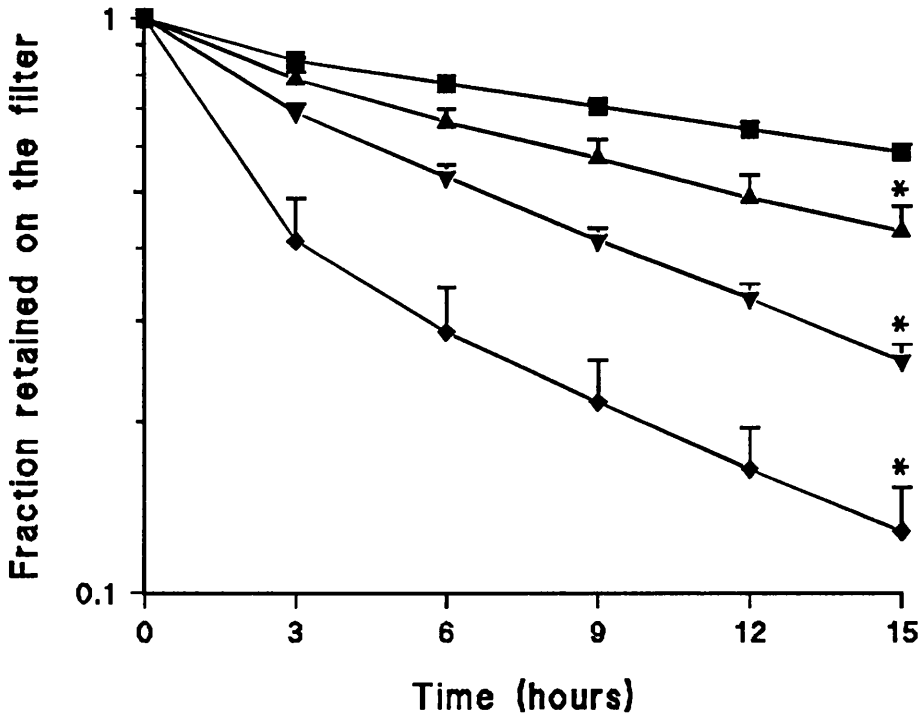

Fig. 6.1 The effect of quinones on the elution kinetics of DNA from rat hepatocytes. Hepatocytes (10^6 cells/ml) were exposed to DMSO alone (■), menadione 50 μM (◆) 2,3-diOMe-1,4-NQ 50 μM (▲) or 100 μM (▼) for 15 min at 37°C. 8 x 10^5 cells were then diluted (x 10) in ice cold phosphate buffered saline, washed and lysed on the filter before alkaline elution. Values represent the mean ± SEM of 3 hepatocyte preparations. * Significantly different from control (DMSO alone treated cells)

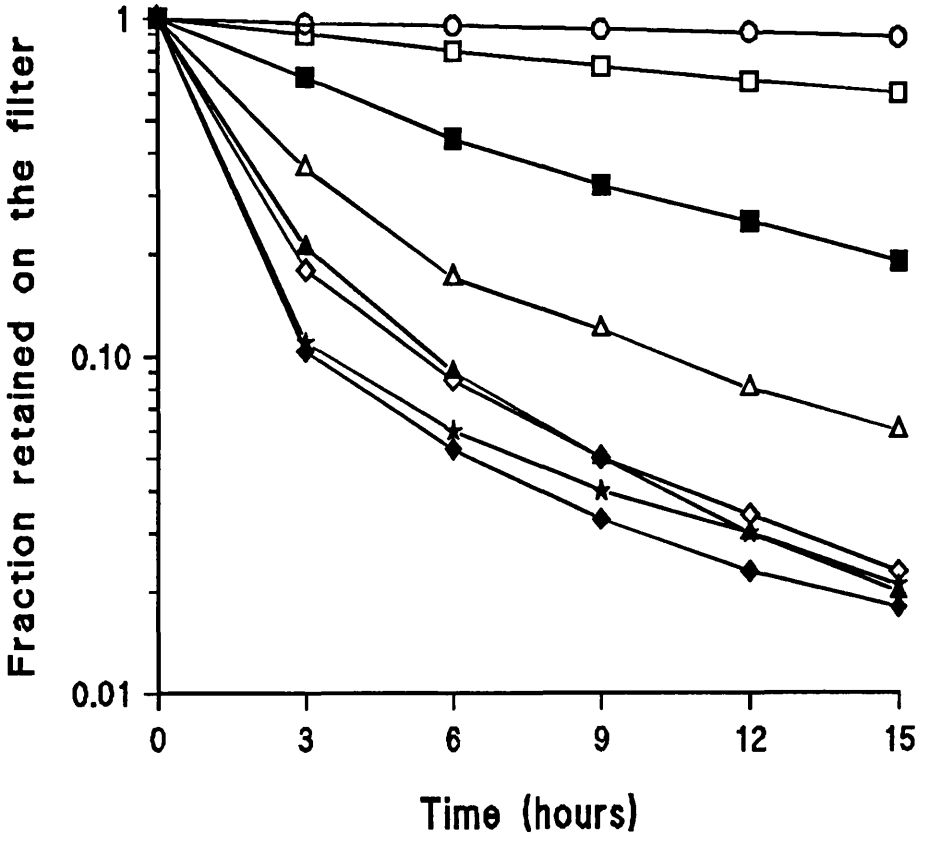

Fig. 6.2 The effect of incubation time on the elution kinetics of DNA from K562 cells. The cells (10^6 cells/ml) were exposed to 2,3-diOMe-1,4-NQ 15 μM for 0 min (○), 1 min (□), 5 min (■), 10 min (△), 15 min (▲), 20 min (◊), 30 min (◆), and 60 min (★) min. At the indicated times, cells were removed and elution kinetics determined. The results represent the mean of at least 2 incubations.

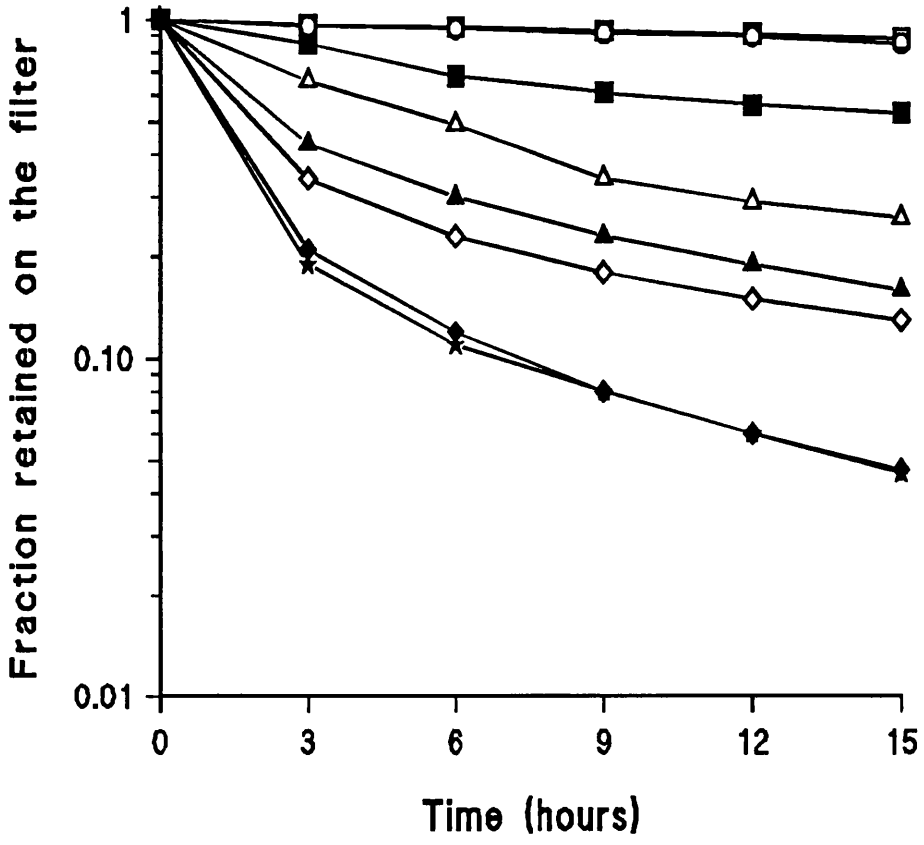

Fig. 6.3 The effect of incubation time on the elution kinetics of DNA from K562 cells. The cells (10^6 cells/ml) were exposed to menadione 15 μM for 0 min (○), 1 min (□), 5 min (■), 10 min (△), 15 min (▲), 20 min (◊), 30 min (◆), and 60 min (★) min. At the indicated times, cells were removed and elution kinetics determined. The results represent the mean of at least 2 incubations.

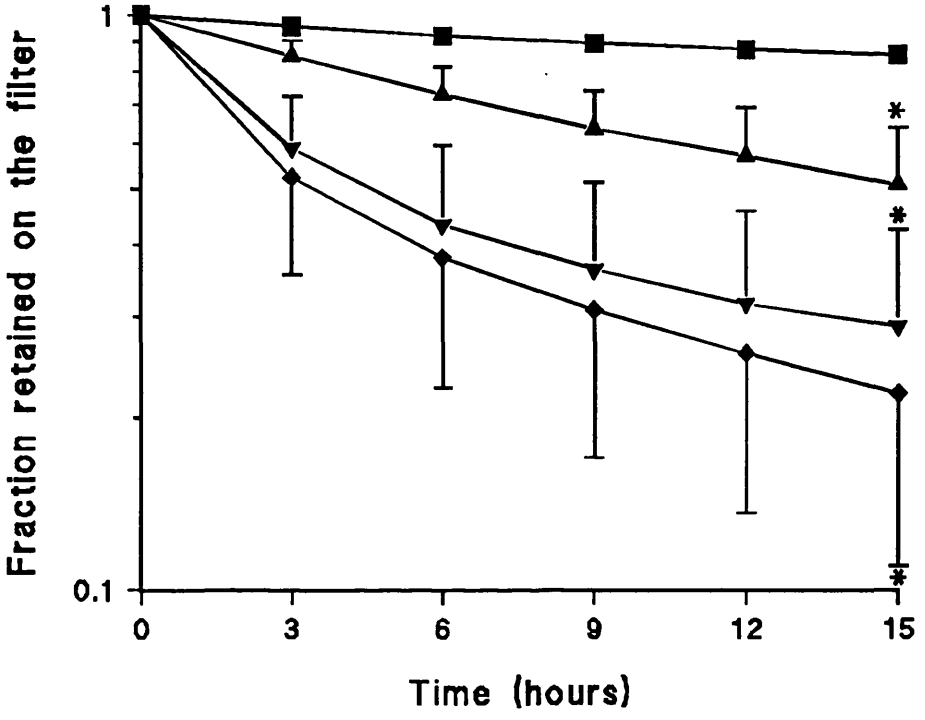

Fig. 6.4 The effect of quinone concentration on the elution kinetics of DNA from K562 cells. Cells were exposed to 2,3-diOMe-1,4-NQ at the following concentrations: 0 μM (■), 5 μM (▲), 10 μM (▼), 15 μM (◆), for 15 minutes before being removed for alkaline elution. The results represent the mean ± SEM of at least 4 incubations. * Significantly different from untreated cells.

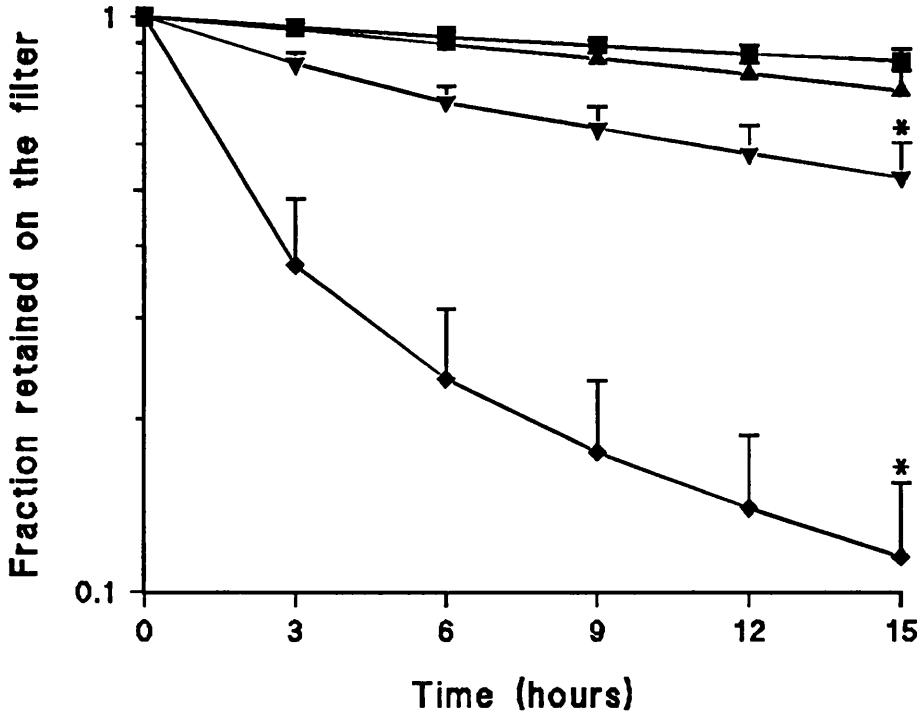

Fig. 6.5 The effect of quinone concentration on the elution kinetics of DNA from K562 cells. Cells were exposed to menadione at the following concentrations: 0 μM (■), 5 μM (▲), 10 μM (▼), 15 μM (◆), for 15 minutes before being removed for alkaline elution. The results represent the mean ± SEM of at least 4 incubations. * Significantly different from untreated cells.

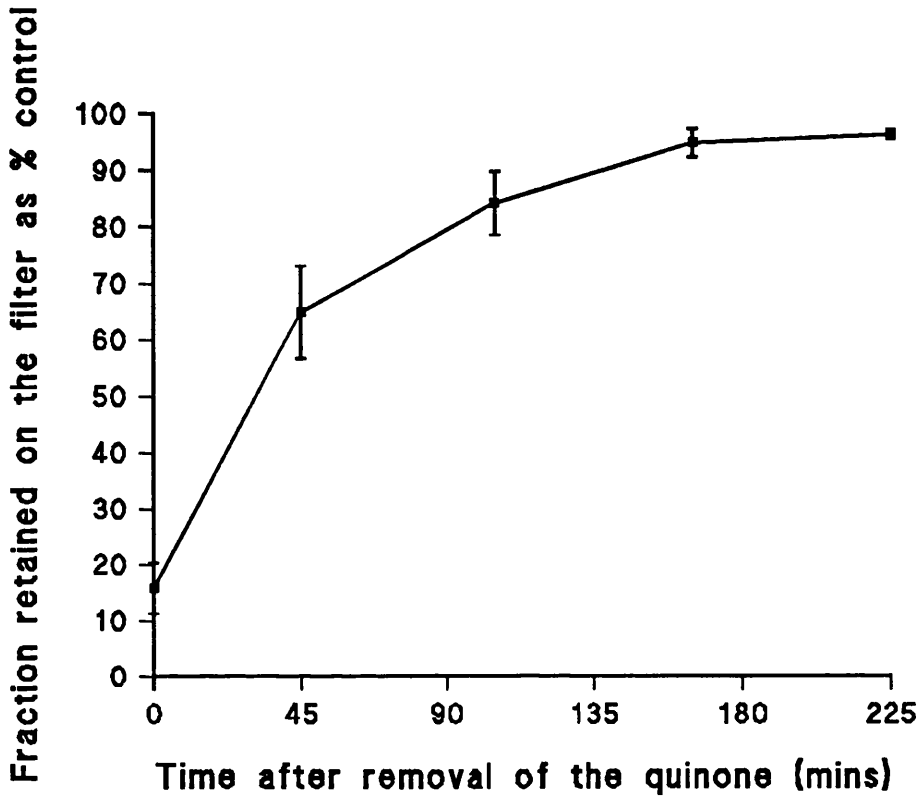

Fig. 6.6 The repair of SSB induced by quinones in K562 cells. Cells were incubated with 2,3-diOMe-1,4-NQ (15 μM) for 15 min then resuspended in fresh medium. At the specified times, 0.8 ml aliquots were removed and elution kinetics determined. Values represent mean ± SEM of at least 5 incubations. Control cells were treated with DMSO for 15 min and then resuspended in fresh medium. The fraction retained on the filter in control cells was always above 83%.

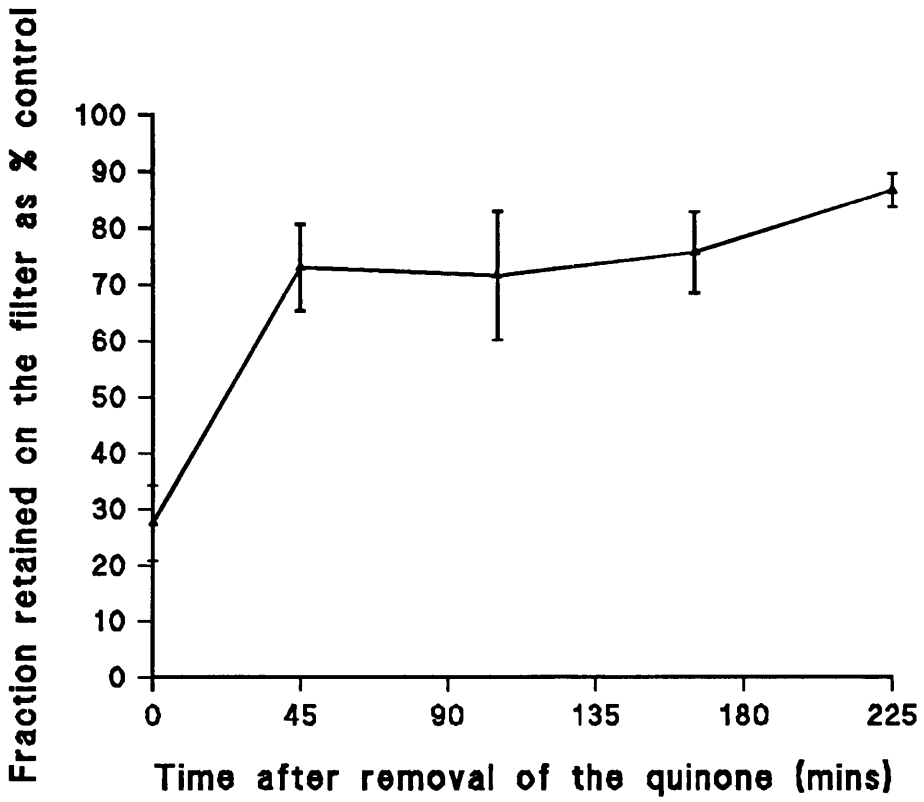

Fig. 6.7 The repair of SSB induced by quinones in K562 cells. Cells were incubated with menadione (15 μM) for 15 min then resuspended in fresh medium. At the specified times, 0.8 ml aliquots were removed and elution kinetics determined. Values represent mean ± SEM of at least 5 incubations. Control cells were treated with DMSO for 15 min and then resuspended in fresh medium. The fraction retained on the filter in control cells was always above 83%.

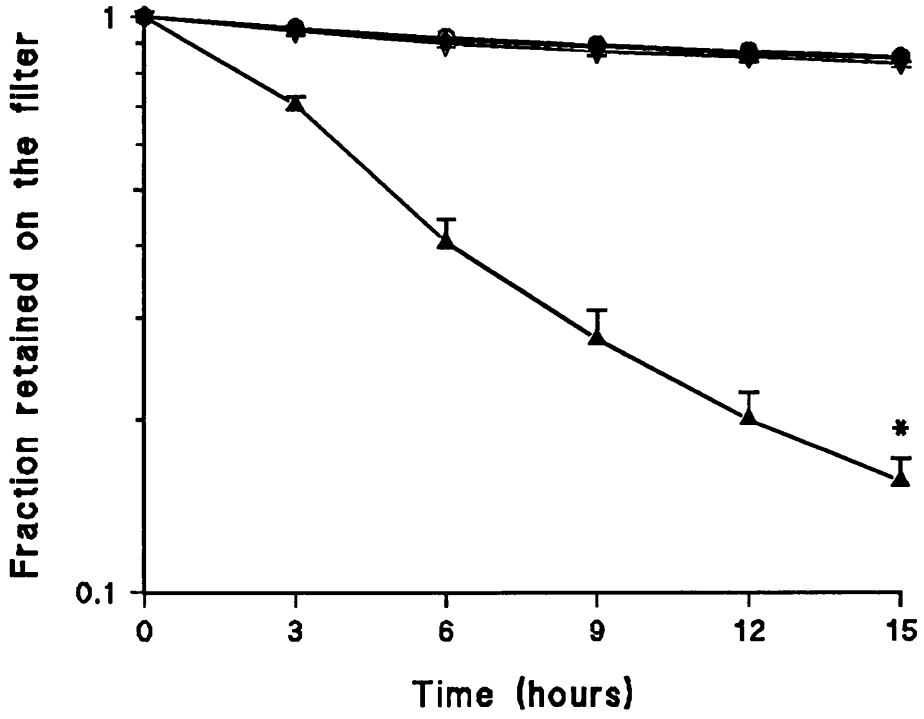

Fig. 6.8 Prevention of SSB by 1,10-phenanthroline in K562 cells. Cells were exposed to 2,3-diOMe-1,4-NQ (15 μM), either alone (▲), or with the quinone (15 μM) and either 25 μM (◆) or 50 μM (▽) phenanthroline. Cells treated with phenanthroline were preincubated for 30 min before exposure to the quinone. Control cells (O) were incubated with phenanthroline (50 μM) alone. The results represent the mean ± SEM of at least 5 incubations. * Significantly different from untreated cells.

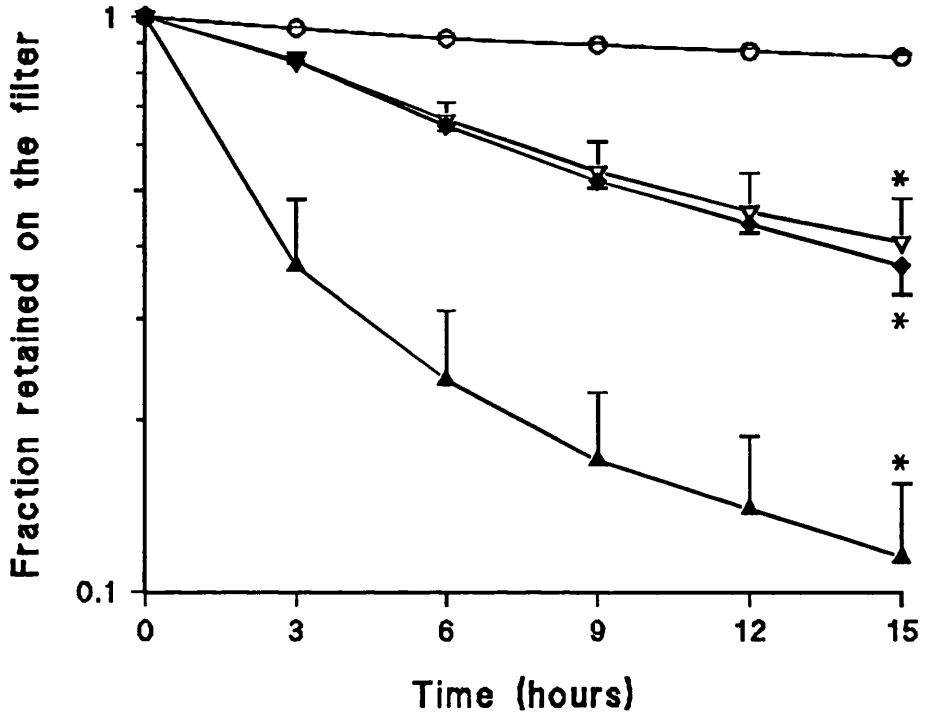

Fig. 6.9 Prevention of SSB by 1,10-phenanthroline in K562 cells. Cells were exposed to menadione (15 μM), either alone (▲), or with the quinone (15 μM) and either 25 μM (◆) or 50 μM (▽) phenanthroline. Cells treated with phenanthroline were preincubated for 30 min before exposure to the quinone. Control cells (O) were incubated with phenanthroline (50 μM) alone. The results represent the mean ± SEM of at least 5 incubations. * Significantly different from untreated cells.

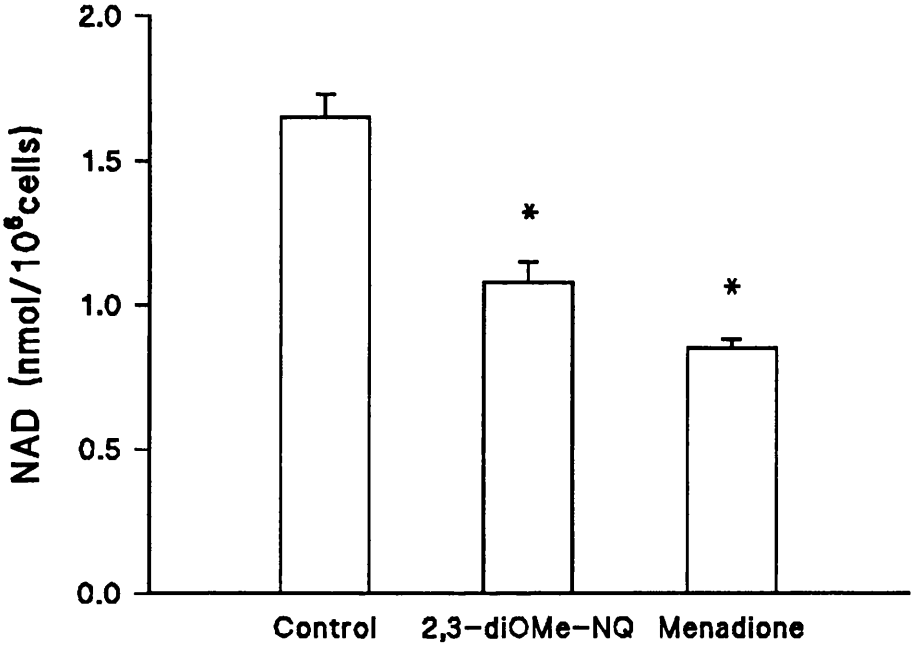

Fig. 6.10 The effect of quinones on the level of NAD^+ in K562 cells. Cells were exposed to either 2,3-diOMe-1,4-NQ (15 μM) or menadione (15 μM) for 15 min after which NAD^+ was determined as described in the materials and methods. Values represent the mean ± SEM of four individual incubations.

* Significantly ($P < 0.05$) different from control.

6.4. DISCUSSION

Previously Stubberfield and Cohen (1989) reported a decrease in NAD^+ in rat hepatocytes exposed to either 2,3-diOMe-1,4-NQ or menadione at non-toxic concentrations as assessed by trypan blue exclusion. In the earlier chapters similar pyridine nucleotide changes were noted. In order to ascertain if this was linked with DNA damage, the extent of SSB in rat hepatocytes exposed to these quinones was investigated. In hepatocytes, both quinones induced significant SSB (Fig. 6.1), which in preliminary studies was partially inhibited by 1,10-phenanthroline, pointing to the involvement of hydroxyl radicals. The presence of SSB in hepatocytes exposed to either quinone suggests that the previously reported decrease in NAD^+ [Stubberfield and Cohen, 1988; Cohen and Stubberfield, 1990] was primarily due to the activation of the enzyme poly(ADP-ribose)polymerase [Schraufstatter et al, 1986b]. Previously, Cohen and Stubberfield (1990), reported that 3-aminobenzamide was unable to inhibit the decrease in NAD^+ induced by redox cycling quinones. They inferred that at low concentrations of the redox cycling quinones, DNA damage and the activation of poly(ADP-ribose)polymerase was not responsible for the depletion of NAD^+.

SSB were detected within 5 min of exposure to either quinone and correlated well with the oxidation of NADPH and other signs of redox cycling [Gant et al, 1988; Stubberfield and Cohen, 1989;Kappus and Sies, 1981]. This observation implicates the process of redox cycling in the early appearance of quinone induced SSB.

In mammalian cells exposed to redox cycling quinones both enzyme mediated DNA fragmentation [McConkey et al, 1988] and hydroxyl radical induced SSB [Coleman et al, 1989; Starke and Farber, 1985] have been reported. Whereas DNA fragmentation

is observed after several hours exposure [Cotter et al, 1990], hydroxyl radical induced SSB may be seen within minutes [Morgan et al, 1992; Schraufstatter et al, 1986b]. The early detection of DNA damage (≤ 5 min) with alkaline elution kinetics consistent with the formation of SSB, points to the generation of hydroxyl radicals as the probable cause of DNA damage in the present study. The generation of hydroxyl radicals is additionally implicated by the inhibition of SSB induced by 2,3-diOMe-1,4-NQ by the iron chelator 1,10-phenanthroline [Cantoni et al, 1989; Mello Filho et al, 1984; Cantoni et al 1991] (Fig. 6.8 and 6.9). As discussed earlier the availability of Fe^{2+} is crucial to the formation of hydroxyl radicals during redox cycling [Mello Filho and Meneghini, 1984]. Although hydroxyl radicals are very reactive they are unable to diffuse over long distances, hence if generated outside the nucleus they are unlikely to cause significant DNA damage. The extensive SSB observed at very low concentrations of both quinones may be due to the binding of iron to DNA [Starke and Farber, 1985; Halliwell and Aruoma, 1991], so allowing the generation of hydroxyl radicals in close proximity to the DNA and maximising the DNA damage.

Previously it had been demonstrated that menadione bound directly to DNA causing SSB [Morrison et al, 1984]. The persistence of some SSB in cells preincubated with 1,10-phenanthroline and exposed to menadione observed in this study (Fig. 6.9) and previously [Cantoni et al, 1991], may be attributed to this effect. The ability of menadione to arylate nucleophiles [Gant et al, 1988] would decrease its effective concentration available to redox cycle and thus reduce its ability to cause SSB at lower concentrations. This may partially explain the observation that SSB in K562 cells exposed to 2,3-diOMe-1,4-NQ (≤10 μM) were greater than those induced by menadione (Fig. 6.4 and 6.5).

A large proportion of the quinone induced SSB was repaired within 45 minutes of the removal of the quinone (Fig. 6.6 and 6.7), in accordance with previous studies [McWilliams et al, 1983]. A complete repair of SSB induced by 2,3-diOMe-1,4-NQ was observed within 4 hours, in contrast to menadione where SSB were still detected (Fig. 6.6 and 6.7). This observation together with the data with 1,10-phenanthroline strongly suggests that the SSB induced by menadione was only partially mediated by the generation of hydroxyl radicals. A depletion in NAD^+ was observed in K562 cells exposed to 2,3-diOMe-1,4-NQ (15 μM) and menadione (15 μM) (Fig. 6.10). As in other cell systems, a depletion in NAD^+ below a critical level may lead to a depletion in ATP and cell death as part of a suicide response [Gaal et al, 1987].

These results reveal that in rat hepatocytes and K562 cells, both menadione and 2,3-diOMe-1,4-NQ induced extensive DNA damage manifested in the form of SSB and possibly mediated by hydroxyl radicals generated during redox cycling.

CHAPTER 7

THE ROLE OF DNA STRAND BREAKAGE AND PYRIDINE NUCLEOTIDE CHANGES IN QUINONE-INDUCED CYTOTOXICITY

Abstract- Although redox cycling quinones are known to induce extensive DNA damage, the mechanisms by which quinone-induced DNA lesions lead to cell death remain unresolved. The quinones 2,3-dimethoxy-1,4-naphthoquinone (2,3-diOMe-1,4-NQ) and menadione induce extensive DNA damage in human chronic myelogenous leukaemic cells (K562). The strand breaks induced by 2,3-diOMe-1,4-NQ (15-100 μM) are followed by a transient decrease in NAD^+ and at least partial repair of strand breaks. However, in the ensuing 72 hours, cell proliferation is significantly reduced in cells exposed 2,3-diOMe-1,4-NQ (50-100 μM). Greater DNA damage was observed in cells exposed to menadione (50-100 μM), while no strand scission repair was detected. Furthermore cell death was preceded by a permanent depletion of NAD^+ and ATP. These results suggest that the DNA damage induced by redox cycling quinones may cause cell death by activating secondary events such as the depletion of NAD^+ and ATP.

7.1. INTRODUCTION

The exposure of mammalian cells to certain redox cycling quinones has been associated with a number of biochemical changes including DNA damage and the depletion of the pyridine nucleotide NAD^+ [Cantoni et al, 1991; Stubberfield and Cohen, 1989]. In particular, the generation of hydroxyl radicals ($OH^\cdot$) during the metabolism of redox cycling quinones is known to cause single strand breaks (SSB) in DNA, which are usually not cytotoxic as most are rapidly repaired [Cantoni et al, 1991; McWilliams et al, 1983]. Where extensive SSB are formed in close proximity, lethal double strand breaks (DSB) may result [Bradley and Erickson, 1981]. Additionally, certain quinones may also cause DNA double strand breaks by interferring with the breakage-reunion reaction of mammalian DNA topoisomerase II, by stabilizing the enzyme in the cleaving form [Tewey et al, 1984].

During oxidative stress, cell death may result as a direct consequence of DNA damage. Alternatively strand breakage may elicit secondary lethal events such as the activation of poly(ADP-ribose)polymerase which hydrolyses NAD^+ to nicotinamide and ADP-ribose [Gaal et al, 1987]. Although the ribosylation of certain nuclear proteins has been shown to regulate both DNA strand scission repair and chromatin conformation [Shall, 1989], cell death may result from the excessive depletion of NAD^+ and the subsequent depletion of ATP [Berger, 1985]. In certain mammalian cells, the depletion of NAD^+, ATP and the early onset of cell death, may be prevented by inhibitors of poly(ADP-ribose)polymerase [Schraufstatter et al, 1986b]. However the long term viability of such cells may be compromised as the poly(ADP-

ribose)polymerase inhibitors prevent strand scission repair [Shall, 1989]. Furthermore 3-aminobenzamide an inhibitor of poly(ADP-ribose)polymerase has been shown to potentiate the cytotoxicity of H_2O_2 [Cantoni et al, 1986].

In the previous chapter, low concentrations of the redox cycling quinones 2,3-diOMe-1,4-NQ (15 μM) and menadione (15 μM) were reported to induce significant DNA strand breakage in rat hepatocytes and K562 cells without inducing the early loss of membrane integrity. This study investigates the long term consequences of DNA damage and the importance of the depletion of NAD^+ and ATP in the mechanisms of cytotoxicity of redox cycling quinones.

7.2. Materials and Methods

7.2.1 Cell Culture and Treatment.

Human chronic myelogenous leukaemic cells (K562) and U937 cells [Lennon et al, 1991], from the Department of Oncology, University College and Middlesex School of Medicine, were cultured in RPMI 1640 supplemented with 5% heat inactivated foetal calf serum and L-glutamine (2 mM) at 37°C. Cells (10^6/ml) in exponential growth phase were exposed to the quinone (in DMSO 0.1% v/v) and incubated for 15 min at 37°C. The cells were then washed once in RPMI before resuspension in fresh medium (2 x 10^5/ml) at 37°C. At various times aliquots of cell suspension were removed for determination of DNA damage, NAD^+, $NADP^+$, ATP and GSH.

7.2.2 Determination of Growth Inhibition.

K562 cells (10^6 cells/ml) were exposed to various concentrations of the quinones for 15 min after which they were resuspended in fresh medium and diluted to 10^5 cells/ml. The cells were then incubated for 72 hours at 37°C during which time cell number was determined at 24 hour intervals.

7.2.3 Determination of DNA Strand Breakage.

DNA strand breakage was determined using the fluorescence analysis of the rate of unwinding according to the method of Birnboim and Jevcak (1981), as described in chapter 2. Briefly, cells were washed once in HEPES buffer and resuspended in a buffer containing 0.25 mM meso-inositol, 10 mM sodium phosphate and 1.0 mM $MgCl_2$ (pH 7.2). The cells were lysed for 10 min in a buffer containing 9 M urea, 10

mM NaOH, 2.5 mM cyclohexanediaminetetraacetate and 0.5% Triton X-100. The DNA was allowed to unwind for 30 min at 0°C, after which the tubes containing the blank sample were sonicated for 3 sec to allow complete unwinding. The DNA was then allowed to unwind for a further 15 min at 15°C and unwinding was stopped by the addition of a solution containing 1 M glucose and 14 mM mercaptoethanol. The amount of double stranded DNA remaining was assayed by the addition of ethidium bromide (6.7 µg/ ml) and fluorescence measured (emission,590 nM excitation, 520 nM)[Coleman et al, 1989]. The assay was performed in reduced lighting. DNA strand breakage was expressed as percentage D (percentage of double stranded DNA remaining), where;

$$\%D = (P-B)/(T-B) \times 100 \quad \text{(see section 2.10.2)}$$

7.2.4 Determination of NAD^+, $NADP^+$, ATP and GSH.

Intracellular $NADP^+$ and NAD^+ was assayed as previously described in chapter 2. Briefly, aliquots of cell suspension were sedimented by bench centrifugation at 1000 rpm for 3 min and the supernatant fraction aspirated. NAD^+, $NADP^+$, ATP and GSH were extracted by addition of 0.5M perchloric acid and the acid extract stored at -80°C prior to analysis.

ATP levels were determined using a luciferase-linked luminescence method as described earlier, while intracellular GSH was determined by the o-PT method as previouly described in chapter 2.

7.3.5 Quantification of DNA Fragmentation

The method used to quantify DNA fragmentation is partly based on the that previously reported by McConkey et al (1988). At the appropriate times, cells (3 x 10^6) were resuspended in a lysis buffer containing Tris (5 mM), EDTA (20 mM) and 1% Triton X-100 (v/v), pH 8.0. The cell suspension was allowed to lyse for 30 min on ice before centrifugation (13,000g) for 40 min in a Eppendorf microcentrifuge (centrifuge 5413) to separate the intact chromatin (pellet) from DNA fragments (supernatant).

DNA was quantified by measuring the increased fluorescence induced by 33258 Hoechst, when the dye is complexed with DNA [Stout and Becker 1982]. DNA was calibrated by preparing a stock solution of calf thymus DNA (0.5 mg/ml) dissolved in NaCl (0.154 M), Na_3citrate (0.015 M) pH 7.0. The DNA standard curve (0-7µg/ml) was made by further dissolving the DNA stock solution in the lysate solution. The assay mixture contained 1.30ml sample/standard, 0.7ml KH_2PO_4 (17 mM) to adjust the pH to 6.8-7.0. and 0.75ml Hoechst 33258. Fluorescence was determined on a Perkin-Elmer model LS-3 spectrophotometer at 450 nm during 360 nm excitation.

As it proved difficult to resuspend the chromatin pellet, DNA fragmentation was quantified by determining the amount of DNA in the supernatant as well as in the lysate solution prior to centrifugation (Total DNA). % DNA fragmentation was then quantified using the following formula:

$$\% \text{ DNA fragmentation} = \frac{\text{DNA in supernatant}}{\text{Total DNA}} \times 100$$

7.3. Results

7.3.1 The Effects of 2,3-diOMe-1,4-NQ and Menadione on Cell Proliferation

Exposure of K562 cells to either 2,3-diOMe-1,4-NQ (15-400 μM) or menadione (15-400 μM) for 15 min had no effect on cell viability as measured by trypan blue exclusion in the ensuing 6 hours. However a 15 min exposure of K562 cells to 2,3-diOMe-1,4-NQ (50-100 μM) resulted in a significant reduction in cell proliferation after 72 hours (Fig. 7.1), while in cells exposed to menadione (50-100 μM) cell proliferation was completely inhibited (Fig. 7.2).

7.3.2 Quinone-Induced DNA Fragmentation

Previously, quinones were reported to cause DNA fragmentation and cell death by a mechanism similar to apoptosis [McConkey et al, 1988]. Arabinofuranosylcytosine (ARA-C) has also been shown to induce a programmed fragmentation of DNA characteristic of apoptosis. In this study, ARA-C (10^{-6}M to 10^{-3}M) induced extensive DNA fragmentation (Fig. 7.3) in U937 cells [Lennon et al 1991] . In contrast, in U937 cells exposed to either 2,3-diOMe-1,4-NQ (50 μM) or menadione (50 μM) no DNA fragmentation was observed (Fig. 7.3).

7.3.3 The Repair of Quinone-Induced DNA Strand Breakage

As reported in the previous chapter, greater DNA damage was observed in cells exposed to 2,3-diOMe-1,4-NQ (15 μM) than to menadione (15 μM), while at higher concentrations (50-100 μM) greater damage was observed in cells exposed to menadione (Fig. 7.4 and 7.5). Similarly, in the previous chapter, significant strand

scission repair was reported within minutes of removal of the quinone. In cells exposed to the lower concentration (15 μM) of both quinones, complete repair was observed within 6 hours of removal of the quinone (Fig. 7.4 and 7.5). At the highest concentration of 2,3-diOMe-11,4-NQ (100 μM), only partial repair was observed (Fig. 7.4), while in cells exposed to the higher concentrations of menadione (50-100 μM) no repair was observed (Fig. 7.5).

7.3.4 The Effects of 2,3-diOMe-1,4-NQ and Menadione on Intracellular NAD^+, ATP, $NADP^+$ and GSH

The repair of DNA damage is often associated with the depletion of NAD^+, while the subsequent depletion of ATP is thought to lead to cell death. In K562 cells exposed to either quinone, a rapid depletion in NAD^+ was observed (Fig. 7.6 and 7.7). In cells exposed to 2,3-diOMe-1,4-NQ (15-100 μM) and to menadione (15 μM), intracellular NAD^+ returned to at least 75% of control values within three hours of the removal of the quinone (Fig. 7.6 and 7.7). In cells exposed to menadione (50-100 μM) no recovery of the the level of NAD^+ was observed (Fig. 7.7).

Although a depletion of NAD^+ may precipitate the subsequent depletion of ATP, quinone-induced ATP depletion has been shown to be independent of the depletion of NAD^+. In cells exposed to either 2,3-diOMe-1,4-NQ (15-100 μM) or menadione (15 μM), no change in the level of ATP was observed (Fig. 7.8), while in cells exposed to menadione (50-100 μM) a significant reduction in the level of ATP was observed (Fig. 7.9).

Cell death resulting from exposure to redox cycling quinones is normally preceded by the oxidative stress characterised by a rapid depletion of GSH and the extensive

oxidation of NADPH. In this study, following a 15 min exposure of K562 cells to either quinone (15-100 μM), no change in the level of $NADP^+$ was observed (fig. 7.10 and fig. 7.11), while a significant depletion of GSH was only bserved in cells exposed to menadione (100 μM)(Fig. 7.12).

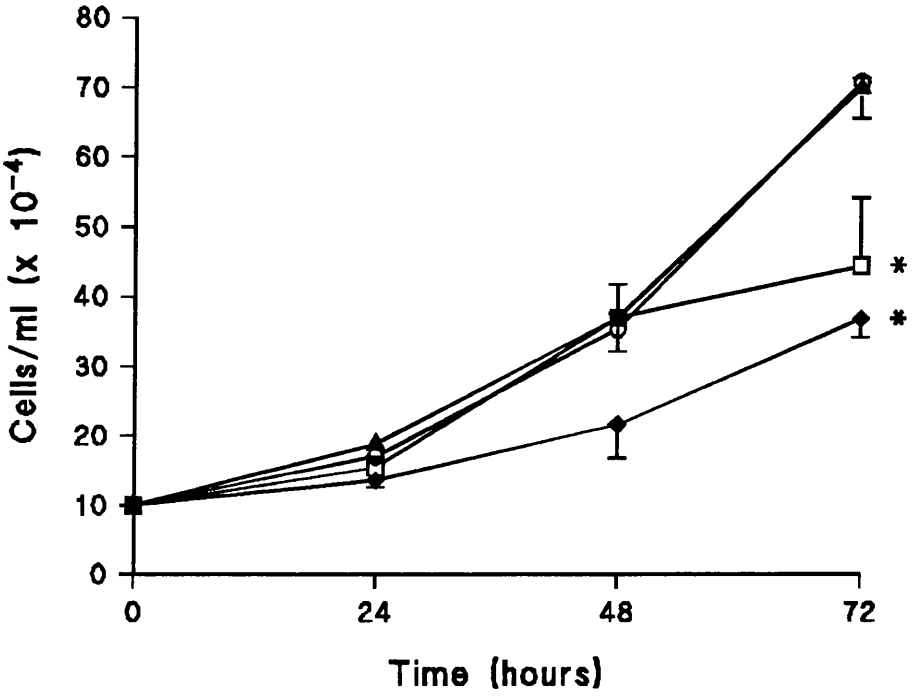

Fig. 7.1 The effect of 2,3-diOMe-1,4-NQ on the proliferation of K562 cells. Cells were exposed to the quinone at the following concentrations: 0 μM (○), 15 μM (▲), 50 μM (□) or 100 μM (♦) for 15 min, then resuspended in fresh medium and diluted to 10^5 cells/ml. The cells were then incubated at 37°C for 72 hours and cell number determined at times indicated. The results represent the mean ± SEM of 3 incubations.

* Significantly ($P < 0.05$) different from control after 72 hours.

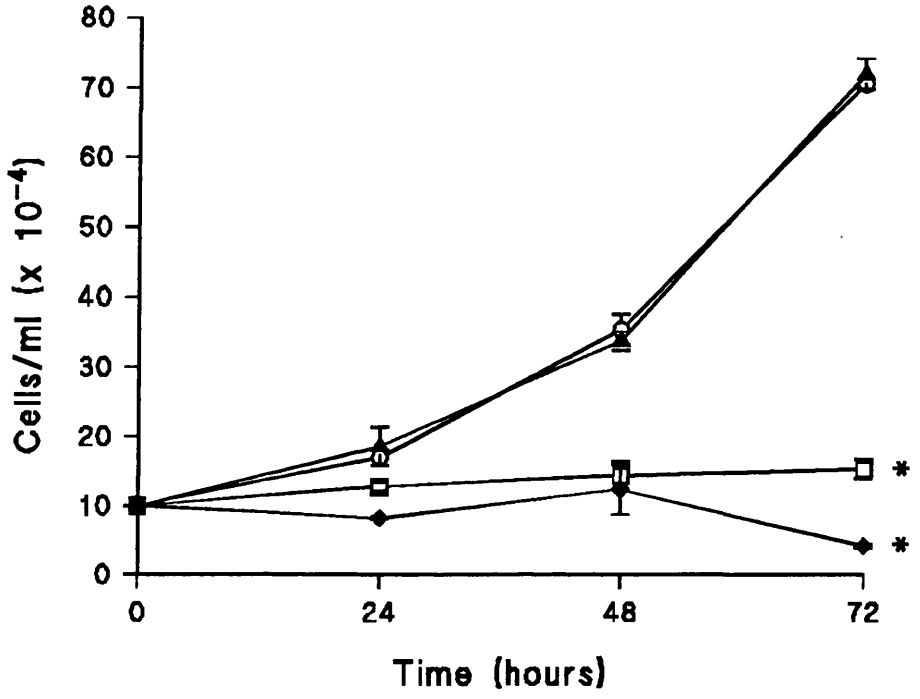

Fig. 7.2 The effect of menadione on the proliferation of K562 cells. Cells were exposed to the quinone at the following concentrations: 0 μM (O), 15 μM (▲), 50 μM (□) or 100 μM (♦) for 15 min, then resuspended in fresh medium and diluted to 10^5 cells/ml. The cells were then incubated at 37°C for 72 hours and cell number determined at times indicated. The results represent the mean ± SEM of 3 incubations.

* Significantly ($P < 0.05$) different from control after 72 hours.

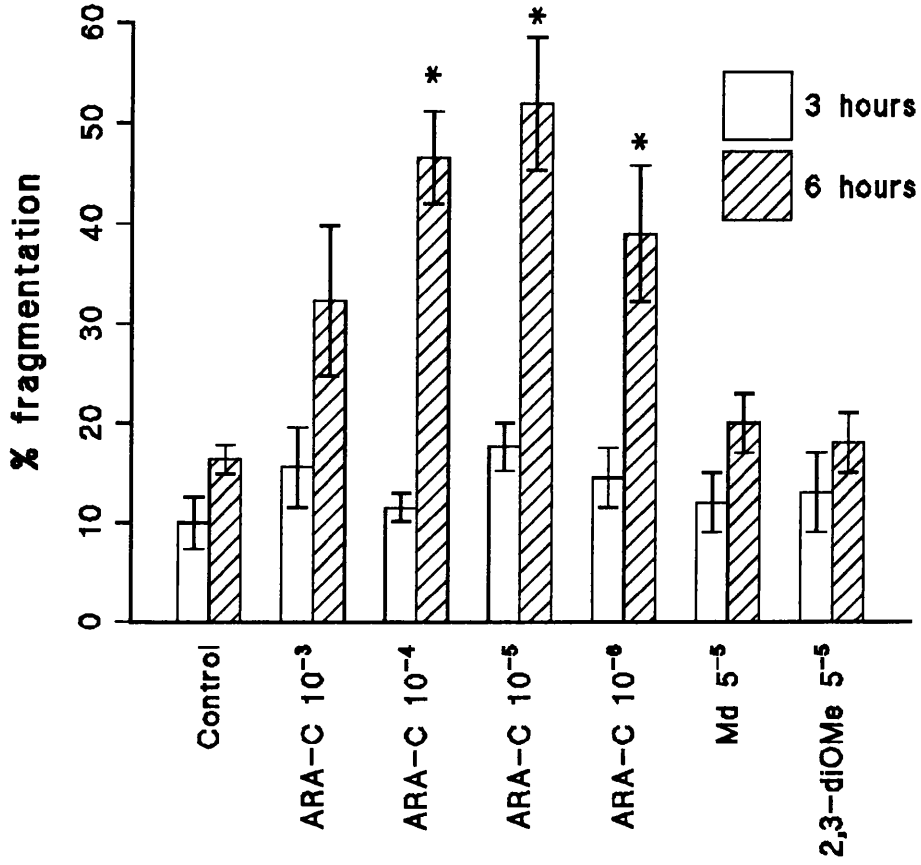

Fig 7.3 DNA fragmentation induced by Arabinofuranosylcytosine (ARA-C), 2,3-diOMe-1,4-NQ (2,3-diOMe) and menadione (Md). U937 cells were exposed to either ARA-C (10^{-6}M-10^{-3}M), 2,3-diOMe (50 μM) and Md (50 μM) for 15 min. At the times indicated, DNA fragmentation was determined as described in the materials and methods. Value represent the mean ± SEM of three separate preparations.

* Significantly ($P < 0.05$) different from control.

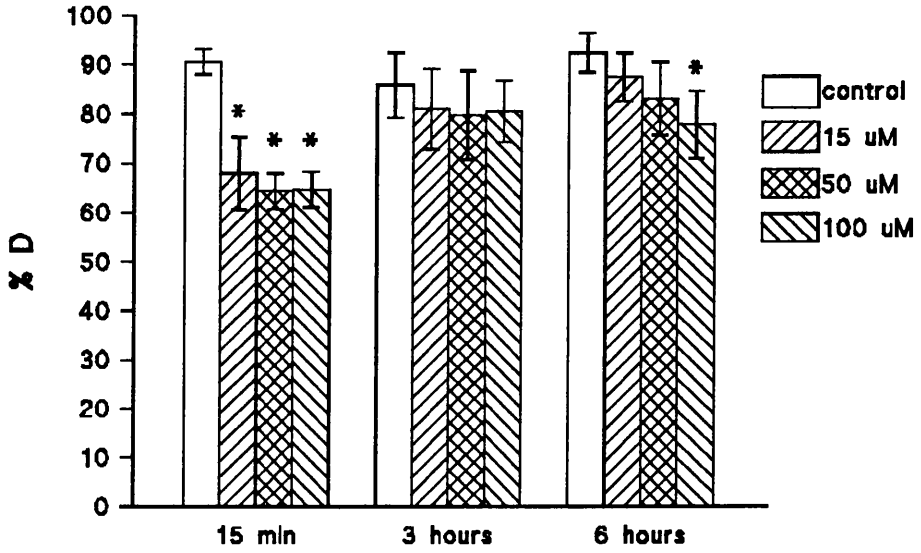

Fig. 7.4 DNA strand breakage and repair in K562 cells exposed to 2,3-diOMe-1,4-NQ. Cells were exposed to the quinone for 15 min, then resuspended in fresh medium and diluted to 10^5 cells/ml. The cells were then incubated at 37°C for 6 hours and at the times indicated, DNA strand breakage determined as described in the materials and methods (%D = percentage double stranded DNA remaining at the times indicated). The results represent the mean ± SEM of 3 incubations.

* Significantly ($P < 0.05$) different from control.

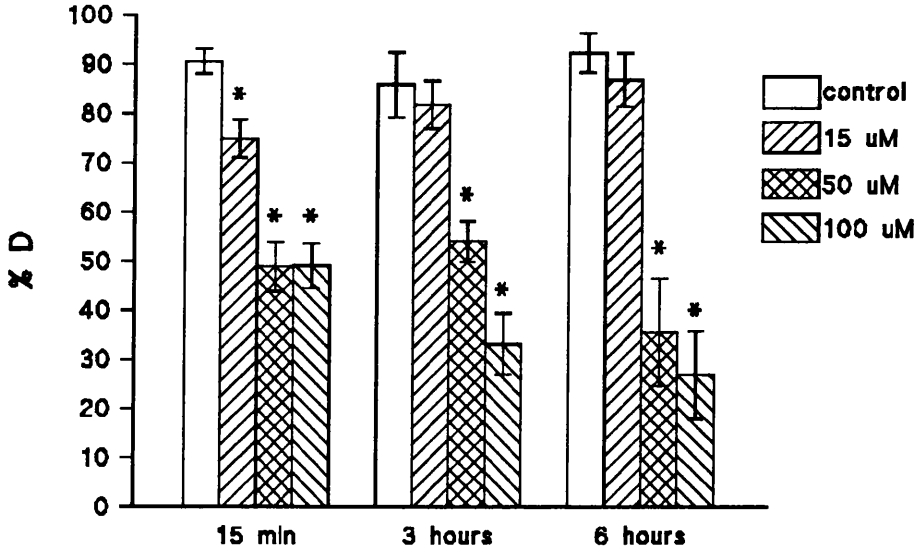

Fig. 7.5 DNA strand breakage and repair in K562 cells exposed to menadione. Cells were exposed to the quinone for 15 min, then resuspended in fresh medium and diluted to 10^5 cells/ml. The cells were then incubated at 37°C for 6 hours and at the times indicated, DNA strand breakage determined as described in the materials and methods(%D = percentage double stranded DNA remaining at the times indicated). The results represent the mean ± SEM of 3 incubations.

* Significantly ($P < 0.05$) different from control.

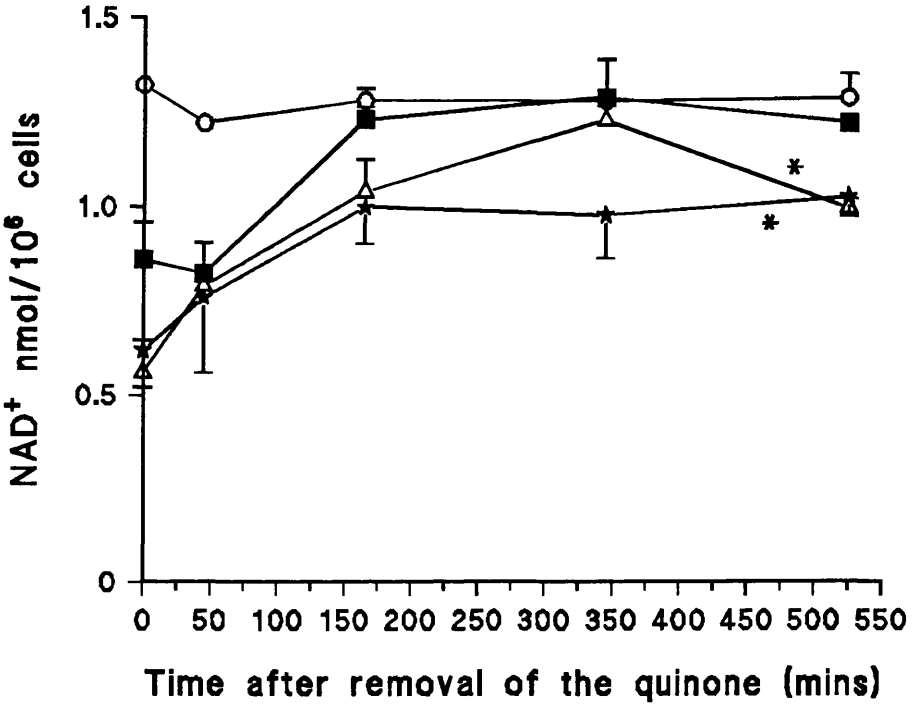

Fig. 7.6 The effect of 2,3-diOMe-1,4-NQ on the intracellular NAD^+. K562 cells were exposed to the quinone at the following concentrations: 0 μM (○), 15 μM (■), 50 μM (△) or 100 μM (★) for 15 min, then resuspended in fresh medium and diluted to 10^5 cells/ml. The cells were then incubated at 37°C for 9 hours and at the times indicated, intracellular NAD^+ determined as described in the materials and methods. The results represent the mean ± SEM of 3 incubations.

* Significantly ($P < 0.05$) different from control after 9 hours.

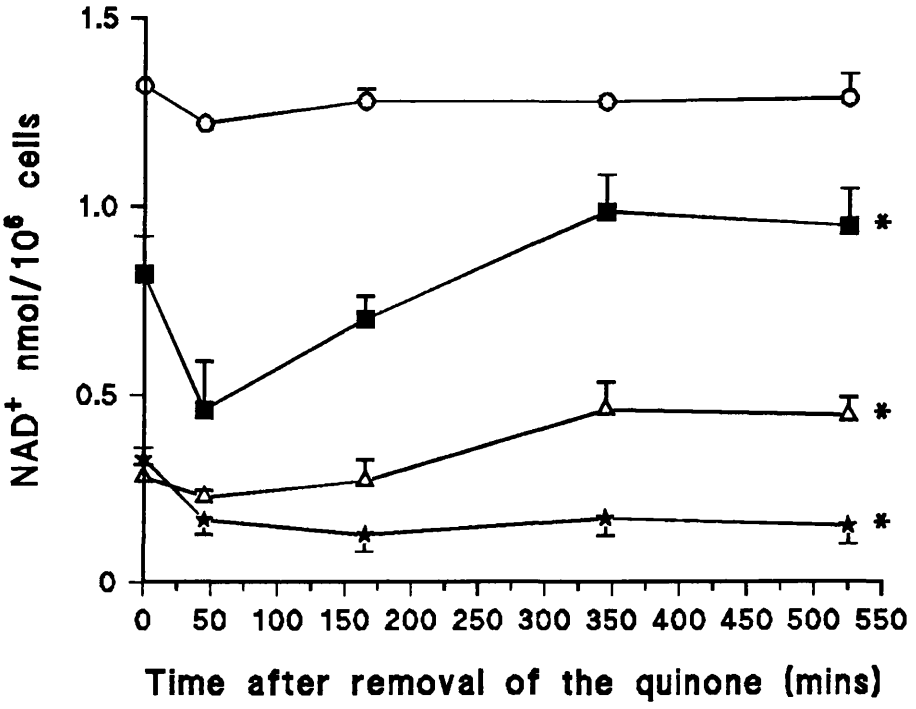

Fig. 7.7 The effect of menadione on the intracellular NAD^+. K562 cells were exposed to the quinone at the following concentrations: 0 μM (○), 15 μM (■), 50 μM (△) or 100 μM (★) for 15 min, then resuspended in fresh medium and diluted to 10^5 cells/ml. The cells were then incubated at 37°C for 9 hours and at the times indicated, intracellular NAD^+ determined as described in the materials and methods. The results represent the mean ± SEM of 3 incubations.

* Significantly ($P < 0.05$) different from control after 9 hours.

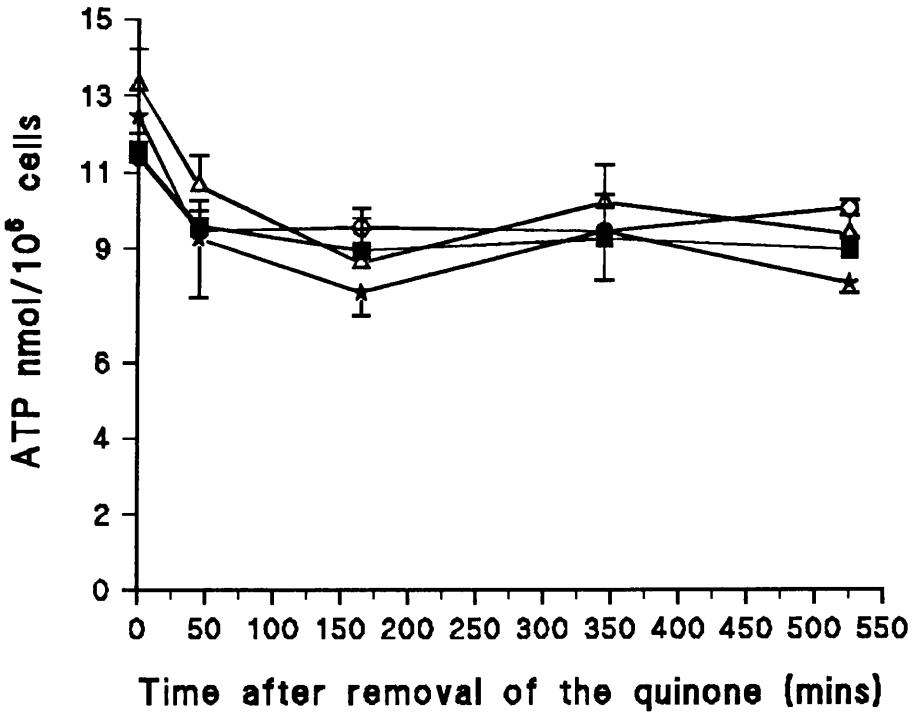

Fig. 7.8 The effect of 2,3-diOMe-1,4-NQ on the intracellular ATP. K562 cells were exposed to the quinone at the following concentrations: 0 μM (○), 15 μM (■), 50 μM (△) or 100 μM (★) for 15 min, then resuspended in fresh medium and diluted to 10^5 cells/ml. The cells were then incubated at 37°C for 9 hours and at the times indicated, intracellular ATP determined as described in the materials and methods. The results represent the mean ± SEM of 3 incubations.

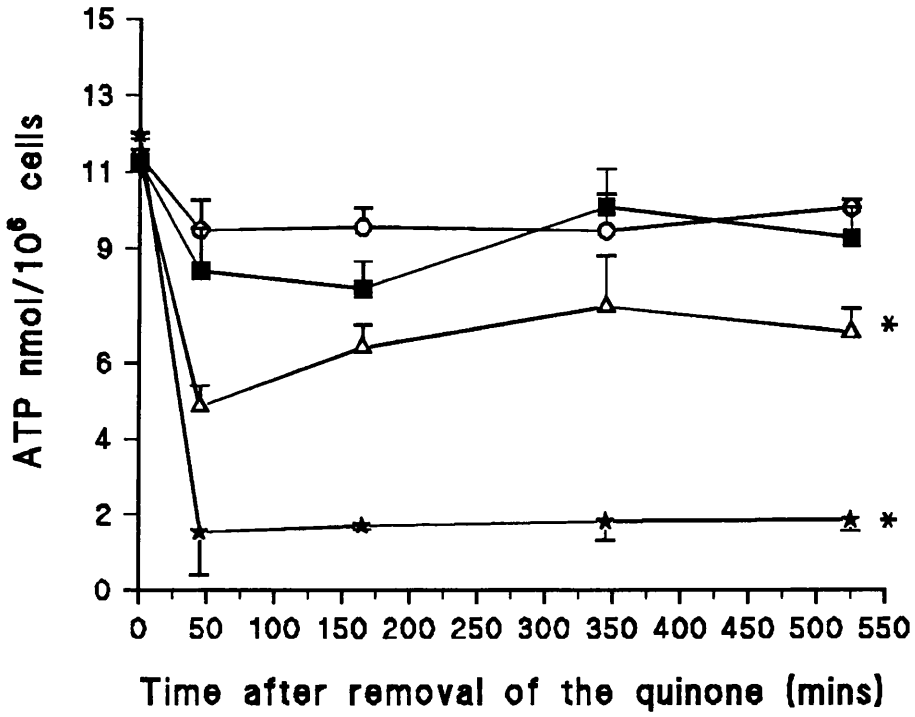

Fig. 7.9 The effect of menadione on the intracellular ATP. K562 cells were exposed to the quinone at the following concentrations: 0 μM (○), 15 μM (■), 50 μM (△) or 100 μM (★) for 15 min, then resuspended in fresh medium and diluted to 10^5 cells/ml. The cells were then incubated at 37°C for 9 hours and at the times indicated, intracellular ATP determined as described in the materials and methods. The results represent the mean ± SEM of 3 incubations.

* Significantly ($P < 0.05$) different from control after 9 hours.

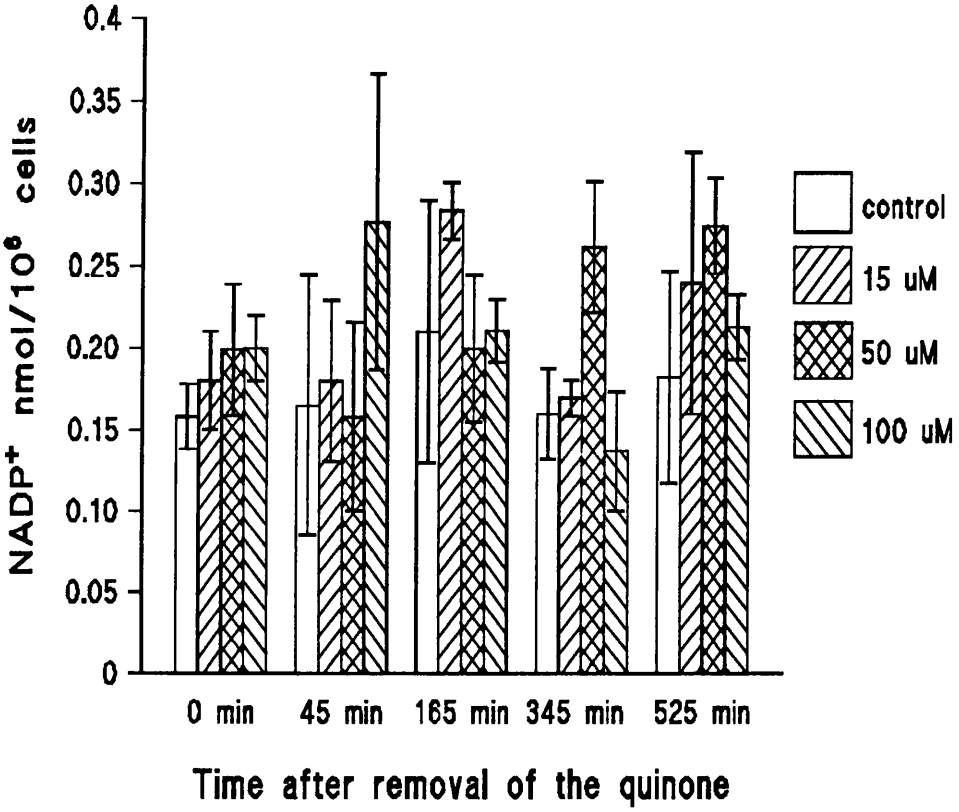

Fig. 7.10 The effect of 2,3-diOMe-1,4-NQ on the intracellular $NADP^+$. K562 cells were exposed to increasing concentrations of the quinone for 15 min, then resuspended in fresh medium and diluted to 10^5 cells/ml. The cells were then incubated at 37°C for 9 hours and at the times indicated, intracellular $NADP^+$ determined as described in the materials and methods. The results represent the mean ± SEM of 3 incubations.

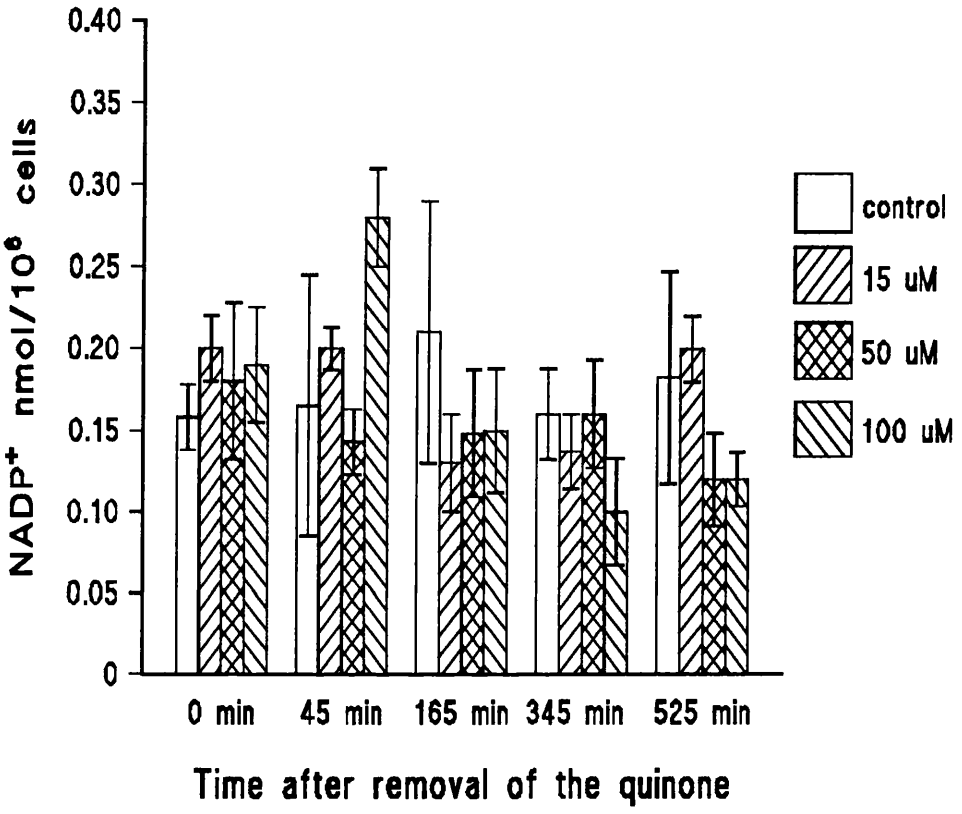

Fig. 7.11 The effect of menadione on the intracellular $NADP^+$. K562 cells were exposed to increasing concentrations of the quinone for 15 min, then resuspended in fresh medium and diluted to 10^5 cells/ml. The cells were then incubated at 37°C for 9 hours and at the times indicated, intracellular NAD^+ determined as described in the materials and methods. The results represent the mean ± SEM of 3 incubations.

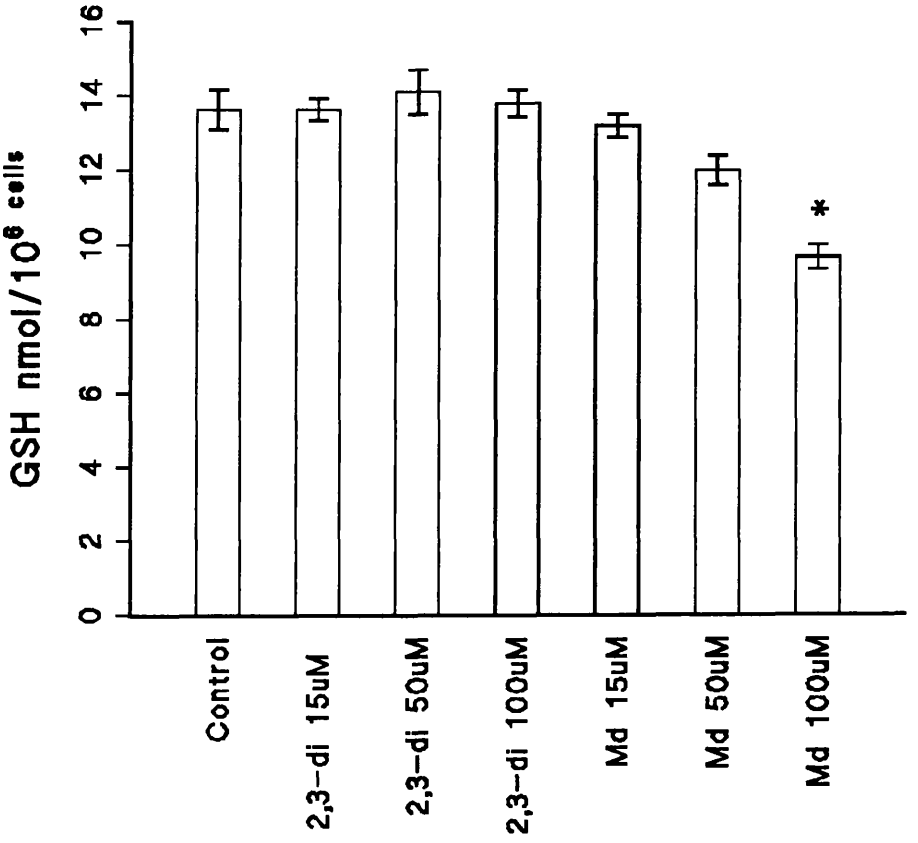

Fig 7.12 The effect of 2,3-diOMe-1,4-NQ (2,3-di) and menadione (Md) on intracellular GSH. K562 cells were exposed to the quinones for 15 min. GSH was determined as described in the materials and methods. Value represent the mean ± SEM of three separate preparations.

* Significantly different from control.

7.4. Discussion

In earlier studies both the redox cycling quinone and tert-butyl hydroperoxide were reported to cause distinct changes in the pyridine nucleotides. At concentrations which induced an early loss of membrane integrity, a prolonged increase in $NADP^+$ and a rapid depletion of NAD^+ were observed, whereas at lower concentrations where no loss of membrane integrity was detected, only a rapid depletion of NAD^+ was seen [Stubberfield and Cohen, 1989]. In the previous chapter, low concentrations of 2,3-diOMe-1,4-NQ (15 μM) and menadione (15 μM) were reported to cause DNA damage and a rapid depletion of NAD^+ in K562 cells, while low concentrations of menadione (25 μM) has been reported to cause DNA strand breaks in hepatocytes [Morrison et al, 1984]. Although the mechanisms by which redox cycling quinones induced an early loss of membrane integrity in mammalian cells were discussed in the earlier chapters, the relationship between DNA strand breakage and cell death has not been extensively studied.

7.4.1 DNA Damage and Cell Proliferation

As mentioned earlier, redox cycling quinones may cause cell death by numerous mechanisms [Monks et al, 1992]. Although evidence of DNA damage is observed at very low concentrations, prolonged exposure to the quinone often results in cell death from the effects of oxidative stress as discussed earlier. In an attempt to determine the long term consequences of quinone-induced DNA damage, cells were exposed to either 2,3-diOMe-1,4-NQ (15-100 μM) or menadione (15-100 μM) for 15 min, after

which the quinone was removed and cell proliferation determined over 72 hours. In cells exposed to either 2,3-diOMe-1,4-NQ (15 μM) or menadione (15 μM), no change in the rate cell of proliferation was detected although significant DNA damage was observed. At the higher concentrations (50-100 μM), both quinones caused extensive DNA damage and a reduction in cell proliferation. Although a clear relationship exists between the extent of DNA damage and the reduction in cell proliferation, an increase in the quinone concentration results in cytotoxicity from other quinone-induced processes including oxidative stress.

7.4.2 Oxidative Stress, DNA Fragmentation and Cytotoxicity.

As mentioned above, the prolonged exposure of mammalian cells to redox cycling quinones may result in oxidative stress characterised by the extensive oxidation of NADPH, GSH and increased intracellular Ca^{2+} [Smith et al, 1987; Gant et al, 1988; Fawthrop et al, 1991]. However, following a 15 min exposure of K562 cells to either 2,3-diOMe-1,4-NQ (15-100 μM) or menadione (15-50 μM), no significant change in the intracellular level of $NADP^{+}$ and GSH was observed in the subsequent 6 hours (Fig. 7.10 to 7.12). Similarly, increased intracellular Ca^{2+} is thought to activate Ca^{2+}-dependent enzymes including proteases and endonucleases [Orrenius, 1985]. In a recent study menadione was reported to cause cell death by a mechanism similar to apoptosis [McConkey et al, 1988]. It was envisaged that during oxidative stress, the activation of a Ca^{2+}-dependent endonuclease caused the fragmentation of DNA into multiples of 200 base-pair fragments. The possibility of quinone-induced DNA fragmentation was also investigated using U937 cells which have been extensively used as a model for apoptosis [Lennon et al, 1991].

However in U937 cells exposed to either 2,3-diOMe-1,4-NQ (50 μM) or menadione (50 μM), no DNA fragmentation was observed. These results suggest that the mechanism by which redox cycling quinones induced DNA damage and the subsequent reduction in cell proliferation may not involve oxidative stress or the induction of apoptosis.

7.4.3 DNA Repair and Cytotoxicity

Although numerous studies have investigated the mechanisms of cytotoxicity of compounds which cause DNA damage, no correlation has been found between the ability to induce DNA single strand breaks and cytotoxicity [Coleman et al, 1989]. Similarly, in this study K562 cells exposed to either 2,3-diOMe-1,4-NQ or menadione (15-400 μM) remained viable for up to 6 hours without a loss of membrane integrity despite extensive DNA strand breakage. One possible explanation is the rapid repair of such DNA lesions [Cantoni et al, 1986]. However at concentrations greater than 50 μM, less repair is observed (Fig. 7.4 and 7.5). The cytotoxicity of both quinones was found to correlate well with the extent of DNA damage and rate of DNA repair. In cells exposed to either quinone (15 μM), strand scission repair was almost complete within 3 hours of the removal of the quinone, while no change in the rate of cell proliferation was observed in the ensuing 72 hours. In cells exposed to 2,3-diOMe-1,4-NQ (100 μM), where only partial strand scission repair was observed after 6 hours, the rate of cell proliferation was significantly reduced. In cells exposed to menadione (50-100 μM), no strand scission repair was observed and cell proliferation was completely inhibited.

The partial repair of strand breaks induced by 2,3-diOMe-1,4-NQ (15-100 μM) may be due to the formation of mainly single strand breaks [Cantoni et al, 1986]. Conversely, the lack strand scission repair in cells exposed to menadione (50-100 μM) may result from the formation of double strand breaks where numerous single strand breaks are formed in close proximity, such breaks are usually more difficult to repair. Furthermore, in the previous chapter it was suggested that the mechanism by which menadione induced strand breakage may only be partly due to the generation of hydroxyl radicals [Cantoni et al, 1991].

7.4.4 Intracellular NAD^+ and ATP

DNA repair is mediated by poly(ADP-ribose)polymerase which consumes NAD^+ as a source of ADP-ribose [Berger, 1985]. In this study, the initial depletion of NAD^+ closely matched the extent of DNA damage induced by the quinones, while the rate of recovery of the nucleotide reflected the pattern of DNA repair. As the availability of NAD^+ is essential for DNA repair, where the nucleotide is only partially depleted such as following exposure to 2,3-diOMe-1,4-NQ (15-100 μM) and to menadione (15 μM), widespread repair is observed. Conversely, in cells exposed to menadione (50-100 μM), the nucleotide is almost completely depleted and no DNA strand scission repair is observed.

Berger et al (1979) proposed that the sequence of events which follow DNA damage, the depletion of NAD^+ and the subsequent depletion of ATP may represent a molecular response to prevent the survival of cells which suffer extensive DNA damage. Similarly, in this study a depletion of ATP was only observed in cells which suffered extensive DNA damage. In cells exposed to 2,3-diOMe-1,4-NQ (15-100 μM)

and to menadione (15 μM) DNA strand breakage and the decrease in NAD^+ were transient. In cells exposed to menadione (50-100 μM) no DNA repair was observed and this was accompanied a permanent depletion of NAD^+ and ATP.

These results suggest that redox cycling quinones induce extensive DNA damage, which does not lead to the early loss of membrane integrity. Where strand scission repair is delayed a reduction in the rate of cell proliferation may result, such as following exposure to 2,3-diOMe-1,4-NQ (Fig. 7.4). In cells which suffer extensive strand breakage cell death is thought to result from the consequences of the depletion of NAD^+. These studies highlight the importance of the marker used when assessing cytotoxicity [Grisham and Smith, 1984].

CHAPTER 8

FINAL DISCUSSION

8.1 INTRODUCTION

These studies attempted to determine the role of pyridine nucleotides in the mechanism of cell death induced by redox cycling quinones. Although the cytotoxicity of quinones has been extensively studied, their exact mechanism of cell killing remains unresolved. Furthermore, as new scientific data are reported, the re-examination of previous work becomes necessary. The present study reports for the first time the pyridine nucleotide changes induced by several BABQ. These studies also re-examined the pyridine nucleotide changes induced by the naphthoquinone 2,3-diOMe-1,4-NQ previously reported by Stubberfield and Cohen (1989). In an attempt to explain the pyridine nucleotide changes induced by redox cycling naphthoquinones, Stubberfield and Cohen (1989) proposed an interconversion of NAD(H) to NADP(H). This study examined the evidence for pyridine nucleotide interconversion in cells exposed to a number of compounds which are thought to cause oxidant cell injury. The evidence of nucleotide interconversion is partially based on the observation of Stubberfield and Cohen (1988) and later by Yamamoto and Farber (1992) of the absence of poly(ADP-ribose)polymerase activity in rat hepatocytes during oxidative stress. This present study also examined the role of poly(ADP-ribose)polymerase in the depletion of NAD^+ during oxidative stress. Finally, in an attempt to correlate DNA strand breakage with the pyridine nucleotide changes, quinone-induced DNA strand breakage was determined.

8.2 BABQ-Induced Pyridine Nucleotide Changes and Cytotoxicity in Rat Hepatocytes.

The ubiquity of quinones and in particular their increasing use as therapeutic agents has resulted in an increased interest in their mechanism of action in relation to cytotoxicity. Recently, Stubberfield and Cohen (1988,1989) published a series of studies on quinone-induced pyridine nucleotide changes. They made several observations including pyridine nucleotide interconversion (see section 8.3) and that redox cycling naphthoquinones caused a prolonged increase in $NADP^+$ prior to cell death, while the more cytotoxic benzoquinone which is incapable of redox cycling had no effect on the intracellular level of $NADP^+$. At non-toxic concentrations they also observed a transient decrease in NAD^+ in cells exposed to redox cycling naphthoquinones while no change was observed in cells exposed to benzoquinones. These observations suggested that the determination of intracellular pyridine changes may provide an insight into the mechanism of action of quinones.

Aziridinylbenzoquinones are increasingly being examined as potential chemotherapeutic agents. These compounds were designed with two active groups; the alkylating aziridinyl groups and the quinone moiety. However, the relative importance of redox cycling of the quinone moiety and the arylation of the aziridinyl groups in the cytotoxicity of these quinones remains unresolved [Gutierrez et al, 1986; Lea et al, 1988]. Recently, Prins et al (1989) reported that the cytotoxicity of these compounds as measured by trypan blue exclusion was closely related to their ability to redox cycle. Here, pyridine nucleotide changes induced by several BABQ were compared to the those induced by the naphthoquinone 2,3-diOMe-1,4-NQ.

The BABQ induced extensive oxidation of NADP(H) and plasma membrane

blebbing prior to cell death in a manner similar to the naphthoquinones. The close association between increased $NADP^+$, plasma membrane blebbing and cell death suggests that the mechanism of cell killing of the redox cycling naphthoquinones and the BABQ may result from the loss of reducing equivalents (GSH and NAD(P)H) during oxidative stress and the subsequent perturbation of intracellular Ca^{2+}. Furthermore, of the three BABQ used in the study, the least cytotoxic as measured by trypan blue exclusion was Carboquone, which is incapable of undergoing a one electron reduction. However, the decrease in the level of NADPH observed in cells exposed to this quinone may result from its two electron reduction in a manner similar to that proposed for 2-hydroxy-1,4-naphthoquinone [Cohen and Stubberfield, 1990].

Although similar changes in the redox status of NADP(H) were induced by the naphthoquinones and the BABQ, a significant difference was observed between the changes in NAD(H) induced by the two sets of quinones. Whereas the naphthoquinones induced a transient decrease in NAD^+ at low non-toxic concentrations as measured by trypan blue exclusion, the BABQ caused a permanent decrease in NAD^+. As a rapid decrease in NAD^+ is often associated with DNA repair, the transient nature of the naphthoquinone-induced decrease in NAD^+ probably results from the rapid repair of DNA single strand breaks. Conversely, a prolonged decrease in NAD^+ may be due to the formation of DNA damage which is either slowly repaired or not repaired. BABQ have been reported to cause both DNA strand breakage and DNA cross-linkage in mammalian cells. The determination of BABQ-induced pyridine nucleotide changes suggests two potential mechanisms of cell killing. The redox cycling of the quinone moiety may be responsible for the rapid loss of membrane integrity observed at high concentrations (> 100 μM) (as with the naphthoquinones).

While the permanent depletion of NAD^+ at lower concentrations (< 100 μM) may be due DNA damage resulting from the activation of the aziridinyl groups possibly leading to crosslinking of DNA bases. However the 3 hour incubation used in this study would not reveal the cytotoxicity associated with the prolonged decrease on NAD^+. Alternatively, a five or six hour incubation may have revealed a decrease in ATP followed by a loss of membrane integrity in cells exposed to Carboquone as well as TW13 (100 μM) and TW25 (50 μM).

8.3 Redox Cycling, Oxidative Stress and Nucleotide Interconversion

When the concept of pyridine nucleotide interconversion was first proposed by Stubberfield and Cohen (1989) and later by Yamamoto and Farber (1992), it was suggested that it may represent a novel cellular response to oxidative stress. It was envisaged that during oxidative stress intracellular NAD^+ was converted to $NADP^+$ and later to NADPH. On first examination, the evidence for nucleotide interconversion was almost irresistible; the decrease in NAD^+ was matched by an increase in $NADP^+$; increased intracellular Ca^{2+} was thought to activate NAD^+ kinase and no evidence of poly(ADP-ribose)polymerase activity was detected.

Despite the evidence above, pyridine nucleotide interconversion would only be possible if several assumptions were made. Firstly, that at concentrations of the redox cycling quinones and tBH which were reported to cause nucleotide interconversion, no DNA strand breakage had taken place. Alternatively, if strand breakage had taken place, the process of strand scission repair was not initiated. However, numerous compounds which induce oxidative stress including menadione, 2,3-diOMe-1,4-NQ, H_2O_2 and tBH have been shown to induce DNA strand breakage [Morrison et al,

1984;Schraufstatter et al, 1986b; Coleman et al, 1990]. Furthermore in the present study, in cells exposed to tBH which causes oxidative stress without redox cycling, the depletion of NAD^+ was significantly greater that the increase in $NADP^+$. A similar result was observed with the BABQ. Additionally, under circumstances where a significant increase $NADP^+$ has been reported, such as in mammary tissue during lactation a concurrent decrease in NAD^+ has not been reported [Kaplan, 1985].

8.4 Poly(ADP-ribose)polymerase Inhibitors and NAD^+ Hydrolysis

In cells which suffer DNA damage, the activation of poly(ADP-ribose)polymerase results in the rapid depletion of NAD^+. DNA strand scission repair is thought to involve the hydrolysis of the nucleotide as a source of ADP-ribose [Berger et al, 1979]. Recently, the depletion of NAD^+ induced by a number of redox cycling quinones as well as tBH has been suggested to be independent of the activation of poly(ADP-ribose)polymerase or a related enzyme [Stubberfield and Cohen, 1988; Yamamoto and Farber, 1992] . The evidence was primarily based on the observation of a depletion of NAD^+ in the presence of inhibitors of poly(ADP-ribose)polymerase.

A number of difficulties exist in trying to inhibit poly(ADP-ribose)polymerase in intact cells; primarily that of getting an effective concentration of the inhibitor inside the cell [Rankin et al, 1989]. By designing the inhibitor experiments in a manner which enabled the accumulation of the inhibitor inside the cell, a significant inhibition of the depletion of NAD^+ was observed, using inhibitors which had been shown to be ineffective in previous studies [Cohen and Stubberfield, 1990; Yamamoto and Farber, 1992]. At the concentrations of the inhibitors used, the extent of inhibition was less than would be expected from the reported inhibitor constants. However such values

were determined in cell free systems; in the absence of both plasma and nuclear membranes. Furthermore, in the studies of Stubberfield and Cohen (1988) a significant inhibition of NAD^+ depletion was only observed in cells preincubated with 3-aminobenzamide and exposed to dimethyl sulphate. In cells preincubated with either nicotinamide or theophylline, far less inhibition was observed. The inhibitor studies were complicated by several other factors including the transient nature of the decrease in NAD^+ at low concentrations. This restricted the effective experimental time to the first 30 min of exposure to the quinones and tBH. At higher concentrations of the toxicants where the decrease is permanent, the greater rate of NAD^+ loss prevents an effective inhibition as only a fraction of the extracellular inhibitor concentration is thought to enter the intact cell [Rankin et al, 1989]. The time during which the inhibitor studies could be carried out was also restricted by the background increase in NAD^+, resulting from the inhibition of the normal recycling of the nucleotide. In the previous studies of Stubberfield and Cohen (1988) several fundamental factors were not considered, including the time course of entry of the inhibitor into the cell and in particular into the nucleus.

In addition to inhibitor studies, a direct determination of NAD^+ hydrolysis was made. By radiolabelling the intracellular nucleotides at the nicotinamide moiety, it was possible to determine the fate of NAD^+. These studies provided convincing evidence of the simultaneous hydrolysis of NAD^+ and the formation of nicotinamide. Intracellular NAD^+ has several fates; phosphorylation to $NADP^+$; reduction to NADH or hydrolysis primarily to nicotinamide and ADP-ribose. During oxidative stress no increase in NADH was observed, similarly the increase in $NADP^+$ induced by most compounds can be accounted for by the oxidation of NADPH. Hence the most likely

explanation of the depletion of NAD^+ is hydrolysis.

In determining the hydrolysis of NAD^+, the efficiency of the pyridine nucleotide cycle facilitated the separation of the radiolabelled nucleotides. As mentioned in chapter 1, large quantities of the intermediates in the pyridine nucleotide cycle are not detected, hence radioactivity is concentrated in peaks containing either nicotinamide, NAD^+ and $NADP^+$. Further evidence of the efficiency of the NAD^+ salvage pathways may be gained from the observation that in cells exposed to low concentrations of the redox cycling quinones as well as tBH, the increase in radioactivity seen in the nicotinamide peak at 15 and 30 min is not present after 1 hour, while a recovery in the radioactivity is observed in the NAD^+ peak is observed after 60 min.

8.5 Quinone-Induced DNA Strand Breakage

Quinones may induce DNA damage in mammalian cells by a number of mechanisms, including the activation of Ca^{2+} dependent endonucleases, the stabilization of DNA topoisomerase II in the form that cleaves but does not religate or through the generation of active oxygen species, in particular hydroxyl radicals. As mentioned above, the transient decrease in intracellular NAD^+ induced by low concentrations of 2,3-diOMe-1,4-NQ and menadione is indicative of DNA damage. In an attempt to determine the nature of the DNA damage, DNA strand breakage was determined using the technique of alkaline elution. Several factors were considered including the time course of DNA damage, the quinone concentration and the rate of repair. In the earlier discussion on the fate of intracellular NAD^+, it was suggested that the early depletion of the nucleotide was due to the activation of poly(ADP-ribose)polymerase. This suggestion is supported by the observation of DNA strand

breakage in cells within 5 min of exposure to either quinone, while further ruling out the possibility of nucleotide interconversion as the two processes are incompatible. Several factors point to DNA single strand breakage mediated by the generation of hydroxyl radicals. The early detection of strand breakage is consistent with the rapid generation of active oxygen species following exposure to redox cycling quinones [Cohen and d'Arcy Docherty, 1987; Gant et al, 1988], while single strand breaks caused by active oxygen species are usually rapidly repaired [Cantoni et al, 1986]. Finally, the inhibition of strand breaks in the presence of phenanthroline suggest the mechanism by which redox cycling quinones cause DNA damage may involve a Haber-Weiss type reaction [Haber and Weiss, 1934; Mello Filho and Meneghini, 1984]. Furthermore in this study, no evidence of DNA fragmentation was detected in cells exposed to menadione or 2,3-diOMe-1,4-NQ in contrast to that previously reported by McConkey et al (1988).

The detection of DNA damage at very low concentrations of the redox cycling quinones has other significant implications. Previously it was suggested that arylating quinones such benzoquinone were more cytotoxic than redox cycling quinones as they caused a loss of membrane integrity at a much lower concentration; 100 µM [Gant et al, 1988; Stubberfield and Cohen 1989]. Whereas the redox cycling quinone 2,3-diOMe-1,4-NQ induced a loss of membrane integrity at a much higher concentration; 400 µM. However in preliminary studies in hepatocytes exposed to benzoquinone (50 µM) no DNA damage was detected, whereas in hepatocytes exposed to 2,3-diOMe-1,4-NQ (50 µM) and menadione (50 µM) extensive DNA damage was observed. Using DNA damage as a determinant of cytotoxicity there is strong evidence that the redox cycling quinones may be more cytotoxic at the lower concentrations.

Having discovered that a short exposure of mammalian cells to low concentrations of certain redox cycling quinones results in extensive DNA strand breakage, the consequences for long term cell viability were examined. Although compounds which cause oxidative cell injury are known to induce extensive DNA strand breakage, early loss of membrane integrity is normally attributed to other consequences of oxidative stress including the oxidation of cellular thiols, increased intracellular Ca^{2+} and lipid peroxidation [Fawthrop et al, 1991]. Furthermore in numerous studies, cell death has been dissociated from the formation of DNA single strand breaks. However studies which attempt to correlate DNA strand breakage with cell death often use compounds which have multiple mechanisms of action or expose the cells to very high concentrations. This often results in cell death before the effects of DNA damage can be seen [Dypbukt et al, 1990]. Other studies were carried out in non-proliferating cells [Coleman et al, 1989]. These studies revealed that following extensive DNA damage long term viability is dependent on the rapid repair of strand breaks which was in turn probably dependent on the availability of NAD^+. Extensive depletion of NAD^+ during strand scission repair may precipitate cell death.

8.6 Final Summary and Some Possible Future Experiments.

Pyridine nucleotides exist in two forms; NAD(H) and NADP(H). The cytotoxicity of redox cycling quinones has been shown to result from their ability to significantly alter the redox status of NADPH over several hours. Additionally, quinones which cause DNA damage have been shown to alter the level of NAD(H), in particular the measurement of NAD^+ provides a simple means of assaying DNA damage. Hence the determination of cellular pyridine nucleotides provides an additional tool in assessing

the mechanism of cytotoxicity compounds which cause oxidant-induced cell injury.

These studies also provide the basis for a number future studies into the mechanisms of cytotoxicity of redox cycling quinones and other oxidants. A determination of oxidant-induced pyridine nucleotide changes on a subcellular basis may be informative as the pyridine nucleotide changes reported in this study represent changes at the cellular level. For example, it is worthwhile exploring whether the oxidation of mitochondrial NADPH is more important than cytosolic NADPH. Does alteration in the redox status of NADPH alter the compartmentalization of the nucleotide ? etc. These studies only implicate the ribosylation of nuclear proteins. Studies could be carried out to clarify the relationship between the decrease of NAD^+ and increased ribosylation of nuclear and other proteins. Further studies could also be undertaken to clarify the relationship between the extent of DNA damage, the rate of repair and cytotoxicity. Additionally, confirmation of the role of hydroxyl radicals in quinone-induced DNA strand breakage could be found by looking at strand breakage in the presence of hydroxyl radical scavengers. Finally, other forms of oxidant-induced DNA damage should be investigated, including double strand breakage, DNA-protein cross-links and the frequency of incorrect DNA repair.

REFERENCES

Ames BN, Dietery carcinogens and anticarcinogens. Science 221:1256-1264, 1983

Althaus RF and Richter C, ADP-ribosylation of proteins: Enzymology and Biological Significance. Springer-Verlag, Heidleberg, New York, London, Paris, 1987.

Aruoma OI, Halliwell B, Damage to the bases in DNA induced by hydrogen peroxide amd ferric ion chelates. J. Biol Chem 264:20509-20512, 1989.

Aw TY, Nicotera P, Manzo and Orrenius S, Trybutyltin stimulates apoptosis in rat thymocytes. Arch. Biochem. Biophys. 283:46-50, 1990.

Bauer NA, Halkam A and Kun E, Mechanism of poly(ADP-ribose) polymerase catalysis; mono ADP-ribosylation of poly(ADP-ribose) polymerase at nanomolar concentrations of NAD. FEBS Lett 195:331-338, 1986.

Bellomo G, Mirabelli F, Di Monte D, Richelmi P, Thor H, Orrenius G and Orrenius S, Formation and reduction of glutathione-protein mixed disulphides during oxidative stress. Biochem Pharmacol 36: 1313-1320, 1987.

Benjamin NA and Gill DM, Poly(ADP-ribose) synthesis in vitro programmed by damaged DNA. J Biol Chem. 255:10502-10508, 1980.

Berger NA, Poly(ADP-ribose) in the cellular response to DNA damage. Radiation Res. 101:4-15, 1985.

Berger NA, Sikorski GW, Petzold SJ and Kurohara KK, Association of poly(adenosine diphosphoribose) synthesis with DNA damage and repair in normal human lymphocytes. J Clin Invest. 63:1164-1171, 1979.

Berger NA, Sims JL Catino DM and Berger SJ, Poly(ADP-ribose) polymerase mediates the suicide response to massive DNA damage: studies in normal and DNA-repair defective cells. In ADP-ribosylation, and DNA Repair and Cancer, pp. 219-226. Japan Sci. Soc. Press, Tokyo/VNU Science Press, Utrecht, 1983.

Berger NA and Petzold SJ, Identification of the requirements of DNA for activation of poly(ADP-ribose) polymerase. Biochemistry 24:4352-4355, 1985.

Bernosky C and Swan M, An improved cycling assay for nicotinamide adenine dinucleotide. Anal Biochem. 53:452-458, 1973.

Birnboim HC and Jevcak JJ, Fluorometric method for rapid detection of DNA strand breaks in human white blood cells produced by low doses of radiation. Cancer Res. 41: 1889-1892, 1981.

Blum RH and Carter SK, Adriamycin: A new anticancer drug with significant clinical activity. Annals Int. Med. 80: 247-259, 1974.

Boobis AR, Fawthrop DJ and Davies DS, Mechanisms of cell death. TIPS 10:275-

280, 1989.

Bradley MO and Kohn KW, X-ray-induced DNA double strand break production and repair in mammalian cells as measured by neutral filter elution.

Bucher Th, In "Pyridine nucleotide dependent dehydrogenase" (H Sund, ed) pp. 439-461, Springer-Verlag, Berlin, Heidelberg, New York, 1970.

Bus JS and Gibson JE, Role of activated oxygen in chemical toxicity. In " Drug metabolism and drug toxicity" (ed Mitchell JR and Horning MG) pp 21-32. Raven press, New York, 1984.

Cadenas E, Oxidative stress and formation of excited species. In " Oxidative stress" (ed. Seis H). pp311-330 Academic press Inc. London 1985.

Canbonera D and Azzone GF, Permeability of inner mitochondrial membrane and oxidative stress. Biochim et Biophys Acta 943:245-285, 1988.

Cantoni O, Murry D and Meyn RE, Effects of 3-aminobenzamine on DNA strand-break rejoining and toxicity in CHO cells treated with hydrogen peroxide. Biochimica et Biophysica acta. 867:135-143, 1986.

Cantoni O, Sestili P, Cattabeni F, Bellomo G, Pou S, Cohen M and Cerutti P, Calcium chelator quin 2 prevents hydrogen- peroxide-induced DNA breakage and cytotoxicity, Eur. J. Biochem. 182:209-212, 1989

Cantoni O, Fiorani M, Cattabeni F and Bellomo G, DNA breakage caused by hydrogen peroxide during the metabolism of 2-methyl-1,4-naphthoquinone (menadione) does not contribute to the cytotoxic action of the quinone. Biochem. Pharmacol. 42: S220-222, 1991.

Carter SK and Crook ST, Mitomycin C. Current status and New development. Academic press London 1974.

Chance B, Seis H and Boveris A, Hydroperoxide metabolism in mammalian organs. Physiol. Rev. 59:529-605, 1979.

Chasseaud LF, The role of glutathione and glutathione-S-transferase in the metabolism of chemical carcinogens and other electrophilic agents. Adv. Cancer Res. 29: 175-274, 1979.

Chaykin S, Degani M, Johnson L and Samli M, The fate of nicotinamide in the mouse. Urinary metabolites. J. Biol Chem. 240: 932-938, 1965.

Chien KR, Pfau RG and Farber JL, Ischemic myocardial cell injury. Prevention by chlorpromazine of an accelerated phospholipid degradation and associated membrane dysfunction. Am. J. Pathol. 97:505-529, 1979.

Coleman JB, Gilfor D and Farber JL, Dissociation of the accumulation of single strand breaks in DNA from the killing of cultured hepatocytes by oxidative stress, Molecular Pharmacol 36: 193- 200, 1989.

Cohen GM and d'Arcy Docherty M, Free radical mediated cell toxicity by redox cycling chemicals. Br. J. Cancer 55:46-52, 1987.

Cohen GM and Stubberfield CR, Pyridine nucleotide changes in hepatocytes exposed to quinones. Free Rad. Res. Comms. 8:355-363, 1990.

Cotter TG, Lennon JG, Glynn JG and Martin SJ, Cell death *via* apoptosis and its relationship to growth. Developments and differentiation of both tumour and normal cells, Anticancer Res. 10: 1153-1160, 1990.

Creissen D and Shall S, Regulation of DNA ligase activity by Poly(ADP-ribose). Nature 296:271-272, 1982.

Di Monte D, Bellomo G, Thor H, Nicotera P and Orrenius S, Menadione-induced cytotoxicity is associated with protein thiol oxidation and alterations in intracellular Ca^{2+} homeostasis. Arch. Biochem. Biophys. 235: 343-350, 1984a.

Di Monte D, Ross D, Bellomo G, Eklow L and Orrenius S, Alterations in intracellular thiol homeostasis during the metabolism of menadione by isolated rat hepatocytes. Arch. Biochem. Biophys. 235: 334-342, 1984b.

Dorr TR, Bowden T, Alberts DS and Liddil JD. Interaction of mitomycin C with Mammalian DNA detected by alkaline elution. Cancer Research 45:3510-3516, 1985.

Driebergen RJ, Holthuis JJM, Hulshoff A, Postma-Kelder SJ, Verboom W, Reinhoudt DN and Lelieveld P, Electrochemistry of potential reductive alkylating quinones: its use in the development of new aziridinylquinones. Anticancer. Res. 6:605-620, 1986.

Durkacz BW, Omidiji O, Gray DA and Shall S, $(ADP\text{-}ribose)_n$ participates in DNA excision repair. Nature 283:593-596, 1980.

Dypbukt JM Thor H and Nicotera P, Intracellular Ca^{2+} chelators prevents DNA damage and protects hepatoma ICIC7 cells from quinone-induced cell death. Free Rad Res Commun 8:347-354, 1990.

Dzielendziak A, Butler J, Hoey BM, Lea JS and Ward TH, Comparison of the structural and cytotoxic activity of novel 2,5-bis(carboethoxyamino)-3,6-diaziridinyl-1,4-benzoquinone analogues. Cancer Research 50: 2003-2008, 1990.

Epel D, Patton C, Wallace RW and Cheung WY, Calmodulin activates NAD kinase of sea urchin eggs: an early event of fertilization. Cell 23:543-549, 1981.

Fawthrop DJ, Boobis AR and Davies DS, Mechanisms of cell death. Arch. Toxicol.

65:437-444, 1991.

Fee JA and Valentine JS, Chemical and physiological properties of superoxide . In "Superoxide and Superoxide Dismutase " (ed Michaelson AM) pp 19-60. Academic press Inc. London 1977.

Foster JW and Baskowsky-Foster AM, Pyridine nucleotide cycle of Salmonella typhimurium: In vivo recycling of nicotinamide adenine dinucleotide. J. Bacteriol. 142: 1032-1035, 1980.

Foster JW and Moat AG, Nicotinamide adenine dinucleotide biosynthesis and pyridine nucleotide cycle metabolism in microbial systems. Microbial Rev. 44: 83-105, 1980.

Frei B, Winterhalter KH and Richter C, Menadione (2-methyl- 1,4-naphthoquinone) dependent enzymatic redox cycling and calcium release by mitochondria. Biochemistry 25: 4438-4443, 1986.

Freidovich I, Superoxide radical: An endogenous toxicant. Ann Rev. Pharmacol Toxicol. 23:239-257, 1983.

Gaal JC, Smith RK and Pearson CK, Cellular euthanasia mediated by a nuclear enzyme: a central role for nuclear ADP-ribosylation in cellular metabolism. TIPS 12:129-130, 1987.

Gant TW, Rao DNR, Mason RP and Cohen GM, Redox cycling and sulphydryl arylation; their relative importance in the mechanism of quinone cytotoxicity to isolated hepatocytes. Chem-Biol. Interact 65:157-173, 1988.

Gholson RK, The pyridine nucleotide cycle. Nature 212:933-935, 1966.

Gillette JR, A perspective on the role of chemically reactive metabolites of foreign compounds in toxicity. Correlation of changes in covalent binding of reactive metabolites with the changes in the incidence of toxicity. Biochem. Pharmacol. 23:2785-2794, 1974.

Giloni L, Takeshita M, Johnson F, Iden C and Grollman AP, Bleomycin-induced strand-scission of DNA: Mechanism of deoxyribose cleavage. J. Biol. Chem. 256:8608-8615, 1981.

Glende EA and Pushpendran CK, Activation of phospholipase A_2 by carbon tetrachloride in isolated hepatocytes. Biochem Pharmacol 35: 3301-3307, 1986.

Greenbaum AL and Pinder S, The biosynthesis of nicotinamide adenine dinucleotide in rat mammary glands. Biochem. J. 107: 55-62, 1968.

Grisham JW and Smith GJ, Predictive and mechanistic evaluation of toxic responses in mammalian cell culture systems, Pharmacol. Rev: 36,151S-171S, 1984.

Gutierrez PL, Fox BM, Mossoba MM, Egorin M, Nakazawa H and Bachur NR, Electron spin resonance of electrochemically generated free radicals from diaziquone and its derivatives. Biophys. Chem. 22: 115-123, 1985.

Gutierrez PL, Biswal S, Nardino R and Biswal N, Reductive activation of diaziquone and possible involvement of free radical and the hydroquinone dianion. Cancer Res. 46:5779-5785, 1986.

Gunji H, Kharbanda S and Kufe D, Induction of intranucleosomal DNA fragmentation in myeloid leukaemic cells by 1-β-D-arabinofuranosylcytosine. Cancer Res. 51:741-743, 1991.

Haber F and Weiss J, The catalytic decomposition of hydrogen peroxide by iron salts. Proc. R. Sco. London Ser. A 147: 332-351, 1934.

Halliwell B and Gutteridge JMC, Oxygen toxicity, oxygen radicals, transitional metals and disease. Biochem. J. 219: 1-14, 1984.

Halliwell B and Aruoma OI, DNA damage by oxygen derived species:Its mechanism and measurement in mammalian systems. Febs Lett 281: 9-19, 1991.

Hanawalt CP, Cooper PK, Sanesan AK and Smith CA, DNA repair in bacteria and mammalian cells. Ann. Rev. Biochem. 48: 783-836, 1983.

Hatefi Y, The mitochondrial electron transport chain and oxidative phosphorylation system. Ann Rev. Biochem 54: 1015-1069, 1985.

Heldt HW, Greif N, Klingenberg M, Scholz R Panten, U, Grunst, J and Bucher T, The problem of acid-labile triphosphopyridine nucleotide in biological materials. J.Biol Chem. 240: 4659-4661, 1965

Hayaishi O and Ueda K, Poly(ADP-ribose) and ADP-ribosylation of proteins. Ann Rev. Biochem 46: 95-116, 1977.

Hiltz H, Bredehorst R, Amamietz P and Wielkens K, Subfraction and subcellular distribution of mono(ADP-ribosyl) protein in eukaryotic cells. In "ADP-ribosylation reactions" (ed Hayashi O and Ueda K) pp 208-221, Academic press Inc. London, 1982.

Hissin PJ and Hilf R, Fluorometric determination of glutathione using o-phthaldialdehyde. Anal. Biochem. 74:214-226, 1976.

Imlay TA and Linns BA, DNA damage and oxygen radical toxicity. Science 240:1302-1309, 1988.

Imsande J and Handler P, Biosynthesis of diphosphopyridine nucleotide 111. nicotinic acid pyrophosphatase. J.Biol Chem. 236: 525-530, 1961.

Ito S, Schizuta Y and Hayaishi O, Purification and classification of poly(ADP-ribose) synthetase from calf thymus. J. Biol. Chem. 254:3647-3651, 1979.

James MR and Lehmann AR, Role of poly(adenosine diphosphate ribose) in deoxyribonucleic acid repair in human fibroblasts. Biochemistry 21:4007-4013, 1982.

Jewell SA, DiMonte D, Richelmi P, Bellomo G and Orrenius S, Tert-Butylhydroperoxide-induced toxicity in isolated rat hepatocytes:Contribution of thiol oxidation and lipid peroxidation. J Biochem Toxicol 1:13-22, 1986.

Jones DP, The role of oxygen concentration in oxidative:Hypoxic and Hyperoxic models. In "Oxidative Stress" (ed Seis H) pp 151-195, 1985.

Jones DP, Eklow L, Thor H and Orrenius S, Metabolism of hydroperoxide in isolated hepatocytes:relative contribution of catalase and glutathione peroxidase in decomposition of endogenously generated hydrogen peroxide. Arch. Biochem. Biophys. 210:510-516, 1981.

Kalhorn TF, Thummel KE, Nelson SD and Slattery JT, Analysis of oxidized and reduced pyridine nucleotides in rat liver by high-performance liquid chromatography. Anal Biochem. 151:343-347, 1985.

Kameshita I Matsuda Z, Taniguchi T and Shizuta Y, Poly(ADP-ribose) synthetase. Separation and identification of three proteolytic fragments as the substrate binding domain, the DNA binding domain and the automodification domain. J. Biol Chem. 259:4770-4776, 1984.

Kaplan NO, Goldin A, Humpherys SR and Stolzenbach FE, Pyridine precursor of mouse liver diphosphopyridine nucleotides. J. Biol Chem. 226: 365-371, 1957

Kaplan N, Metabolic pathways involving niacin and its derivatives . In "Metabolic Pathways" (Greenberg D, ed), Vol 2, pp 627-672. Academic press, Inc., New York, 1961.

Kaplan N, The role of pyridine nucleotides in regulating cellular metabolism. Current topics in cellular regulation 20: 271-281, 1985.

Kappus H, Overview of enzyme systems involved in bioreduction of drugs and redox cycling. Biochem. Pharmacol. 35: 1-6, 1986.

Kappus H, Oxidative stress in chemical toxicity. Arch. Toxicol. 60:114-149, 1987.

Kappus H and Sies H, Toxic drug effects associated with oxygen metabolism: Redox cycling and lipid peroxidation. Experientia 37: 1233-1241. 1981

Kawaichi M, Ueda K and Hayaishi O, Initiation of poly(ADP-ribosyl) histone synthesis by poly(ADP-ribose) synthetase. J Biol. Chem. 255:816-819, 1980.

Kawaichi M, Ueda K and Hayaishi O, Multiple auto poly(ADP-ribosyl)ation of rat liver of rat poly(ADP-ribose) synthetase. J Biol. Chem. 256:9483-9489, 1981.

Kawamura M Tanigawa Y, Kitamura, Miyaki Y and Shimoyama M, Effects of polyamines on purified poly(ADP-ribose) synthetase from rat liver nuclei. Biochim Biophys Acta 652:9483-9489, 1981.

Kidwell WR, Nolan N and Stone PR, Variation in poly(ADPribose) and poly(ADPribose)synthetase in synchronously dividing cells. In "ADP-ribosylation reactions" (ed Hayaishi O and Ueda K) pp 374-388, Academic press Inc. London 1982.

Kohn KW, Ewig RAG, Erickson LC and Zwelling LA, Measurements of strand breaks and crosslinks in DNA by alkaline elution. In "DNA Repair: A laboratory manual of research techniques", (Friedberg EC and Hanawalt PC, eds). pp379-401. New York : Marcel Dekker 1981.

Lagunas R, Mclean P and Greenbaum AL, The effect of raising the NAD^+ content on the pathway of carbohydrate metabolism and lipogenesis in rat liver. Eur. J. Biochem. 15: 170-190, 1970.

Lasko SA, Lorentzen RJ and Ts'o POP, Role of superoxide in deoxyribosenucleic acid strand scission. Biochemistry 19:3023-3028, 1980.

Lea JS, Garner HJ, Butler J, Hoey BM and Ward TH, The lack of correlation between toxicity and free radical formation of two diaziridinyl benzoquinones. Biochem. Pharmacol 37:2023-2025, 1988.

Lehninger AL, Vercesi A and Bababunmi EA, Regulation of Ca^{2+} release from mitochondria by the oxidation-reduction state of pyridine nucleotides. Proc. Natl. Acad. Sci USA 75:1690-1694, 1978.

Lemasters JC and Hackenbrock CR, Firefly luciferase assay for ATP production in mitochondria . Methods Enzymol 57: 36-50, 1978.

Lennon SV, Martin SJ and Cotter TG, Dose-dependent induction of apoptosis in human tumour cell lines by widely diverging stimuli. Cell Prolif. 24:203-214, 1991.

Lin AJ, Cosby LA Shansky CW and Sortorelli AC, Potential bioreductive alkylating agents. 1. Benzoquinone derivatives. J. Med Chem. 15:1247-1252, 1972.

Lind C, Hochstein P and Earnster, DT-diaphorase as a quinone reductive: A cellular control devise against semiquinone and superoxide radical formation. Arch. Biochem Biophys. 216:178-185, 1982.

Lindquist R and Olivera BM, Pyridine nucleotide metabolism in E coli. 1. Exponential growth. J. Biol Chem. 246 : 1107-1116, 1971.

Little JW, Zimmermann SB, Oshinshy CK and Gillert, Enzymic joining of DNA strands II. An enzyme-adenylate intermediate in the dpn-dependent DNA ligase reaction. Proc. Natl. Acad. Sci. 58: 2004-2011 1967.

Loeb LA, James EA, Waltersdorph AM and Klebanoff SJ, Mutagenesis by autoxidation of iron with isolated DNA, Proc. Natl Acad. Sci.USA. 85:3918-3922, 1988.

Lowry OH, Roseborough OH Farr AL and Randall RJ, Protein measurements with the folin phenol reagent. J. Biol. Chem. 193:265-275, 1951

Lotscher H, Winterhalter KH, Carafoli E and Richter C, Hydroperoxide-induced loss of pyridine nucleotides and release of calcium from rat liver mitochondria. J. Biol Chem. 255: 9325-9330, 1980.

Lozzio CB and Lozzio BB, Human chronic myelogenous leukemia cell line with positive Philadelphia chromosome, Blood 45: 321-324, 1975.

Lusthof KJ, DE Mol N, Janssen LHM, Verboom W and Reinhoudt DN, DNA alkylation and formation of DNA interstrand cross-links by potential 2,5-bis(1-aziridinyl)-1,4-benzoquinones. Chem-Biol.Interact. 701: 249-262, 1989.

Lusthof KJ, DE Mol N, Janssen LHM, Prins B, Verboom W and Reinhoudt DN, Interactions between potential antitumour 2,5-(1-aziridinyl)-1,4-benzoquinone derivaties and glutathione: reductive activation, conjugation and DNA damage. Anti-Cancer Drug Design 6:253-260, 1990.

Marks DI and Fox RM, DNA damage, poly(ADP-ribosyl)ation and apoptotic cell death as a potential common pathway of cytotoxic drug action. Biochem. Pharmacol. 42: 1859-1867, 1991.

McConkey DJ, Hartzell P, Nicotera P, Wyllie AH and Orrenius S, Stimulation of endogenous endonuclease activity in hepatocytes exposed to oxidative stress, Tox Lett 42: 123- 130, 1988.

McConkey DJ, Hartzell P, Amador Perez JF, Orrenius S and Jondal M, Calcium-dependent killing of immature thymocytes by stimulation via CD3/T cell receptor complex. J. Immunol. 143:1801-1806, 1989a.

McConkey DJ, Nicotera P, HartzellP, Bellomo G Wyllie AH and Orrenius S, Glucocorticoid activates a suicide response in thymocytes through an elevation of cytosolic Ca^{2+} concentration. Arch. Biochem. Biophys. 269:365-370, 1989b.

McCord JM and Fridivich I, Superoxide dismutase : An enzymic function of erythrocuprein. J Biol Chem. 244:6049-6055, 1969.

Mclean J, Ngo DJC and Olivera BM, Pyridine nucleotide metabolism in E. Coli.

111. Biosynthesis from alternative precursors *in vivo* J. Biol Chem. 248: 5144-5159, 1973.

Mcwilliams RC, Cross WG, Kaplan JG and Birnboim HC, Rapid rejoining of DNA strand breaks in resting human lymphocytes after irradiation damage by low doses of ^{60}Co gamma rays or 14.6 MeV neutrons, Radiat. Res. 94: 499-507, 1983.

Mellgren RL, Calcium-dependent proteases: an enzyme system active at cellular membranes ?. FASEB 1:110-115, 1987.

Mello Filho AC, Hoffmann ME and Meneghini R, Cell killing and DNA damage by hydrogen peroxide are mediated by intracellular iron, Biochem. J. 218:273-275, 1984.

Mello Filho AC and Meneghini R, In vivo formation of strand breaks in DNA by hydrogen peroxide is mediated by the Haber-Weiss reaction. Biochimica Biophysica acta 781:56-63, 1984.

Mirabelli F, Salis A, Marinoni V, Finardi G, Bellomo G Thor H and Orenius S, Menadione-induced bleb fromation in hepatocytes is associated with the oxidation of thiol groups in actin. Arch. Biochem. Biophys. 264:261-269, 1988.

Mirabelli F, Salis A, Vairetti M, Bellomo G Thor H and Orenius S, Cytoskeleton alterations in human platelets exposed to oxidative stress are mediated by oxidative and Ca^{2+}-dependent mechanisms. Arch. Biochem. Biophys. 270:478-488, 1989.

Moldeus P, Hogberg J and Orrenius S, Isolation and use of liver cells, Methods Enzymol 52: 60-71, 1978.

Monks TJ Hanzlik RP, Cohen GM Ross D and Graham DG, Contempory issues in toxicology: Quinone chemistry and toxicology. Tox. and Appl. Pharm 112:2-16, 1992.

Moore M, Thor H, Moore G, Nelson S, Moldeus P and Orrenius S, The toxicity of acetaminophen and N-acetyl-benzoquinoneimine in isolated hepatocytes is associated with thiol depletion and increased cytosolic Ca^{2+}. J. Biol. Chem. 260:13035-13040, 1985.

Moore GA, O'Brien PJ and Orrenius S, Menadione (2-methyl-1,4-naphthoquinone)-induced Ca^{2+} release from rat-liver mitochondria is caused by NAD(P)H oxidation, Xenobiotica 16:873-882, 1986.

Morgan WA, Hartley JA and Cohen GM, Quinone induced DNA single strand breaks in rat hepatocytes and human myelogenous leulaemic K562 cells. Biochem. Pharmacol. 44: 215-221, 1992.

Morrison H, Jernstron B, Nordenskjold M, Thor H and Orrenius S, Induction of DNA damage by menadione (2-methyl-1,4- naphthoquinone) in primary cultures of

rat hepatocytes. Biochem Pharmacol 33: 1763-1769, 1984.

Moser B, Winterhalter KH and Richter C, Purification and properties of mitochondrial NAD^+ glycohydrolase. Arch. Biochem Biophys. 224:356-364, 1983.

Niedergang C, Okazaki H and Mendel P, Properties of purified calf thymus poly(adenosine diphosphate ribose) polymerase. Eur J Biochem. 102:43-57, 1979

Nickerson WJ, Falcone G and Strauss G, Studies on quinone thioethers 1. Mechanism of formation and properties of thiodone. Biochemistry 2: 537-543, 1963.

Nishizuka Y, Ueda K, Honjo T and Hayaishi O, Enzymic adenosine diphosphate ribosylation of histones and poly(adenosine diphophate ribose) synthesis. J. Biol. Chem. 243: 3765-3769, 1968.

Nicotera P, Hartzell P, Davis G and Orrenius S, The formation of plasma membrane blebs in hepatocytes exposed to agents that increase cytosolic Ca^{2+} is mediated by the activation of a non-lysosomal proteolytic system, FEBS Lett. 209:139-144, 1986.

Nicotera P, McConkey D, Svensson S, Bellomo G and Orrenius S, Correlation between cytosolic Ca^{2+} concentration and cytotoxicity in hepatocytes exposed to oxidative stress, Toxicology 52: 55-63, 1988.

Nohl H, Jordan W and Youngman RJ, Quinone in biology: Function in electron transfer and oxygen activation. Adv. Free Radical Biol and Med 2:211-279, 1986.

Ogushi H Yoshihara K and Kaniya T, Bovine thymus poly(ADP-ribose) polymerase. Physical properties and binding to DNA. J Biol. Chem. 255:6205-6211, 1980.

Oka H and Field JB, Inhibition of rat liver nicotinamide adenine dinucleotide kinase by reduced nicotinamide adenine dinucleotide phosphate. J. Biol Chem 243:815-819, 1968.

Okayama H, Edson CM, Fukushima M, Ueda K and Hayaishi O, Purification and properties of poly(Adenosine diphosphate ribose) synthetase. J Biol. Chem. 252:7000-7005, 1977.

Orrenius S, Biochemical mechanism of cytotoxicity. Trends in Phmarmacol. Sci. November FEST supplement: 1-4, 1985.

Orrenius S, McConkey DJ, Bellomo G and Nicotera P, Role of Ca^{2+} in toxic cell killing. TIPS 10:281-285, 1989.

Phelps OC and Crane FL, Inhibition of mitochondrial electron transport by hydroxy substituted 1,4-quinones. Biochemistry 14: 116-122, 1985.

Powis G and Appel GA, Relationship of single electron reduction potential of quinones to their reduction by flavoproteins. Biochem. Biophys Res Comm. 251:25-35, 1986.

Powis G, Svingen BA and Appel P, Quinone stimulated superoxide formation by subcellular fractions, isolated hepatocytes and other cells. Mol. Pharmacol. 20:387-394, 1981.

Priess J and Handler P, Biosynthesis of diphosphopyridine nucleotide 1. Identification of intermediates. J. Biol Chem 233: 488-492, 1958a.

Priess J and Handler P, Biosynthesis of diphosphopyridine nucleotide 11. Enzymic aspects. J. Biol Chem 233: 493-500, 1958b.

Prins B, Koster ASj, Verboom W and Reinhoudt DN, Microsomal superoxide anion production and NADPH-oxidation in a series of 22 aziridinylbenzoquinones. Biochem. Pharmacol. 38: 3753-3757, 1989.

Pryor WA, Hales BJ Premovic PI and Church DF, The radicals in cigarette tar: Their nature and suggested physiological implications. Science 220: 425-427, 1983.

Purnell MR and Whish WJD, Novel inhibitors of poly(ADP-ribose)synthetase. Biochem J. 185:775-777, 1980.

Purvis JL and Lowenstein JM, The relationship between intra- and extramitochondrial pyridine nucleotides. J. Biol. Chem. 236:2794-2803, 1961.

Rankin PW, Jacobson EL, Benjamin RC, Moss J and Jacobson MR, Quantitative studies of inhibitors of ADP-ribosylation in vitro and in vivo. J Biol Chem. 264:4312-4317, 1989.

Rechsteiner M and Cantanzarite V, The biosynthesis and turnover of nicotinamide adenine dinucleotide in enucleated culture cells. J. Cell Physiol 84:409-422, 1974.

Rechsteiner M, Hillyard D and Olivera BM, Magnitude and significance of NAD^+ turnover in human cell line D98/AH2. Nature 259: 695-696, 1976.

Redegeld FAM, Moison RMW, Barentsen HM, Koster ASj and Noordhoek J, Alterations in energy status by menadione metabolism in hepatocytes from fasted and fed rats. Arch. Biochem Biophys. 273:215-222, 1989.

Reed DJ, Regulation of reductive processes by glutathione. Biochem. Pharmacol. 35:7-13, 1986.

Richter C and Frei B, Ca^{2+} movement induced by hydroperoxides in mitochondria. In "Oxidative Stress" (ed Seis H) pp 221-241 Academic press Inc. London 1985.

Richter C and Kass GE, Oxidative stress in mitochondria: Its relationship to

cellular ca^{2+} homeostasis cell death, proliferation and differentiation. Chem Biol Interact. 77:1-23, 1991.

Richter C Theus M and Schlegel J, Cyclosporin A inhibits mitochondrial pyridine nucleotide hydrolysis and calcium release . Biochem Pharmacol 40:779-782, 1990.

Richter C, Winterhalter KH, Baumhuter S, Lotscher HR and Moser B, ADP-ribosylation in the inner membrane of rat liver mitochondria. Proc. Natl. Acad. Sci. USA. 80:3188-3192, 1983.

Schraufstatter IU Hyslop PA, Hinshaw DB, Spragg RG and Cochrane CG, Oxidant injury of cells, J Clin Invest 77:1312-1320, 1986a.

Schaufstatter IU, Hyslop PA, Hinshaw DB, Spragg RG, Sklar LA and Cochrane CG, Hydrogen peroxide-induced injury of cells and its prevention by inhibitors of poly(ADP-ribose)polymerase. Proc. Natl. Acad. Sci. USA 83:4908-4912, 1986b.

Schutzle D, Sampling of vehicle emissions for chemical analysis and biological testing. Environ. Health Perspect. 47:65-80, 1983.

Sies H, Nicotinamide nucleotide compartmentation. In: "Metabolic Compartmentation" (ed Seis H), pp 205-231. Academic press London 1982.

Sies H and Cadenas E, Biological basis of detoxification of oxygen free radicals . In "Biological basis of detoxification" (ed Caldwell J and Jackoby W) pp 181-221, Academic press, New York and London 1983.

Sies H, Hydroperoxides and thiol oxidants in the study of oxidative stress in intact cells and organs. In "Oxidative stress " (ed. Seis H) pp. 73-90, Academic press Inc. London. 1985.

Shall S, ADP-ribosylation of proteins:A Ubiquitous cellular control mechanism. Biochem. Soc. Trans. 17:317-322, 1989.

Silva JM and O'Brien JO, Diaziquone-induced cytotoxicity in isolated rat hepatocytes. Cancer Res. 49:5550-5554, 1989.

Sims JC, Sikorski GW Catino DM, Berger SJ and Berger NA, Poly(adenosine diphosphate ribose)polymerase inhibitors stimulate unscheduled DNA synthesis in normal human lymphocytes. Biochemistry 21: 1813-1821, 1982.

Skidmore CJ, Davies MI, Goodwin P, Halldorsson H, Lewis PJ, Shall S and Zia'ee A, The involvement of poly(ADP-ribose)polymerase in the degradation of NAD caused by X-radiation and N-methyl-N-Nitrosourea. Eur. J Biochem. 101: 135-142, 1979.

Smith PF, Alberts DW and Rush GF, Menadione-induced oxidative stress in

hepatocytes isolated from fed and fasted rats:the role of NADPH-regenerating pathways. Toxicol. Appl. Pharmacol. 89:190-201, 1987.

Stanley PE and Williams SG, Use of the liquid scintillation spectrophotometer for determining adenosine triphosphate by luciferase enzyme. Anal Biochem. 29: 381-392, 1969.

Starke PE and Farber JL, Ferric iron and superoxide ions are required for the killing of cultured hepatocytes by hydrogen peroxide, J Biol Chem 260: 10099-10104, 1985.

Starke PE, Hoek JB and Farber JL, Calcium-dependent and calcium-independent mechanisms of irreversible cell injury in cultured hepatocytes. J Biol Chem 261:3006-3012, 1986.

Stout DL and Becker FF, Fluorometric quantitation of single-stranded DNA: A method applicable to the technique of alkaline elution, Anal. Biochem. 127: 302-307, 1982.

Steenken S, Purine base nucleosides and nucleotides: Aqueous solution redox chemistry and transformation reactions of their radical cations and e^- and OH Adducts. Chem Rev. 89:503-520, 1989.

Streeter A, Dahlin DC, Nelson SD and Baillie TA, Covalent binding of acetaminophen to protein: evidence of cysteine residues as major sites of arylation in vitro. Chem. Biol Interact. 48:349-366, 1984.

Strehler BL, Biolumensecence assay: principles and practice. Meth Biochem Anal 16:99-181, 1968.

Striffer C and Benes J, Nicotinamide mononucleotide- determination of its enzymic formation *in vitro* and its physiological role in the biosynthesis of nicotinamide-adenine dinucleotide in mice. Eur. J. Biochem 21: 357-362, 1971.

Stubberfield CR and Cohen CR, NAD^+ depletion and cytotoxicity in isolated rat hepatocytes. Biochem. Pharmacol. 37:3967-3974, 1988.

Stubberfield CR and Cohen GM, Interconversion of NAD(H) to NADP(H): A cellular response to quinone-induced oxidative stress in isolated hepatocytes. Biochem. Pharmacol. 38:2631-2637, 1989.

Szmigiero L Erickson L Ewig RA and Kohn KW, DNA strand scission and crossing-linking by diaziquone in human cells in relation to cell killing. Cancer Res. 44:4447-4452, 1984.

Tanaka Y, Hashida R, YoshiharaH and Yoshihara K, Bovine thymus poly(ADP-ribose) polymerase histone-dependent and Mg^{2+}-dependent reaction. J Biol Chem. 254:12433-12438, 1979.

Tanaka Y, Yoshihara K, Ohashi Y, Haya A, Nahano T Ito K and Kamiya T, A method for determining oligo- and poly(ADP-ribosyl)ated enzymes and proteins. Ann Biochem 145:137-143, 1985.

Tee LBGT, Boobis AR, Huggett AC and Davies DS, Reversal of acetaminophen toxicity in isolated Hamster hepatocytes by dithiothreitol. Toxicol. Appl. Pharmacol. 83:294-314, 1986.

Teoule R, Radiation-induced DNA damage and its repair. Int J. Radiat Biol. 51:573-589, 1987.

Tewey KM, Rowe TC, Yang L, Halligan BD and Liu LF, Adriamycin-induced DNA damage mediated by mammalian DNA topoisomerase II. Science 226:466-468, 1984.

Thor H, Smith MT, Hartzell P, Bellomo G, Jewell SA and Orrenius S, The mechanism of menadione (2-methyl-1,4-naphthoquinone) by isolated rat hepatocytes. J. Biol. Chem. 257: 12419-12425, 1982.

Thompton RH, In " Naturally occuring quinones" Academic press London and New York 1971.

Thurman RG and Kauffman FC, Factors regulating drug metabolism in intact hepatocytes. Pharm. Reviews 31: 229-251, 1980.

Tischler, ME Friedrichs D, Coll K and Williamson JR, Pyridine nucleotide distribution and enzyme mass action ratios in hepatocytes from fed and starved rats. Arch. Biochem Biophys. 184: 222-236, 1969.

Trakshel GM, Rowley PT and Maines MD, Regulation of the activity of heme degradative enzymes in K562 erythroleukemic cells: induction by thymidine, Exp. Hematol 15:859-863, 1987.

Ueda K and Hayaishi O, ADP-ribosylation. Ann. Rev. Biochem. 54:73-100, 1985.

Vercesi AE, The participation of $NADP^+$, the transmembrane potential and the energy-linked NAD(P) transhydrogensae in the process of Ca^{2+} effux from rat liver mitochondria. Arch.Biochem. Biophys 265: 415-424, 1987.

Von Sonntag C, In "The chemical basis of radiation biology" Taylor and Francis London, 1987.

Warburg O, Christian W and Giese A, The active group of the coenzyme from red blood cells. Biochem. Z. 279:143-144, 1935.

White HD, Biosynthetic and Salvage pathways of pyridine nucleotide coenzymes . In "Pyridine Nucleotide Coenzymes" (ed. Kaplan N) pp225-241, Academic press Inc 1982.

Wyllie AH, Glucocorticoid-induced thymocyte apoptosis as associated with endogenous endonuclease activation. Nature 284:555-556, 1980.

Wyllie AH and Morris RG, Hormone-induced cell death: purification and properties of thymocytes undergoing apoptosis after glucocorticoid treatment. Am J Pathol 109:78-87, 1982.

Wyllie AH, Morris RG, Smith AL and Dunlop D, Chromatin cleavage in apoptosis: association with chromatin morphology and dependence on macromolecule synthesis. J Pathol. 142:67-77, 1984.

Yamamoto K and Farber JL, Metabolism of pyridine nucleotides in cultured hepatocytes intoxicated with tert-butyl hydroperoxide. Biochem. Pharmacol. 43:1119-1126, 1992.

Yoshihara K, Hashida T, Yoshihara H, Tanaka Y and Ohgushi H, Enzyme-bound early products of purified poly(ADP-ribose)polymerase. Biochem Biophys Res Commun 78:1281-1288, 1977.

LIST OF PUBLICATIONS

Krishnamurthi S, Morgan WA and Kakkar VV, Extracellular Na^+ removal enhances granule secretion in platelet - evidence that Na^+/H^+ exchanger is inhibitory to secretion induced by some agonist. FEBS. Letts. 250 195-200, 1989.

Krishnamurthi S, Morgan WA and Kakkar VV, Extracellular Na^+, but not Na^+/H^+ exchange, is necessary for receptor-mediated arachidonate release in platelet. Biochem. J. 265: 155-160, 1990.

Krishnamurthi S, Patel Y, Morgan WA Wheeler-Jones CP and Kakkar VV, Na^+/H^+ exchanger is not necessary for protein kinase C-mediated effects of platelet. FEBS Letts. 252:147-152, 1989.

Morgan WA, Hartley JA and Cohen GM, Quinone induced DNA single strand breaks in rat hepatocytes and human chronic myelogenous leukaemic K562 cells. Biochem. Pharmacol 44:215-221, 1992.

Ghatineh S, Morgan WA, Timbrell JA and Preece NE, The course of energy failure in hydrazine toxicity. A biochemical and NMR spectroscopic study in the isolated hepatocyte. Arch Toxcol. 66:660-668,1992.

Winston A Morgan, Bram Prins, Andries Sj Koster* and
Gerald M Cohen, Pyridine nucleotide changes induced by aziridinylbenzoquinone in rat hepatocytes. 12th European workshop on drug metabolism. Basel Sept. 1990.

Papers in preparation.

Morgan WA and Cohen GM, Pyridine nucleotide hydrolysis and interconversion in rat hepatocytes during oxidative stress.
To be submitted to Biochem Pharmacol EARLY 1993.

Winston A. Morgan, Bram Prins, Andries Sj. Koster* and
Gerald M. Cohen, Aziridinylbenzoquinone-induced pyridine nucleotide changes may provide an insight into their mechanisms of cytotoxicity. Manuscript in preparation.

Morgan WA and Cohen GM, The role of DNA strand scission repair, intracellular NAD^+ and ATP in quinone-induced cytotoxicity. Manuscript in preparation.